United States
Environmental Protection
Agency

Health Effects Research
Laboratory
Research Triangle Park NC 27711

EPA 600 1-79-035
September 1979

Research and Development

EPA

Comprehensive Progress Report for Fourier Transform NMR of Metals of Environmental Significance

EP 600/1
79-035

RESEARCH REPORTING SERIES

Research reports of the Office of Research and Development, U.S. Environmental Protection Agency, have been grouped into nine series. These nine broad categories were established to facilitate further development and application of environmental technology. Elimination of traditional grouping was consciously planned to foster technology transfer and a maximum interface in related fields. The nine series are.

1. Environmental Health Effects Research
2. Environmental Protection Technology
3. Ecological Research
4. Environmental Monitoring
5. Socioeconomic Environmental Studies
6. Scientific and Technical Assessment Reports (STAR)
7. Interagency Energy-Environment Research and Development
8. "Special" Reports
9. Miscellaneous Reports

This report has been assigned to the ENVIRONMENTAL HEALTH EFFECTS RESEARCH series. This series describes projects and studies relating to the tolerances of man for unhealthful substances or conditions. This work is generally assessed from a medical viewpoint, including physiological or psychological studies. In addition to toxicology and other medical specialities, study areas include biomedical instrumentation and health research techniques utilizing animals — but always with intended application to human health measures

This document is available to the public through the National Technical Information Service, Springfield, Virginia 22161

EPA-600/1-79-035
September 1979

Comprehensive Progress Report
for
Fourier Transform NMR of Metals of Environmental Significance

by

Paul D. Ellis and Jerome D. Odom
Department of Chemistry
University of South Carolina
Columbia, South Carolina 29208

Grant R804359

Project Officer
Nancy K. Wilson
Environmental Toxicology Division
Health Effects Research Laboratory
Research Triangle Park, North Carolina 27711

Disclaimer

This report has been reviewed by the Health Effects Research Laboratory, U.S. Environmental Protection Agency, and approved for publication . Approval does not signify that the contents necessarily reflect the views and policies of the U.S. Environmental Protection Agency, nor does mention of trade names or commercial products constitute endorsement or recommendation for use.

Forward

The many benefits of our modern, developing, industrial society are accompanied by certain hazards. Careful assessment of the relative risk of existing and new man-made environmental hazards is necessary for the establishment of sound regulatory policy. These regulations serve to enhance the quality of our environment in order to promote the public health and welfare and the productive capacity of our Nation's population.

The Health Effects Research Laboratory, Research Triangle Park conducts a coordinated environmental health research program in toxicology, epidemiology, and clinical studies using human volunteer subjects. These studies address problems in air pollution, non-ionizing radiation, environmental carcinogenesis and the toxicology of pesticides as well as other chemical pollutants. The Laboratory develops and revises air quality criteria documents on pollutants for which national ambient air quality standards exist or are proposed, provides the data for registration of new pesticides or proposed suspension of those already in use, conducts research on hazardous and toxic materials, and is preparing the health basis for non-ionizing radiation standards. Direct support to the regulatory function of the Agency is provided in the form of expert testimony and preparation of affidavits as well as expert advice to the Administrator to assure the adequacy of health care and surveillance of persons having suffered imminent and substantial endangerment of their health.

This report presents results of extensive studies of the interactions of the toxic metals selenium and cadmium with biological systems, particularly metalloproteins. Improved analytical methods for examination of these interactions, using nuclear magnetic resonance spectroscopy, were developed and are described in this report.

F. Gordon Hueter
Director
Health Effects Research Laboratory

Abstract

Metals or metalloids of primary importance to this study are cadmium and selenium. These nuclei are ideally suited for a multinuclear magnetic resonance study involving direct observation of the metal nucleus by Fourier transform techniques because of their respective receptiveness to an nmr experiment and because they are spin $\frac{1}{2}$ nuclei. The principal objectives of this project included: i) the study of the interactions of cadmium with various amino acids, ii) a detailed examination of the nmr parameters of cadmium substituted metalloproteins, iii) the development of a systematic understanding of the relaxation behavior of ^{77}Se, and iv) the development of the necessary nmr technology to bring these objectives to fruition on a reasonable time scale per experiment.

Our work with the cadmium/glutathione system indicate that the conditions necessary to observe a ^{113}Cd resonance are such that the results of such a study would have little relevance to a real biological system. Hence, our research with ^{113}Cd nmr has been largely devoted to a critical examination of three metalloproteins; concanavalin A, bovine superoxide dismutase, and carboxypeptidase A. Our work to date indicates that this new spectroscopic probe, i.e. ^{113}Cd nmr, is providing new and significant information to the biochemist with respect to the fundamental mode of action of these proteins and the relationship between the function of the protein and the metal associated with it.

Furthermore, we have been involved in an intensive effort to find other nmr active spin $\frac{1}{2}$ nuclei that could be exploited in biological applications. Such a nucleus is ^{77}Se. Although extensive chemical shift information is available for ^{77}Se, little, if any relaxation time information was available before our efforts in this area of research. The spin lattice relaxation time is a parameter of paramount importance in determining the overall utility of a given nucleus in a biological application, that is, it is intimately related to the signal-to-noise per unit time. To this end, we have carried out an extensive study on the nature of the specific mechanism(s) of spin lattice relaxation and the corresponding values of T_1. The systems that we have investigated to date are: organoselenium compounds, RSeR', selenols RSeH, diselenides, RSeSeR', selenates, SeO_4^{-2}, and selenocysteamine. As a result of this research it is clear that ^{77}Se may be very useful to studying active site sulfhydryls in sulfhydryl proteins.

In order to pursue these research topics in the most efficient fashion, it was necessary for us to develop some novel modifications of our nmr instrumentation. One of these is a unique nmr probe, capable of spinning 18 mm nmr tubes, decoupling at any frequency, and observing any nmr active nucleus. Further, the most important design parameter was signal-to-noise ratio per unit volume. That is, we did not take the "milk-bottle" approach in our system. But rather, we tried to optimize the signal-to-noise on a 5 ml coil volume. The net result is that the probe leads to a timesaving of approximately a factor of twelve over conventional 12 mm nmr systems.

Finally, we have solved a rather severe experimental problem in nmr spectroscopy. That is, the required power levels for efficient broad band heteronuclear spin decoupling. This problem reaches critical proportions when examining

biological systems, e.g. proteins in high salt concentrations, on nmr spectrometers employing superconducting magnets. The basic approach employs a linear frequency modulation scheme, i.e. a "Chirp",followed by a 180° -phase modulation of the "Chirp". The relative rates of "Chirp" to 180° -phase modulation must be kept in a 4 to 1 ratio for the method to succeed. The net result is that uniform decoupling can be achieved over a range in excess of 2kHz with only 2 watts of power. For those systems not employing a Faraday shield, efficient decoupling can be affected with power levels between 1 and 2 watts.

Table of Contents

LIST OF ABBREVIATIONS AND SYMBOLS

ABBREVIATIONS

Asp	--	aspartic acid
CD	--	circular dichroism
Con A	--	Concanavalin A
CW	--	continous wave
esr	--	electron spin resonance
FT	--	Fourier transform
His	--	histidine
MCD	--	Magnetic circular dichroism
nmr	--	nuclear magnetic resonance
NOE	--	Nuclear Overhauser Effect
ORD	--	optical rotary dispersion
ppm	--	parts per million
SOD	--	Superoxide Dismutase

SYMBOLS

H, H^1	--	Hameltonians for the spin system
I	--	spin I
I_x, I_y, I_z	--	x,y, of z components of the I spin angular momentum.
J_R	--	resudual indirect nuclear spin coupling constant.
R,R',V	--	rotating frame transformations
S	--	spin S
T_1	--	spin lattice relaxation time
T_2	--	transverse relaxation time
ω_I, ω_S	--	resonance frequency for spin I or S in radians per second.
90°, 180°	--	pulse flip angles

Acknowledgement

The authors wish to acnowledge the work of Professors James Fee, Dave Behnke as well as Drs. Bill Dawson, Vladameir Basus and graduate students Dave Bailey, Allen Cardin, Allen Palmer, and Andy Byrd. The authors are particularly grateful to Dr. Nancy Wilson of the Health Effects Research Laboratory for her invaluable help at the early stages of this research.

I. Introductory Comments

Within the scope of EPA Grant R804359 there are four principal objectives. These objectives include: i) the study of interactions of spin 1/2 metals, e.g. ^{113}Cd, with various amino acids, ii) a detailed examination of the nmr parameters (chemical shifts, T_1 and T_2) of cadmium substituted metalloproteins, iii) the development of a systematic understanding of the magnetic resonance parameters of those spin 1/2 nuclei which are not well characterized and are of importance to environmental research problems, e.g. ^{77}Se, and iv) the development of the necessary nmr technology to bring these objectives to fruition on a resonable time scale per experiment. This progress report is divided into these four categories.

II. Interactions of Spin 1/2 Metals With Amino Acids.

The main objective of this project was to examine the relaxation parameters and chemical shifts of metals in the presence of various amino acids. If these results were positive, then these same methods would be applied to a study of metals interacting with hormones. Our initial efforts were directed toward a study of the ^{113}Cd/glutathione system. Glutathione was chosen because of the existance of sulfhydryl residues in reduced form and disulfide bonds in the oxidized form. The results of these experiments were very frustrating. That is, the ^{113}Cd nmr signal disappeared in the presence of the amino aicd. The only way the resonance could be observed was to raise the sample temperature to above 60°. Admittedly the system could then be studied, but the results would have little, if any, relevance to a in vivo biological system. Further, most of the hormones (which are very expensive) would denature or decompose at these temperatures. Since it was important for these studies to be applicable to biological environments we chose to defer this study until some better biological models were developed.

Recently a short note on the ^{113}Cd nmr of the cadmium/glutathione system has appeared[1]. Their results are consistent with our observations.

III. Cadmium-113 NMR of Cadmium Substituted Metalloproteins.

We have examined the ^{113}Cd nmr of three metalloproteins, Concanavalin A, Carboxypeptidase A, and bovine superoxide dismutase. During the course of these studies (to be described in detail below) three brief reports on the ^{113}Cd nmr of metalloproteins have appeared[2-4]. These studies dealt with three proteins: Alkaline Phosphatase[2,4] and Carbonic Anhydrase B[2,3] from bovine and human sources. These studies demonstrated the utility of ^{113}Cd nmr in studying metalloproteins, even though the results of Armitage et al.[2] on carbonic anhydrase B are in direct disagreement with those of Sudmeier and Bell[3].

A. Cadmium-113 NMR Studies of Cadmium Substituted Concanavalin A[5-7]

This research has been performed in collaboration with Professor David Behnke of the University of Cincinnati Medical School.

Concanavalin A (Con A), a lectin isolated from the jack bean, has been extensively studied due to its unusual biological properties[8-10]. These properties include: preferential agglutination of suspended malignant cells as compared to normal parent cells[11], stimulation of blastogenesis in lymphocytes[12], stimulation of cell mediated immunological responses[13], and pronounced effects on the phenomena of delayed hypersensitivity[14]. As variant as the above list appears, all of these properties seem to depend on the ability of Con A to bind to cell surfaces, which in turn involves specific interactions between saccharide binding sites on the cell surface with the Con A moiety[15]. Because of this, the fundamental requirements for the saccharide binding activity of Con A have been an area of intensive research over the last several years.

It has been known for some time that one of the requirements for the saccharide binding activity of Con A involves certain metals bound to the protein. The nature and location of these metals have been studied by X-ray crystallography[16-21], esr[22], nmr[23-34] and circular dichroism[33-35]. These studies reveal that Con A consists of a dimer (pH $\leq$ 6) or tetramer (pH $\geq$ 7) composed of identical subunits with a molecular weight of 25,500[36,37]. Each subunit requires two metals to bind saccharide. One of the essential metals binds to a site denoted S1. This site is occupied by Mn(II) in the native protein but will also accept other transition metals as well[38,39]. The second site, denoted S2, contains Ca(II) in the native protein but may also bind Cd(II), and to a lesser extent Mn(II)[34,38]. It has been proposed that an ion must have a high affinity for nitrogen ligands to bind at S1 and must have an ionic radius of very nearly 1A to bind at S2[39]. Studies involving the removal and replacement of various metals, both native and non-native reveal that the S1 site must be occupied before the second metal will bind in the S2 site, and that both sites must be occupied to allow the protein to display saccharide binding activity[38,40]. Although the location of the saccharide binding site has been the subject of some controversy in the past[37-40], it now appears that this site is about 11A distant from the S1 metal[21].

Recent developments in multinuclear Fourier Transform (FT) nmr techniques[41-45] have given researchers the capability of using a variety of nmr nuclei as probes to investigate chemical and biological systems. One application of interest is the use of metal nuclides as probes of metal-protein interactions in metalloproteins and enzymes. The native metals found in these proteins have, in general, poor high resoultion nmr characteristics but may in many cases be replaced by metals with more favorable properties. One substitute nuclide with excellent nmr properties is ^{113}Cd. Several studies have been published that have investigated the ^{113}Cd nmr spectra of a variety of inorganic and organometallic models systems[39-43]. More recently, Armitage and co-workers[2,4] have investigated the ^{113}Cd nmr of Cd(II) substituted alkaline phosphatase, human and bovine carbonic anhydrase B. These three metalloproteins are all similar in that each has basically the same symmetry around the metal site (four-coordinate or tetrahedral) and for each protein, three of the ligands binding the metal are nitrogen. Despite these similarities, the reported ^{113}Cd chemical shifts of these proteins are in a range of over 40 ppm. Sudmeier and Bell[3] have also investigated the ^{113}Cd nmr of Cd(II) human carbonic anhydrase B with findings that differ considerably from the former work. The difference in the chemical shifts reported is 80 ppm. In any case, the sensitivity of ^{113}Cd nmr as a probe metal environment has been clearly demonstrated.

We wish to report here our findings on the ^{113}Cd nmr of $^{113}Cd(II)$ substituted Con A. The general areas of concern in this report include: (i) the differences between locked and unlocked Con A and (ii) the interaction of Con A with saccharides as viewed by ^{113}Cd nmr.

Native Con A was isolated from jack bean meal (purchased from Sigma Chemical Co. or Pfaltz and Bauer, Inc.) as previously described[51]. Enriched ^{113}CdO (96%) was purchased from the Atomic Energy Commission (Oak Ridge Laboratories) and converted to the chloride using a metal free HCl solution. Other metals salts used for metal competition studies ($Pb(NO_3)_2$, $ZnCl_2$, $CaCl_2 \cdot 2H_2O$) were obtained commercially and used without further purification. All buffers used in the dialysis of the apo-protein and for assays were rendered metal free by dithizone extraction. Protein concentrations were measured spectrophometrically at 280 nm using $\varepsilon_{1cm}^{0.1\%} = 1.24$[52] with the appropriate dilution factor and a monomeric molecular weight of 25500[50].

Apo Con A was prepared using a modified version of the procedure given by Brown et al.[34]. Approximately 1.0 g of native Con A was dissolved in 8 ml of deionized water and the pH lowered to 1.3 by dropwise addition of 1 M HCl to the solution while stirring at 2°. After stirring for 45 minutes at 2° the solution was transferred to dialysis bags and dialyzed against deionized water. After dialysis against water, the solution was perevaporated until the total volume was approximately 10 ml. This step was found useful in concentrating the Con A solutions. The concentrated protein was then dialyzed against the appropriate metal-free buffer with the final dialysis against a D_2O based buffer to provide an internal lock for nmr experiments. The solution was centrifuged to remove precipitate and the Con A concentration of the supernatant was determined. Typical protein concentrations run from 1 - 2.3 mM, in protomer. The remetallated proteins were prepared by direct addition of the appropriate salts to the apoprotein or by dialysis of the of the metal into the Con A preparations. Saccharide binding activity was checked using the mannan assay previously described[56].

All ^{113}Cd nmr studies were carried out on a highly modified Varian XL-100-15 spectrometer equipped with the Gyro Observe® option. Some experiments were carried out using a frequency synthesizer mode of operation to be described elsewhere[45]. All studies involved the use of a home-built multinuclear 18 mm nmr probe[44]. The sample volume necessary to observe ^{113}Cd on this probe is 5 ml. Due to the broad lines encountered in these systems, it was not found necessary to spin the samples. All ^{113}Cd chemical shifts are referenced to an external standard of 0.1 M $Cd(ClO_4)_2$ in 50/50 H_2O/D_2O[48]. A positive chemical shift denotes resonances to lower shielding.

Brown et al.[34] have recently investigated the various conformational states of Con A by the method of ^1H nuclear magnetic relaxation dispersion. They found that Con A can be qualitatively described as existing in either of two states, a metastable, unlocked form(s) or in a locked form(s). The unlocked conformation(s) is characterized by rapid exchange of Ca(II) and Mn(II) with the Con A moiety. The locked form(s) is characterized by slow exchange of Mn(II) and Ca(II) with the protein. Further, it appears that the ground state energies of both conformations are approximately equal with a relatively high (22 kcal/mole) barrier separating the two states. This barrier allows the conformers to be isolated and studied independently. Thus, at 5° the unlocked conformer may be observed for a reasonably long time (several hours), whereas, at 25° the metastable state will rapidly convert to the locked conformation. Although the data described by these workers was only for the native metals

(Mn(II) at S1 and Ca(II) at S2), subsequent data indicates that similar properties exist in preparations where Cd(II) is used as the S2 metal[52]. It is of interest to investigate both conformations using ^{113}Cd nmr techniques.

The Locked Conformation of Con A. Figure 1a depicts the ^{113}Cd nmr spectrum for a sample of Con A with two equivalents of ^{113}Cd(II) per protomer. The spectrum consists of three resonances at 68, 43, and -125 ppm. It is interesting to note that there are three resonances in this system, and that the resonance at -125 represents the most shielded ^{113}Cd resonance reported to date.

Experiments using several different metals to compete for the ^{113}Cd(II) were used to assign these sites. Manganese, which occurs in the native state at S1 was used to compete for that site. Figure 1b shows the spectrum of Con A to which 1.0 equivalent of Mn(II) and 2.2 equivalents of ^{113}Cd(II) have been added. Again peaks at 68, 46, and -125 ppm can be seen, although the peaks show differences in intensity and lineshape from the peaks of the 2 Cd spectrum. The resonance at 46 ppm is reduced in intensity, most likely due to Mn(II) competition. This site was tentatively labeled S1. The peak at -125 ppm shows increased linewidth. This could be due to paramagnetic relaxation of the Cd(II) brought about by nearby Mn(II) or due to a slight difference in chemical shift of the shielded site in those protein molecules containing either Cd(II) or Mn(II) at S1. Finally the peak at 68 ppm shows a greatly increased intensity and line broadening. The increase is greater than can be explained by extra Cd(II) driven out of S1. Both the increase and the broadening can be explained be efficient paramagnetic relaxation of ^{113}Cd(II) which originally had a relaxation time greater than the .4 second recycle time during data acquisition. Relaxation times of cadmium salts in solution are much longer than the relaxation times of protein bound ions; this suggests that the resonance at 68 ppm might be from non-bound ions.

To assign the S2 site, a calcium competition experiment was prepared. Figure 1c represents Con A to which 2.2 equivalents of Cd and 1.0 equivalent of Ca(II) have been added per protomer. The peak at -125 ppm has disappeared, or is below the noise level. The peak at 46 ppm has gained intensity, and has shifted to 43 ppm, leaving a small peak in the original position, addition of an excess of Ca(II) causes the entire peak to shift to 43 ppm. The peak at 68 ppm has gained intensity, but shows no other change. These two experiments indicate that the Mn(II) site (S1) is at 46 ppm, and the Ca(II) site (S2) is at -125 ppm. They also imply that the site at 68 ppm is free in solution, or at best, is nonspecifically and loosely associated with the protein.

In order to confirm the non-bound nature of the resonance at 68 ppm, an experiment using a varying chloride ion concentration was used. Chloride ion in aqueous solution has a very high affinity for Cd(II), and has a large deshielding effect on the ^{113}Cd(II) chemical shift. A spectrum of 2 ^{113}Cd(II) Con A in a chloride free buffer (.05M acetate, pH 5.2) had three peaks at 46, 8, and -125 ppm. The peaks at 46 and -125 ppm were independent of the chloride concentration. The chemical shift of the resonance and the chemical shift of 4mM $^{113}Cd(NO_3)_2$ in the same buffer was plotted (Fig.2) as a function of chloride concentration. The moving resonance was shown to have a chloride dependence almost exactly the same as the chloride dependence of the resonance in the absence of protein.

Unlocked Conformation(s) of Con A. Attention will now be turned to the the unlocked conformation of Con A. This conformer is easily prepared by

adding the desired metals to cold apo Con A and keeping the resultant remetallized protein at 5°C. As described earlier, unlocked Con A is characterized by rapid exchange of the metals with the surrounding solution. So far these experiments have been carried out only with mixed metal preparations of Con A (Mn(II): Ca(II), or Mn(II): Cd(II)). It will be of interest to investigate how the 2 Cd(II) protein will behave in the unlocked form.

Fig. 3a shows the spectrum of unlocked 2 Cd(II) Con A. The major difference between this spectrum and that of the locked species is that only one resonance (at 68 ppm) is observed. This unlocked species may be converted to the locked by allowing the sample to stand at room temperature for a few hours. The ^{113}Cd nmr spectrum of the sample after standing is the same as that of the locked species, shown in Fig. 1a. The origin of the resonance in Fig. 3a may be due to one of several different possible environments for Cd(II). These possibilities are: free Cd(II) with no interaction with the protein, Cd(II) in the unlocked S1 site only, Cd(II) in the unlocked S2 site only, or Cd(II) in rapid exchange between all possible sites, including the free environment outside the protein. The third possibility may be immediately ruled out on the basis of the known binding order for Con A (S1 before S2). To decide between the remaining possibilities a metal competition experiment in which the ^{113}Cd nmr spectrum of an unlocked 1 Cd(II): excess Zn(II) Con A sample was obtained. The spectrum, reproduced in Fig. 3b, shows a shift of the resonance to 72 ppm. If the resonance was due to free Cd(II) only, no shift would have occurred. Since the chemical shift in the presence of excess Zn(II) is deshielded with respect to the resonance in the absence of Zn(II), implies that the chemical shifts of ^{113}Cd(II) in the S1 sites of the locked and unlocked conformers are similar. Thus, it appears that the resonance observed in the unlocked form is due to Cd(II) in rapid exchange with all possible binding sites.

The magnitude of the contribution of the anion to the observed chemical shift of Cd(II) in the unlocked species may be estimated by repeating the 2 Cd(II)-unlocked Con A experiment in a NO_3^- containing buffer as opposed to a Cl^- containing buffer solution. The results of this experiment are shown in Fig. 3c. Again, only one resonance appears, however, now at -12 ppm. This shift is similar in direction and magnitude to that seen in going from $CdCl_x^{2-x}$ species free in solution. In summary, it is evident that the unlocked two Cd(II)-Con A species can be characterized as having cadmium in rapid exchange with the unlocked protein. Further, the observed chemical shift is highly dependent upon the nature of the salt employed in the buffer solution.

Interactions of Saccharides with Con A. The final portion of this report is concerned with the ^{113}Cd nmr of 2 Cd(II) Con A in the presence of binding saccharides. Since the saccharide binding site has been determined to be 10-12 A from the S1 site[25] it should be expected that some change should occur in the spectra especially in the S1 and S2 resonances. First, as may be anticipated, the ^{113}Cd nmr spectrum of unlocked 2 Cd(II) Con A manifests no change upon addition of saccharide. This result confirms that the protein must be in the locked conformer to exhibit binding activity and has been independently measured using mannan rate assay and circular dichroism studies, with excellent agreement among the methods.

Fig. 4 reproduces the ^{113}Cd nmr spectrum of locked 2 Cd(II) Con A to which a slight excess of the binding monosaccharide, methyl-α-D mannopyranoside has been added. The structure of this saccharide is given below.

This sugar is known to bind tightly to Con A. The spectrum is similar to the spectrum of Con A in the absence of sugars, but the -125 ppm resonance has moved

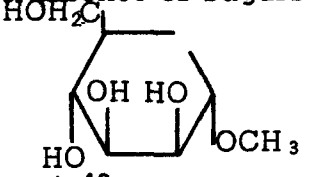

to -133 ppm. The resonance at 46 ppm may again be assigned to the S1 site using methods analogous to those discussed above. As the saccharide binding site is too far from the metal site for direct interaction (over 10A)[21], it appears from this spectrum that a conformational change occurs upon binding the monosaccharide which affects the S2 binding site. Edelman and coworkers[21] have reported dramatic conformational changes within Con A when the monosaccharide 2-deoxy-2-iodo-methyl-α-D-mannopyranoside binds. The most significant changes occur in the metal-binding region when the entire region seems to move 4-6 A with respect to the rest of the molecule. It is evident from the ^{113}Cd nmr that the monosaccharide methyl-α-D-mannopyranoside is producing similar changes within the 2Cd(II) Con A upon binding. There are suggestions in the literature[56] that Con A binds differently to some monosaccharides than to some trisaccharides. This is not supported by our own ^{113}Cd nmr works; however, nmr experiments using ^{13}C and other nuclei are currently underway in our laboratory to further list these observations.

Conclusions. Cadmium-113 nmr studies reported here demonstrate that two ^{113}Cd(II)-Con A can exist in locked or unlocked forms as defined by Brown et al.[34]. The ^{113}Cd nmr spectrum of the locked two ^{113}Cd(II)-Con A preparation yielded three resonances, two of which can be assigned to cadmium bound to the S1 and S2 sites. The third resonance is attributed to ^{113}Cd either not bound or very loosely associated to the protein. The S1 and S2 site are not affected by changes in the buffer. Saccharide binding by those sugars that inhibit the activity of Con A may be monitored by a chemical shift at the S2 site, suggesting that a conformational change takes place when a sugar is bound. In summary, it is clear that ^{113}Cd nmr spectroscopy of cadmium substituted metalloproteins is an excellent tool for delineating subtle changes about the metal site in these proteins.

B. Cadmium-113 NMR Studies of Cadmium Substituted Superoxide Dismutase[56].

This research has been performed in collaboration with Professor James Fee of the University of Michigan. A paper summarizing this work will be submitted to the Proceedings of the National Academy of Sciences.

Superoxide dismutases, which are found in both aerobic and strictly anaerobic organisms[57] are a disparate class of proteins which possess Fe, Mn or Cu as co-factors necessary for catalysis of the reaction

$$2O_2^- + 2H^+ \rightleftarrows H_2O_2 + O_2.$$

The protein isolated from bovine erthyrocytes has received the greatest amount of attention and is the subject of this paper. This protein has a molecular weight near 32,000 daltons and is made up of two identical subunits, each of which binds a Zn(II) and a Cu(II)[58].

The Richardson's group[59,60] has determined the structure of bovine superoxide dismutase by the methods of x-ray crystallography to a resolution on 3.2 A. The metal binding site is shown in Scheme I.

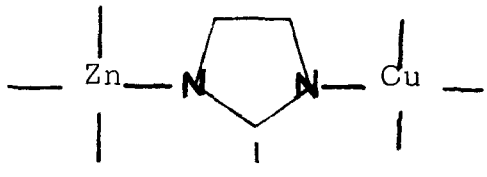

The two metals are approximately 6-7 A apart. The Cu(II) resides in a nearly square planar arrangement of imidazole ligands and a water molecule appears to act as an axial ligand directed toward the exterior of the protein[61]. One of the imidazoles has lost both its protons and forms a bridge to the Zn(II). The Zn(II) resides in an irregular tetrahedron of ligand atoms supplied by three histidines and a carboxyl group.

During catalysis of superoxide dismutation the Cu ion cycles between the (II) and (I) valence states[61,62]. A number of experiments support the contention[64] that the bridge between the two metals is broken concomitant with the uptake of a proton when Cu(II) is reduced and with the release of a proton when Cu(I) is oxidized.

This communication is in part concerned with the question of whether The Zn-N or the Cu-N coordinate bond is broken on reduction. (Scheme II)

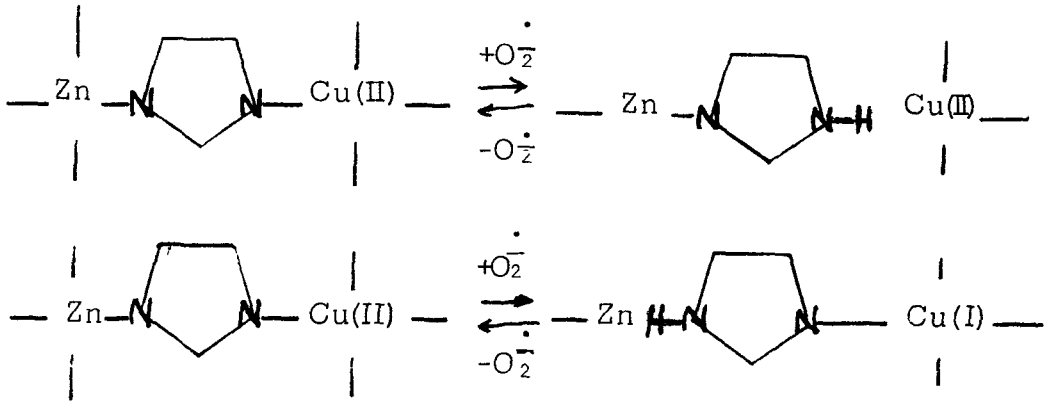

Already two lines of evidence suggest that it is the Cu-N bond that is broken i.e. IIa. First, the optical spectrum of the 2Co(II) protein (Co(II) in the Zn(II) site and the Cu site unoccupied) is very similar to that of the 2Co(II)-2Cu(I) protein (Cu(I) in the Cu site)[65,66]. Thus one can infer from this result that the Cu-N bond is broken in 2Co(II)-2Cu(I) protein resulting in an isolation of the Cu(I) bonding site from the Co(II) site. The second line of evidence comes from x-ray absorption studies[67] which reveal that the Zn(II) undergoes only minor structural perturbations upon reduction of Cu(II), consistent with the Zn(II)-N bond remaining intact.

In this study, ^{113}Cd(II) has been substituted for Zn(II) allowing direct observation of the cadmium nucleus by NMR spectroscopy. Using this technique we have examined the NMR properties of various cadmium derivatives of superoxide dismutase, and one of our conclusions from these efforts is that the Cd(II)-N bond is not broken upon reduction of the Cu(II).

Materials and Methods

Bovine superoxide dismutase (SOD) was isolated from bovine erythrocytes according to the method of McCord and Fridovich[68]. Enriched ^{113}CdO (96% enrichment) was obtained from Oak Ridge National Laboratories and converted to the chloride salt using metal free HCl. Copper sulfate was obtained commercially and used without further purification. Doubly distilled water was used through out and all other chemicals were of reagent grade.

The preparation of apoprotein was carried out using the method published [68], and the Cd derivatives were prepared by adding the desired metals directly to dilute apoprotein (1-2 mg/ml) in a 0.1 M acetate buffer the pH 5.5 and allowing this solution to stand overnight at room temperature. The spectral properties of the 2Cd(II)-2Cu(II) protein were identical to those described by Beem et al.[70] and substitution levels of 90% were obtained. Protein concentrations were determined using the method of Lowry [71]. Copper content of protein sample was measured using ε_{680}=150 M^{-1} [68], and cadmium content was determined by standard atomic absorption techniques.

The preparation of 2Cd(II)-2Cu(I) SOD from the oxidized protein was carried out under strictly anaerobic conditions in a Kewaunnee inert atmosphere glove box. First the 2Cd(II)-2Cu(II) SOD solution was rendered oxygen free by purging the sample with N_2. Solid sodium dithionite was then added directly to the enzyme solution until the characteristic blue-green color of the oxidized protein was completely blanched. The reduced enzyme was then extensively dialysed against the appropriate buffer, also under rigidly oxygen-free conditions, to remove the dithionite. Oxygen free D_2O was added to the sample, either by direct addition or by dialysis, to provide a deuterium lock for the nmr experiments. After dialysis of the enzyme solution, the surface of the dialysis bag occasionally exhibited a pink discoloration. The nature of this material is not known, however, reoxidation of the sample caused the pink color to disappear; the presence of this colored material had no effect on the outcome of the experiments. The pH of the enzyme solution (uncorrected for deuterium isotope effects and henceforth referred to as pH*) was measured inside the inert atmosphere box using a Corning model 109 general purpose pH meter. The pH* of the solutions was adjusted using either 1M H_3PO_4 or 1M NaOH with stirring. The reduced enzyme was finally transferred to an 18 mm nmr tube which was sealed with a rubber stopper, silicone grease and Parafilm®.

The inert atmosphere box was maintained at greater than atmospheric pressure so that a positive pressure was present in the nmr tube during data accumulation. The sample was reoxidized by the admission of air into the enzyme sample after collection of the nmr data; the optical properties of the reoxidized protein were identical to the original 2Cd(II)-2Cu(II) preparation.

All ^{113}Cd nmr spectra were obtained on a highly modified Varian XL-100-15 spectrometer equipped with Gyro-Observe®. Some of the experiments were carried out using a frequency synthesizer mode of operation to be described elsewhere [72]. All experiments involved the use of a home-built multinuclear 18 mm nmr probe [73]. This probe requires 5 ml of sample to obtain a ^{113}Cd nmr spectrum. All ^{113}Cd chemical shifts were referenced to an external sample of 0.1 M $Cd(ClO_4)_2$ in 50/50 H_2O/D_2O. A positive shift denotes resonances to lower shielding. Spin-lattice relaxation times (T_1) were measured using the progressive saturation pulse sequence:

$$-(90° - \tau)_n$$

where τ is the recycle time (including data acquisition) and 90° refers to the angle of the perturbing pulse [74]. No field gradient pulse was employed in these experiments due to the broadness of the line, i.e., $T^*_2 << T_1$. The resulting data were fitted to the following equation using a nonlinear least squares program

$$A(\tau) = A_0 \exp(-\tau / T_1)$$

where $A(\tau)$ is the intensity of the resonance obtained using the pulse interval and A_0 is the intensity obtained for $\tau \geq 5\ T_1$. The use of the nonlinear program obviates the necessity of determining A_0. The Nuclear Overhauser Effect, NOE, was determined using the pulse sequence described above with $\tau = 7T_1$. The "enhanced" spectrum was obtained with the proton decoupler on at all times except during data acquisition. To minimize heating effects and line-broadening, as well as decoupler interference, the NOE supressed spectrum was obtained in the same manner. In the latter case, however, the decoupling frequency was offset 20,000 Hz from the proton chemical shift range and the noise modulation was turned off. The NOE was calculated using the equation:

$$NOE = \frac{A(\text{"enhanced"})}{A(\text{"supressed)"}}$$

Results

The NMR spectra of three derivatives of ^{113}Cd-substituted superoxide dismutase were obtained: 2Cd(II), 2Cd(II)-2Cu(II), 2Cd(II)-2Cu(I) (Figure 5). Some typical spectral parameters are given in Table I . For one of these derivatives, 2Cd(II), a detailed study of the relaxation properties was made. The results of progressive saturation and NOE experiments are shown in Figures 6 and 7 respectively.

Theory and Discussion

Relaxation Properties of 2Cd(II)-Superoxide Dismutase. In any systematic treatment of a molecular system by Fourier transform nmr methods, it is essential to have a working knowledge of the spin lattice relaxation time, T_1, of the nucleus of interest. It is well known that this parameter is a strong function

Table I
Cadmium-113 Chemical Shifts for Various Metal Derivatives of Super Oxide Dismutase

Derivatives[a]	^{113}Cd-Chemical Shift[b]	Linewidth[c]	pH*/Buffer
2Cd(II)	311	27	5.5/.1M Acetate
2Cd(II)/2Cu(II)	-d	-d	
2Cd(II)/2Cu(I)	320	27	4.7 or 8.0/ .1M phosphate 5.5/.1M Acetate

Footnotes for Table I

(a) The designation m Metal refers to the number of metals per dimer of protein

(b) Chemical shifts in ppm with respect to 0.1M $Cd(ClO_4)_2$. A positive sign denotes resonances to lower shielding.

(c) Linewidths are expressed in Hz.

(d) No signal observed.

of molecular structure and the motional dynamics of the system. At the very least, a knowledge of T_1 is essential for optimum data collection rates. Cadmium-metalloproteins are no exception, however it is worth noting that a single T_1 and NOE experiment can represent a significant amount of instrument time, i.e. approximately one week on our XL-100. In this section of the paper we will discuss the measurement and interpretation of the ^{113}Cd T_1 in $^{113}Cd(II)$-substituted superoxide dismutase and its associated NOE.

There are several mechanisms available to an $I=\frac{1}{2}$ nuclide for spin lattice relaxation [75]. However, when this spin is in a metalloprotein in a more or less ionic environment there are basically two principal relaxation mechanisms available: heteronuclear dipole-dipole (usually with protons) and chemical shift anisotropy (CSA). Under ideal conditions these two mechanisms may be separated by a knowledge of the NOE for the spin of interest. The experimental data used to deduce the value of T_1 (1.2 seconds) and the NOE (0.66) are depicted in Figures 6 and 7 respectively. It should be evident from the amount of noise present in these spectra that the error associated with these numbers is appreciable, i.e. approximately 20%. None the less, this error will not invalidate the overall conclusions that one can draw from these experiments.

From simple geometrical models [76], one can calculate the distance 2.8Å, between a hydrogen and the cadmium atom, in a cadmium-histidine complex. If one makes the assumption that two hydrogens per histidine are equivalent (with respect to their distance to the cadmium), then there will be six hydrogens that could provide a dipolar relaxation pathway for the cadmium spin. It is expected that the reorientational correlation time for the ^{113}Cd bound to a protein of 33,000 daltons will be in the range for 10 to 100 nsec. Using these values of the correlation time and the geometrical model discussed above one can predict the dipolar T_1 from standard equations [77]. These values increase from approximately 2.3 seconds for a correlation time of 10 nsec to approximately 16 seconds for a correlation time of 100 nsec. The experimental value is 1.2 sec. Therefore one is forced to conclude that if the geometrical arguments presented are valid, then the spin lattice relaxation is not dominated by dipolar process, but rather that CSA processes are also contributing to the T_1.

The amount of dipole vs. CSA can be estimated by a knowledge of the NOE. The NOE in this type of spin system is not subject to a geometrical conjecture concerning the structure of the active site. The NOE for a given pair of heteronuclear dipolar coupled spins (such as ^{113}Cd coupled to n ^{1}H's) is only a function of the correlation time describing the motion of the internuclear vectors between the spins of interest. If the spin lattice relaxation mechanism was dominated by CSA processes, then the NOE would be equal to one. The largest algebraic value of the NOE if it was dominated by dipolar processes is equal to 0.415 for a system out of the region of extreme narrowing. The experimental value of 0.66 strongly suggests that the two relaxation pathways (CSA and dipole-dipole) are about equally as efficient in providing spin lattice relaxation for the ^{113}Cd nucleus in superoxide dismutase. The value of 0.415 for the NOE represents the limiting value for a system with a correlation time in excess of 50 nsec. If the correlation time for superoxide dismutase is shorter, then the predicted NOE would be algebraically smaller. This would imply a greater importance of CSA process in the mechanism for spin lattice relaxation. Hence, the 50/50 mixture represents a lower limit for the amount to CSA relaxation.

Analysis of the ^{113}Cd NMR of 2Cd(II), 2Cd(II)-2Cu(II), and 2Cd(II)-2Cu(I) Superoxide Dismutase. This section details the analysis of ^{113}Cd nmr spectra of the various metal derivatives of bovine superoxide dismutase. Before beginning this analysis, however, it is prudent to review the known ^{113}Cd nmr data for relevant model complexes of cadmium and of metalloproteins. Attention will be directed to the relationship between the chemical shift and the environment of the ^{113}Cd(II) nucleus, as well as the effects of external variables such as anions and pH on these shifts.

From several reports in the literature the following generalizations are made: octrahedral systems have the smallest chemical shifts (most shielded) followed by progressively larger chemical shifts in tetrahedral and pentacoordinate complexes. Within each of these groups, nitrogen ligands deshield the resonance more than oxygen atoms. Sulfur ligands tend to cause a pronounced deshielding of the cadmium nucleus.

Presently known ^{113}Cd chemical shift data for metalloproteins are summarized in Table II. The most shielded ^{113}Cd chemical shifts reported to date for a metalloprotein are for the lectin Concanavalin A [78a]. This protein exhibits three ^{113}Cd resonances of which those at -125 and 43 ppm are assigned to the known S2 and S1 sites, respectively [78b]. The third resonance at 68 ppm corresponds to "free" cadmium in solution. These sites have been shown by x-ray crystallographic studies to have slightly distorted octahedral symmetry with the majority of the first coordination sphere atoms being the oxygen of amino acid residues or water [79]. The Con A protein resonances do not exhibit an anion dependency.

The majority of the proteins that have been investigated by ^{113}Cd nmr have four coordinate metal sites, although in one case five coordination is possible . The ^{113}Cd substituted metalloenzyme Carboxypeptidase A exhibits no resonance unless an inhibitor such as β-phenyl propionate is added, in which case a resonance at 134 ppm occurs in the presence of chloride anion. The crystal structure of this system shows the Cd(II) to be in a roughly teterahedral environment formed by oxygen atoms for two glutamic acid residues and a histidyl nitrogen with the fourth site open to solvent [80]. In the above cases, this fourth site is occupied either by water or chloride anion .

Another metalloenzyme which has been investigated by ^{113}Cd nmr is Cd(II) substituted human Carbonic Anhydrase B, which Sudmeier and Bell [81], and Armitage et al.[82,83] have studied. In the absence of anions, the latter investigators report a chemical shift for the resonance of 146 ppm while the former report 228 ppm for the same system. The nature of this discrepancy is not clear, but may possibly be due to the amount of dissolved CO_2 present in the samples and /or different isozymes of the protein [84]. The x-ray structure of this system shows the metal site to be a distorted tetrahedron composed of three histidyl nitrogens with the fourth site open to solution [85]. In the absence of anions, this site is occupied by H_2O or OH, depending on the pH. Further, the use of a variety of simple halide anions in the fourth site demonstrated a chemical shift dependence of the Cd(II) resonance in this system, with an observed variation of about 100 ppm [82]. Addition of cyanide to this enzyme appears to form the pentacoordinate Cd(II) species with a chemical shift of 410 ppm [81]. The ^{113}Cd chemical shifts of Cd(II) substituted Alkaline Phosphatase and bovine Carbonic Anhydrase B have also been determined [83]. In the absence of competing effects, these metalloenzymes have chemical shifts of 117 and 214 respectively. Although the crystal structures

Table II
Cadmium-113 Chemical Shifts of Various Metalloproteins

Metalloprotein	Metal Coordination	Metal Site Ligands	pH Sensitive	Counter Ion Sensitive	^{113}Cd Chemical Shift(ppm)[a]
Concanavalin A	S2:six coordinate S1:six coordinate	6 oxygens 5 oxygens 1 nitrogen	no	no	-125 to -132 43[b]
Parvalbumin	six coordinate	6 oxygens	--	--	-90 to -100[c]
Carboxypeptidase A	four coordinate	2 nitrogens, 1 oxygen and substrate donor atom (usually oxygen)	yes	yes	133[d]
Carbonic Anhydrase	four or five coordinate	3 nitrogens substrate donor atom(usually oxygen)	yes	yes	145-241[e,f,g] 410[f]
Alkaline Phosphase	four coordinate	3 nitrogens, substrate donor atom (usually oxygen)	yes	yes	55-170[e,g]

Table II cont.

Metalloprotein	Coordination	Metal Site Ligands	pH Sensitive	Counter Ion Sensitive	^{113}Cd Chemical Shift(ppm)[a]
Super Oxide Dismutase	four coordinate	3 nitrogen 1 oxygen	yes	yes	310-330[h]
Metallothionein	possibly four	sulfur	--	--	614,624,643, and 668[i,j,k]

Footnotes for Table II

a) Chemical shifts are in ppm with respect to external 0.1M $Cd(ClO_4)$. A positive sign denotes resonances to lower shielding.

b) D.B. Bailey, P.D. Ellis, A.D. Cardin, and W.D. Behnke, J. Amer. Chem. Soc., 100, 5236 (1978). In this reference the assignment of the S1 and S2 sites was in error. The correct assignments are given here (A.R. Palmer, P.D. Ellis, W.D. Behnke, D.B. Bailey and A.D. Cardin, submitted to J. Amer. Chem. Soc.).

c) T. Drakenberg, B. Lindman, A. Cave', and J. Parello, FEBS Lett, 92, 346 (1978).

d) D.B. Bailey and P.D. Ellis, unpublished results. Both entries denote ^{113}Cd chemical shifts in the presence of β-phenylpropionate. The entry for 133 ppm corresponds to the presence of Cl^-, whereas, the resonance at 217 is in the presence of ClO_4.

e) I.M. Armitage, R.T. Pajer, A.J.M.S. Miterkamp, J.F. Chelbowski, and J.E. Coleman, J. Amer. Chem. Soc., 98 5710 (1976).

f) J.L. Sudmeier and S.J. Bell, J. Amer. Chem. Soc., 99, 4499 (1977).

g) I.M. Armitage, A.J.M.S. Miterkamp, J.F. Chelbowski, and J.E. Coleman, J. Magn. Res., 29, 375 (1978).

h) present work

i) K.T. Suzuki and T. Maitani, Specialia, 34, 1449 (1978).

j) P.J. Sadler, A. Bakka, P.J. Beynon, FEBS Lett., 94, 315 (1978).

k) J.D. Otvos and I.M. Armitage, personal communication.

of these systems have not yet been determined, other work suggests that the metal sites in both proteins are four coordinate, with three of the ligands in each case being histidyl nitrogens .

The ^{113}Cd nmr spectrum of 2Cd(II) dismutase (Fig. 5a) consists of one resonance with a linewidth of 27 Hz. The appearance of only one resonance indicates that if the Cd(II) sites in the two subunits differ, then this difference only manifests a ^{113}Cd chemical shift difference of less than 10 Hz (0.5 ppm). Given the known sensitivity of the ^{113}Cd chemical shifts to environmental changes, this result suggests that the metal sites in the two subunits are identical. The presence of the resonance at 311 ppm is in line with the metal site being either four or possibly five coordinate. The crystallographic study of this system reveals that the Zn(II) site (Cd(II) site) is four coordinate, with three of the ligands due to histidyl nitrogens and the fourth site occupied by an oxygen from an asparate residue [59]. It should be noted that this chemical shift is 90-150 ppm more deshielded than human Carbonic Anhydrase B, which has the same ligand atoms (when no anions are present) and a similar geometry at the Cd(II) site as the dismutase. This deshielding effect is in all probability due to the greater covalent character of the aspartate-cadmium bond in dismutase compared to the water-cadmium bond in Carbonic Anhydrase or to a slightly different local symmetry about the cadmium.

No resonance was observed from the 2Cd(II)-2Cu(II) dismutase derivative.[82] This result is to be expected as the paramagnetic Cu(II) atom is 6-7A from the Cd(II) sites. Approximate calculations indicate that for our signal-to-noise ratio the resonance will be broadened beyond recognition by the dipolar field of the electron if the copper-cadmium interatomic distance is within 11A.

The reduced copper enzyme is of interest for a number of reasons. First, the number of resonances that are observed will indicate the number of chemically different Cd(II) sites in the enzyme. Second, the chemical shifts of this system will indicate the amount of perturbation placed on the Cd(II) sites by the Cu(I). Third, the dependence of this system on pH and buffer conditions will indicate the accessibility of this site to solute molecules. Figure 5c depicts the ^{113}Cd nmr spectrum of 2Cd(II)-2Cu(I) dismutases. Only one resonance is observed with a chemical shift of -320 ppm. Again, this result indicated that if there is any difference between the two Cd(II) sites in the protein, that difference only generates a 0.5 ppm chemical shift. Thus, as with the 2Cd(II)-protein, the two sites are considered equivalent.

The observation of a small chemical shift between the Cu-free protein and the 2Cd(II)-2Cu(I)-protein immediately suggests that only minor changes occur at the Cd coordination site on the binding of Cu(I) to the Cu-site. Mechanism (a) of Scheme II requires the breaking of the Cu(I)-imidazole bond to provide the necessary proton while mechanism (b) has the Zn(II)-imidazole bond breaking. If the correct mechanism were (a), and the Cd(II) system is analogous to the Zn(II) system, the ^{113}Cd nmr properties of the reduced protein would be similar to those of the copper free system. On the other hand, if mechanism (b) were correct, the Cd(II) species would be required to break the Cd-N bond which would either not be replaced (which is unlikely) or would be replaced by water or some component from the solution. In any case, the ^{113}Cd nmr properties of the reduced system would be dramatically different from those of the copper free protein. On this basis, the ^{113}Cd nmr results indicate that mechanism (a) is the more likely. This point can be strengthened by obtaining the ^{113}Cd nmr data with a variety of pH and buffer conditions. The following systems were therefore used: (i) 0.1 M acetate buffer, pH* 5.5 (ii) 0.1 M phosphate buffer, pH* 8.0, and (iii) 0.1 M phosphate buffer,

pH* 4.7. Under all of these conditions there were no changes observed in the ^{113}Cd nmr spectrum of the 2Cd(II)-2Cu(I)-protein. An experiment was also carried out in which the dithionite was not dialysed away from the protein. Again, no change was noted in the chemical shift of the protein.

Several lines of evidence now support the contention that the imidazole bridge between Zn and Cu is broken at the Cu site upon reduction. The Cu(I) which remains very tightly bound to the protein [86] would thus appear to be coordinated to three atoms donated by the protein and to have at least one position open to the solvent [87].

The certainity of this conclusion now allows speculative comment on the role of the bridging imidazole in the catalysis process. Hodgson and Fridovich[88] speculated that during catalysis the bridge breaks at Cu, a proton is then taken up from the solvent as was shown by Fee and DiCorleto [64]. This proton is subsequently donated to Cu(I) bound O_2^- followed by electron transfer from Cu(I) to the superoxide to form Cu(II)-O-O-H and to reform the bridge. The present work in conjunction with other studies provides a rational structural basis for such a mechanism but does not provide any evidence for its occurrence. Two important facts which must be considered in asking how protons are donated to O_2^- in the second step of catalysis [87] are: a-free aquo Cu-ions are $\sim$ 4X more efficient catalysts of superoxide dismutation then Cu-dismutase [89], and b-removing the Zn from the protein lowers activity by at most a factor of two. The question is raised as to whether a protein mediated proton transfer mechanism is necessary in the catalytic process.

While this work was in progress, a report appeared by Armitage et al. [82] concerning similiar studies of SOD. These workers found that the copper free system exhibited a chemical shift of 179 ppm. Further, upon reduction of the 2Cd(II)-2Cu(II) preparation with dithionite, a chemical shift to 7 ppm was observed, with a large increase in the linewidth of the resonance. These observations are diametrically opposed to our own results. The possibility of differences due to pH and buffer composition must be ruled out on the basis of our own work. Further, the results of Armitage et al. suggest that a large change occurs in the Cd(II) site between the copper free protein and the reduced copper system. This change is incompatible with the mechanism proposed for proton insertion by both ourselves and Armitage. Also, the results shown for other systems indicate that the Zn(II) site is extremely stable and not likely to exhibit such pronounced differences in the ^{113}Cd nmr. On these bases, we must conclude that our results are more indicative of the native system than those of Armitage. The difference in results may be due to the method by which the enzyme systems were prepared. The work referenced by Armitage describing the preparation of the apoprotein does not include the perchlorate dialysis to remove tightly bound EDTA [69]. The presence of the EDTA has been previously shown to produce erroneous results .

C. Cadmium-113 NMR Studies of Carboxypeptidase

Carboxypeptidase A is an enzyme that catalyzes the hydrolysis of peptides and esters [90]. It is an exopeptidase active toward the carboxyl terminus of the peptide, where the residue is usually a phenyl derivative. The enzyme also exhibits esterase activity toward esters containing phenyl groups. The protein has a molecular weight of 34,000 and contains one zinc atom per molecule [91]. The zinc is in a roughly tetrahedral environment with one site open to the environment. In a noncatalytic situation this site is filled by water or anion such as Cl^-. During catalysis this site is believed to coordinate the carbonyl of the substrate. This conclusion follows from the X-ray work of Lipscomb and his co-workers [92]. In this research, the X-ray structure was determined on a binary complex of the enzyme and the peptide glycyl-tyrosine. This pseudosubstrate is not cleaved by the enzyme which, of course, raises some questions about the relevence of this structure to the binding of typical reactive substrates. The enzyme can also cleave esters of α-hydroxy acids, such as α-phenyllactic acid; no X-ray work on carboxypeptidase A with a found ester substrate or pseudosubstrate has been done. A unified picture of the enzyme mechanisms with carboxypeptidase A has been recently proposed by Breslow and Wernick [93]. They propose the following schemes:

(i) Peptide substrates bind so as to displace water from Zn(II). A water molecule is then delivered by the glutamic carboxylate.

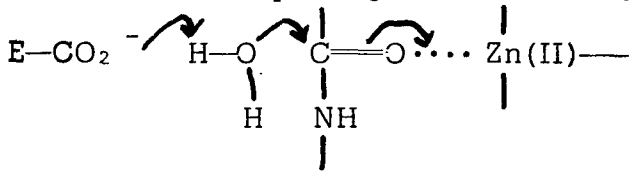

(ii) Ester substrates may bind without displacing the water from Zn(II). This puts the esters in position for a nucleophilic attack by the glutamate.

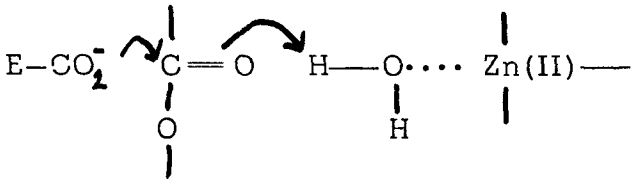

A detailed picture of the peptide hydrolsis mechanism is envisioned by Breslow to be the following:

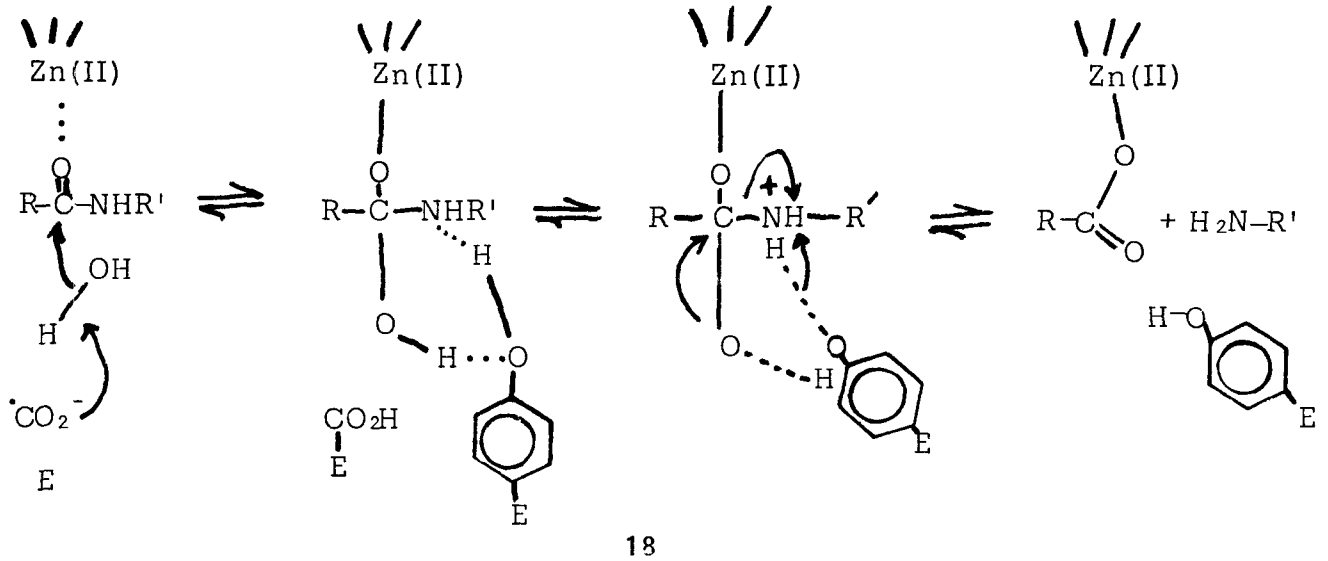

From the preceding mechanistic picture two points are relevant to the present research: (1) ester substrates may not involve carbonyl coordination to the Zn(II), and (2) as the products disassociate in the peptide hydrolysis mehcanism, the resulting acid is coordinated to Zn(II).

Byers and Wolfenden have examined several inhibitors of carboxypeptidase A [94]. In the course of their research, they developed a so-called product inhibitor of the enzyme. That is, the inhibitor, L-benzylsuccinate, resembles the collected products of the peptide hydrolysis, and thus it is bound with an affinity resembling their combined affinity.

If Breslow's detailed mechanistic picture[93] is correct and if Wolfenden's inhibitor indeed resembles disassociated products [94], then one would predict that the Zn(II) would not be accessible to solvent water molecules or anions such as Cl^- in the presence of the inhibitor. However, Byers and Wolfenden[94] have demonstrated that L-benzylsuccinate can bind to apo carboxypeptidase. This binding is sufficiently tight to prevent Zn(II) from coordinating with the enzyme. The results suggest that L-benzylsuccinate may not be bound to the Zn(II). Our research to date on carboxypeptidase has dealt with the question of how L-benzylsuccinate binds to carboxypeptidase.

Cadmium-113 nmr spectroscopy should be able to shed some light on this situation. Before we address ourselves to substrate binding effects, it would be prudent to study carboxypeptidase in the absence of any inhibitors. The results of these experiments have been exceptionally frustrating, in that to date we have been unable to observe the ^{113}Cd resonance for the uninhibited enzyme. This appears to be due to some intermediate exchange condition associated with ligand exchange on and off the cadmium. Our initial efforts have been performed on carboxypeptidase at approximately a 2 mM concentration. This concentration was obtained by having the protein in a 3 M NaCl salt solution in which the chloride ion would be expected to bind to the metal. We have recently found that the enzyme can be solubilized by high concentrations of ClO_4^-. This anion would coordinate the cadmium to a lesser extent than Cl^- ion. We are presently investigating the ^{113}Cd nmr of carboxypeptidase A in the ClO_4^- solutions as a function of the solution pH. An important point to make at this stage is that the cadmium enzyme still maintains its esterase activity in the presence of ClO_4^-.

Our successful ^{113}Cd research on carboxypeptidase A to date has been achieved when the enzyme is in the presence of two inhibitors β-phenyl propionate and D,L-benzylsuccinate. In the case of the β-phenyl propionate, a resonance was observed at 134 ppm deshielded from 0.1 M $Cd(ClO_4)_2$. The resonance was obtained in ClO_4^-/buffer solution and the observed linewidth was approximately 32 Hz. Repeating the experiment using benzyl succinate yielded a resonance at 140 ppm in the ClO_4^-/buffer solution with a linewidth of approximately 90 Hz. The ^{113}Cd resonance, the D,L-benzylsuccinate inhibited enzyme in Cl^-/buffer appeared at 217 ppm with an associated linewidth of 230 Hz. The previous experiments were performed with a pH of 8 for the solution. The corresponding experiment for D,L-benzylsuccinate in the Cl^-/buffer at a pH of 9 yielded a resonance at 209 ppm with a linewidth of 138 Hz.

This large increase in linewidth between D,L-benzylsuccinate and β-phenyl propionate in the ClO_4^- solutions is surprising. Since D,L-benzylsuccinate has a K_I approximately 136 times smaller than β-phenyl propionate, and if both inhibition are bound to the enzyme in the same way, we would have expected a

linewidth narrower for the benzyl succinate than that observed for β-phenyl propionate. These results clearly suggest that the cadmium in the benzyl succinate inhibited enzyme is more accessible to water and ion exchange effects than when β-phenyl propionate is inhibiting the protein. This assertion is further supported by the ^{113}Cd nmr data of the inhibited enzyme in the Cl^- / buffer solutions. That is, the linewidth is substantially greater in these solutions and it is pH dependent. Hence, one obvious conclusion that can be drawn from the research done to date is that D,L-benzylsuccinate binds to carboxypeptidase A in such a way that it does not coordinate the metal. Subsequent experiments are needed to confirm this conclusion. Further, the present data cannot be used to support or refute the notion that the carbonyl oxygen of the inhibitor β-phenyl propionate binds to the Cd(II).

IV. Selenium-77 NMR Investigations of Model Biological Systems.

A preliminary account of this research has been published (W.H. Dawson and J.D. Odom, J. Amer. Chem. Soc., 99, 8352 (1977)). The more detailed summary, to be presented below, will be submitted to the Journal of the American Chemical Society.

While Fourier transform nuclear magnetic resonance (FT NMR) spectroscopy has been used to great advantage to study the chemistry of many elements of the Periodic Table, those of Group VIA have received little attention. For oxygen, and sulphur, the two lightest and most chemically prolific members of this group, the only NMR active isotopes (^{17}O and ^{33}S) are quadrupolar nucleii which suffer from very low natural abundance and relatively low sensitivity. Selenium and tellurium, on the the other hand, both have spin-1/2 isotopes (^{77}Se, ^{123}Te, ^{125}Te) with sufficient sensitivity to make their study readily accessible by FT NMR. For the purposes of this investigation, our interest in selenium stems from the active role it plays in many biological systems, not to mention its increasing involvement in organic synthesis and an extensive inorganic chemistry [95]. Selenium-77 NMR has great potential as a means of exploring the chemistry of this interesting element and as part of our continuing interest in the applications of multinuclear NMR to biological systems[96] we have initiated a program aimed in this direction.

Early continuous wave (CW) nmr studies by Birchall, et al.,[97] followed by the INDOR studies of McFarlane and Wood[98] demonstrated the large chemical shift range of ^{77}Se and the stereospecificity of its coupling constants. To date there have been only a few reports concerned with the direct observation of ^{77}Se by FT NMR[96c,99-103] The nuclear spin-lattice relaxation time, T_1, is a critical parameter in determining the recycle time of FT NMR experiments. More importantly, it can often be used as a powerful, diagnostic tool for the determination of molecular structure, conformation and composition [104]. It can also be employed as a probe to investigate molecular motions and ineractions. Dawson and Odom,[96c] Pan and Fackler,[100] Gansow, et al.[101] and Koch et al.,[102] have briefly examined spin-lattice relaxation times for ^{77}Se in a variety of chemical environments. The result of these studies indicated an importance of spin-rotation (SR) and, to a lesser extent, chemical shift anisotropy (CSA) mechanisms for spin-lattice relaxation.

Relaxation considerations assume an added significance when dealing with large biological macromolecules that contain selenium. Those seleno-systems which are involved in biochemical reactions will eventually be the focus of greatest concern in our nmr studies. However, their high molecular weights impart a motional sluggishness which, from the viewpoint of NMR spectroscopy, requires operating near the limits of the so-called "region of extreme narrowing" ($\omega\tau << 1$) and complicates the task of extracting useful physico-chemical information [105]. It is advantageous to be forearmed with a knowledge of the mechanisms governing T_1 and we have, therefore commenced our biological studies using ^{77}Se NMR with an examination of the spin-relaxation of this nucleus as it appears in a number of functional forms and in both aqueous and non-aqueous solvents.

Spin-lattice relaxation times were determined on a modified Varian XL-100-15 NMR spectrometer. Field-frequency stabilization was achieved by locking to

the deuterium resonance of the solvent (either $CDCl_3$ or D_2O). Selenium-77 resonances were initially detected at 19.1 MHz using the Gyrocode Observe® accessory with the deuterium lock frequency at 15.400960 MHz. Under these conditions, however, it was not possible to simultaneously proton-decouple the sample at 100 MHz using either coherent or modulated (noise or squarewave) irradiation without introducing a prohibitive amount of noise into the receiver. This feature is apparently common to all XL-100 spectrometers[100,106]. A solution to this difficulty was achieved by lowering the field slightly such that ^{77}Se resonates at 18.90 MHz with proton-decoupling at 99.41 MHz. The deuterium lock frequency at this new field strength is exactly 15.30 MHz. During the early stages of this work this latter frequency was obtained by replacing the 15.400960 MHz master crystal by 15.3 MHz from a frequency synthesizer. Since the Gyrocode Observe reference frequencies are ultimately derived from this master frequency, the outputs of this unit using the new frequency were automatically scaled to the required 99.41 MHz decoupling and 18.90 observe frequencies when the "normal" 15.4 MHz Gyrocode settings were used. In the latter stages of this study, the XL-100 was converted to a synthesizer-based instrument, wherein the observe frequencies were derived from a General Radio 1061 frequency synthesizer. The 15.3 MHz master frequency was generated by a home-built frequency synthesizer which was phase locked to the GR 1061 synthesizer. The standard components of the Varian 4412 probe were retunable from 15.4 to 15.3 MHz and 19.1 to 18.9 MHz without any perceptible performance losses.

The inversion-recovery pulse sequency, $(180° - \tau - 90° - T)_n$, was used to obtain the relaxation times (T_1) when the magnitude of this parameter was on the order of 5 sec of less [107]. The 90° and 180° pulse widths were determined in the usual manner with 90° pulse being on the order of 65 μsec. The waiting time between pulses (T) was always set to be greater than 5 T_1's. When T_1's longer than 5 sec were encountered, the homospoil saturation recovery sequence, $(PD- HS - 90° - HS - \tau - AT)_n$, was employed where PD, HS and AT are the pulse delay (nominally 0.1 sec), the homospoil (Z-gradient) pulse, and the acquisition time, respectively [108]. In the case of either pulse sequence, at least one spectrum was obtained with the value of τ exceeding five times T_1 [109]. The value of T_1 was extracted from the experimental data using a non-linear least squares routine in the usual manner. The uncertainty in the T_1 values determined in this way is estimated to be within 10%, although repetition of the measurements for selected samples used in this study indicated that the values are reproducible to well within these limits.

Nuclear Overhauser effect enhancement factors (η) were determined as the difference in integrated intensity between ^1H-decoupled and ^1H-coupled spectra and are reported as NOE = $1 + \eta$ [110]. The measurements were taken from two spectra, one in which the ^1H-decoupling frequency was set exactly on resonance and the second with the decoupling frequency offset at least 10 KHz from this resonance frequency, with the modulation removed. The recycle time between pulses in these experiments was at least seven times the value of T_1 [111].

All spectra were obtained using 250 or 500 Hz spectral widths and transformed using 8K data points (zero-filling as required). Chemical shifts are reported relative to the resonance of dimethylselenide in $CDCl_3$ ($\sim$1.0 M) in the sense that a positive chemical shift denotes a resonance to lower shielding [112].

Temperature control was achieved using standard Varian accessories and temperatures were measured with a copper-constantan thermocouple unit, the "hot" end of which was inserted into an open sample tube containing the appropriate solvent and held at a depth coincident with the receiver coils. The tempertuares reported in this work are estimated to be accurate to ±1°.

All samples were degassed by several freeze-pump-thaw cycles and sealed under dynamic vacuum in 12 mm NMR tubes. The solvents ($CDCl_3$ and D_2O) were treated with dithizone prior to being distilled in an all-glass apparatus. Paramagnetic materials were removed from nmr tubes by allowing the tubes to stand in a nitric acid bath for several days and rinsing them several times with deionized water.

The following materials were obtained from commercial sources: selenium, selenium dioxide, sodium selenate (Alfa-Ventron), d,l-selenomethione and d,l-selenocystine (Sigma Chemical Co.,). Anhydrous hydrogen selenide was a gift from A.J. Zozulin of this department and N,N-dimethylselenourea was a gift from Dr. R.A. Zingaro (Texas A & M University). Dimethyl selenide (b.p. 54-57°; lit.[113] 57°) was prepared from the reaction of CH_3I and Na_2Se in aqueous base [114]. Di-n-butyl selenide (b.p. 196-197°; lit. [113] 82-83°/13 torr), di-n-octyl selenide [115] (b.p. 157-158°/0.1 torr) and di-isopropyl selenide (b.p. 136-137°; lit[116] 135°) were obtained from the reaction of the corresponding alkyl bromides with Na_2Se in liquid NH_3[116]. Methane selenol (B.p. 23-25°; lit. [117] 25.5°) was prepared from the reduction of dimethyl diselenide with hypophosphorous acid [118]. Ethane selenol (b.p. 50-53°;lit.[116] 52°) and decane selenol (b.p. 125-130°/18 torr; lit.[119] 128-129°/13 torr) were synthesized by the reduction of the corresponding dialkyl diselenides with elemental sodium in liquid NH_3[116]. Dimethyl diselenide was obtained as an orange oil (b.p. 156-158°; lit.[120] 155-157°) from the reaction of CH_3I and Na_2Se_2 in aqueous base [114]. Debenzyl diselenide (m.p. 92-93°; lit.[121] 92-93°) was prepared from benzyl chloride and Na_2Se in ethanol [122]. Diphenyl diselenide (m.p. 63.64°; lit.[113] 61-63°) was synthesized by the air oxidation of a solution of benzene selenol [123]. Didecyl diselenide (m.p. 12-16°; lit.[124] 13-14°) was obtained as an orange oil from the reaction of decyl bromide with Na_2Se_2 in liquid NH_3[116]. Trimethyl selenonium iodide (m.p. 150-152°; lit.[125] 150-152°) and dimethylselentine bromide (m.p. 89-92°; lit.[114] 90°) were prepared by mixing cold diethyl ether solutions of dimethyl selenide (20% molar excess) and the corresponding alkyl halide and subsequently removing the volatile materials. Dimethylselenoxide (m.p. 91-93°; lit.[126] 94°) was prepared from both the ozonolysis of dimethyl selenide in $CHCl_3$[113] and the reaction of silver oxide with dimethylselenium dibromide in methanol[114]. Selenocysteamine hydrochloride (m.p. 108-110°; lit. [127] 108-110°) was synthesized by the method of Klayman[127] and methylselenocysteamine hydrochloride (m.p. 149-151°; lit.[128] 149-151°) was prepared according to the method of Tanaka et a.[128]. In addition to the determination of boiling points or melting points, the purity of all compounds was carefully checked by ^1H and ^{77}Se NMR.

Diakyl Selenides

The data for this group of compounds is collected in Table III. In each of these molecules, scalar spin-spin coupling of the ^{77}Se nucleus to nearby alkyl protons is observed. Proton-decoupling reduces the resonances to single sharp line, but in no case was a ^{1}H-^{77}Se NOE observed. Thus, although the presence of these nearby spin-1/2 nuclei must certainly give rise to a ^{1}H-^{77}Se dipole-dipole relaxation, it is apparently very inefficient and its contribution to the observed T_1 is minor relative to the other mechanisms. An earlier study[101] reported an NOE for $(CH_3)_2Se$ of 1.04. One can eliminate in principle a contribution from scalar coupling relaxation since there is no means by which it could be operative in these systems.

In order to distinguish which of the remaining two mechanisms is operative (chemical shift anisotropy (CSA) or spin rotation (SR)) the T_1 was determined as a function of temperature and the data plotted as a semilog plot of $R_1 \equiv T_1^{-1}$ versus the reciprocal temperature (Fig. 8). The temperature dependencies of the relaxation processes dictate that in such a plot the SR mechanism will give a negative slop while the CSA mechanism will yield a positive slope, and under the assumption (valid for these small molecules at the Larmor frequency employed) that the extreme narrowing condition applies[129] . As may be seen from Figure 8 , the negative slope and strict linearity of the plot for dimethylselenide points to the fact that the spin-lattice relaxation of ^{77}Se in this compound is dominated by T_1 (SR) in the temperature range studies. This result is in accordance with theoretical and practical expectations since the SR mechanism requires a coupling of the nucleus to the valence electrons in a manner similar to that which gives rise to the so-called "paramagnetic shielding" term of the chemical shift[130]. As a consequence, heavy, magnetically active nuclei which possess a large chemical shift range will, in small molecules, usually, display significant SR relaxation. This fact has been demonstrated experimentally for a number of heavy nuclei, e.g., ^{113}Cd[96a], ^{199}Hg[96b], and ^{205}Tl[131] . The dioctylselenide molecule should, by virture of its larger size, tumble less rapidly in solution than dimethylselenide and, hence, SR should be less important in this case. In fact, as is seen in Figure , only at the higher temperatures does SR become important and at low temperatures the steep positive slope and lack of an NOE imply a CSA mechanism. The increased importance of the SR mechanism at higher temperatures is undoubtly due to the increased overall motion of the molecule coupled with increased segmental motion of the selenium atom within the chain. The quantitative separation of these motions is beyond the scope of this report.

The slower tumbling experienced by selenium in dioctylselenide at -50° contributes, in this case, to a diminution of the SR mechanism and an enhancement of CSA relaxation. This aspect is of considerable interest to the study of macromolecules containing an RSeR' moiety because of the implication that the CSA mechanism may be important in these systems. If one assumes that the motion of the ^{77}Se nucleus can be described by a single correlation time, τ_c, then the relaxation rate for CSA processes can be expressed[105a] as

$$T_1^{-1}(CSA) = \frac{2}{15}\gamma_{Se}^2 H_o^2 (\Delta\sigma)^2 \frac{\tau_c}{1 + \omega_{Se}^2 \tau_c^2} \qquad [1]$$

Here, γ_{Se} is the magnetogyric ratio for selenium, H_o is the applied magnetic

Table III. Selenium-77 Chemical Shifts and Spin-Lattice Relaxation Times

Compound	Chemical Shift[a] (ppm)	T_1 (sec)	Temp (°C)	Conditions[c]
$(CH_3)_2Se$	0[b]	5.2	55	$CDCl_3$
		7.5	32	
		8.6	12	
		24.4	-60	
	3	4.3	40	acetone
		9.8	030	
$(n\text{-}C_4H_9)_2Se$	167	19.1	40	$CdCl_3$
		23.1	0	
		16.5	-40	
$(n\text{-}C_8H_{17})_2Se$	168	10.4	41	$CDCl_3$
		14.8	0	
		6.0	-42	
$(i\text{-}C_3H_7)_2Se$	432	8.7	41	$CDCl_3$
		13.6	0	
		20.4	-42	
d,ℓ-$CH_3SeCH_2CH_2CH(NH_2)COOH$	75	13.5	34	0.1 M, D_2O, pD 4
$CH_3SeCH_2CH_2NH_2$	44	8.4	43	0.5 M, $CDCl_3$
		15.9	0	
	50	24	43	0.5 M, D_2O, pD 4
		28	10	
$(CH_3Se)_2$	281	9	45	0.5 M$CDCl_3$
		13	0	
$(C_6H_5CH_2Se)_2$	412	27	55	0.5 M, $CDCl_3$
		31	18	
$(C_6H_5Se)_2$	481	20	45	0.5 M, $CDCl_3$
		31	0	
$(n\text{-}C_{10}H_{21}Se)_2$	316	21	43	0.5 M, $CDCl_3$
		14	0	

Compound	Chemical[a] Shift (ppm)	T_1 (sec)	Temp (°C)	Conditions[c]
CH_3SeH	-130	1.3 3.3 3.7	40 -30 -45	acetone-d_6
C_2H_5SeH	39	1.7 4.8 9.5	40 -30 -60	$CDCl_3$
	41	1.5 3.7 7.7	40 -30 -83	acetone-d_6
$n\text{-}C_{10}H_{21}SeH$	-7	1.9 3.4	42 0	$CDCl_3$
$HSeCH_2CH_2NH_2$	-212	7.1	32	0.5 M, D_2O, pD 8.3
d,ℓ-$HSeCH_2CH(NH_2)COOH$	-141	-	-	0.1 M, D_2O, pD 5
H_2Se	-288	0.7 1.0	34 10	1.0 M, D_2O[d]
$(NH_4)_2Se$	-511	-	-	0.5 M, D_2O[d]
$NaSeCH_3$	-330	16.3	43	1.0 M, D_2O[d]
$(CH_3)_3SeI$	258	13.7	32	1.0 M, D_2O, pD 7
$(CH_3)_2Se(Br)CH_2CO_2C_2H_5$	140	1.8 1.7 0.7	32 -1 -30	0.5 M, $CDCl_3$
	298	25 30 21	65 35 8	0.5 M, D_2O, pD 7

Compound	Chemical Shift[a] (ppm)	T_1 (sec)	Temp (°C)	Conditions
H_2SeO_3	1292	3.1 2.1	63 12	1.0 M, D_2O, pH 9.6
	1307	2.8 8.5	63 10	1.0 M, D_2O, pH 1.5
	1281	3.6 2.8	67 10	0.5 M, D_2O, pH 9.8
	1307	10.0 12.5	63 10	0.5 M, D_2O, pH 1.5
Na_2SeO_4	1051	6.5 16.8	61 15	0.5 M, D_2O, pH 6.6
$(CH_3)_2SeO$	819	4.4 8.9	65 30	0.5 M, D_2O, pH 7
$(CH_3)_2NC(Se)NH_2$	147	8.6 10.0	55 32	0.5 M, D_2O, pD 4

[a] Relative to dimethylselenide in $CDCl_3$. The chemical shifts are all temperature dependent and those given are for temperatures between 32 and 42°C.

[b] The exact Larmor frequency for $(CH_3)_2Se$ in $CDCl_3$ is 18.957787 MHz with the ^2H lock frequency (internal $CDCl_3$) at 15.3000000 MHz.

[c] Unless otherwise specified, the samples were 20% (v/v) in the specified solvent.

[d] See text.

field strength, $\Delta\sigma$ is the chemical shift anisotropy and ω_{Se} is the resonance frequency for selenium in radians per second. If one assumes a value of 10^{-10} sec/radian for a correlation time[132] for the ^{77}Se nucleus in dioctylselenide at 50° then from Figure 8 and Eqn [1], one can estimate a value of $\Delta\sigma$ for this system to be 971 ppm. This value is in accord with the value of $\Delta\sigma$ = 1260 ppm determined for a single, crystal of elemental selenium[133]. Hence, for a protein with a correlation time in the range of 10 to 100 nsec, one would expect T_1's in the range of 0.14 to 0.8 sec., respectively. Chemical shift anisotropy contributions to the line width for this hypothetical system can be calculated from Eqn. [2],

$$T_2^{-1}(CSA) = \frac{1}{90}\gamma_{Se}^2 H_o^2 (\Delta\sigma)^2 [8\tau_c + \frac{6\tau_c}{1 + \omega_{Se}^2 \tau^2 c}] \qquad [2]$$

The expected linewidth would be between 5 Hz and 38 Hz for correlation times between 10 and 100 nsec/radian, respectively. If the value of 971 ppm is representative of the CSA for the ^{77}Se nucleus in RSeR' compounds, one can expect that CSA relaxation mechanisms will dominate for molecules undergoing slow molecular motion.

The molecules diisopropylselenide and dibutylselenide have sizes intermediate between those of dimethylselenide and dioctylselenide and their T_1's reflect this transition. The plot for diisopropylselenide (Fig.8) indicates that SR is the dominant mechanism, with the T_1's at equivalent temperatures being marginally longer than for the smaller dimethylselenide. For dibutylselenide the plot displays a pronounced curvature similar to that for dioctylselenide but the T_1's are longer at all temperatures. Clearly, the SR and CSA mechanisms, both of which are contributing here, are less efficient in this compound, a situation that arises because the molecular tumbling is too slow to provide an effective SR relaxation and too fast for an effective CSA relaxation.

For completeness one must also consider the possibility that the changeover in spin-lattice relaxation mechanisms between the dimethyl and dioctylselenides may be due to a difference in either the anisotropy of the chemical shift or the spin rotation coupling constant[105a,130]. However, these parameters should not be radically different for homologous compounds like these dialkyl selenides. The simila. T_1's for dimethyl- and diiso- propylselenide whose resonances are separated by a chemical shift difference of 340 ppm and for which one might expect the differences in these parameters to be the greatest, support the contention that motional arguments provide the most consistent rationale of the data and probable cause of the difference.

The amino acid d, l-selenomethionine, $CH_3SeCH_2CH_2CH(NH_2)COOH$, was studied as a 0.1 M solution in D_2O(pD$\sim$2). The T_1 value of 13±1 sec at 34° falls between that for dimethyl- and dibutylselenide which is in accord with the above data as regards its size relative to the simple dialkyl selenides. The fact that the amino acid will be protonated at pD=2 may increase its effective size as a result of solvation. To study this particular aspect as it relates to the T_1's of dialkyl selenides in aqueous solvents we measured the T_1 of a similar compound methylselenocysteamine, $CH_3SeCH_2CH_2NH_2$, in both $CDCl_3$ and D_2O (pD$\sim$2). The magnitude of the T value in $CDCl_3$ is similar to that of $(CH_3)_2Se$ (Table III) and the temperature dependence of this value implies that SR is the dominant mechanism. The compound appears to be much more mobile in $CDCl_3$ than in D_2O as evidenced by the much longer

T_1's in acidic aqueous solution (Table III). Thus, although the SR mechanism again dominates T_1, solvation in aqueous solution has increased its size and slowed the tumbling of the molecule. The chemical shift of this compound does not reflect this change to the same extent - resonance in D_2O is very similar to that of the amino acid selenomethionine and shifts by only 6 ppm on changing the slovent to $CDCl_3$.

Dialkyl Diselenides

The spin-lattice relaxation of ^{77}Se in the diselenides (Table III) closely resembles that of the dialkylselenides in that spin rotation is the dominant mechanism for the smaller diselenides but CSA relaxation becomes important when the size of the molecule becomes very large, as in didecyl diselenide. These conclusions are based on the temperature dependencies of the T_1's and the lack of a measureable ^1H-^{77}Se NOE for any of the compounds. The T_1's for these compounds are of the same order of magnitude as for diphenyldisenlenide has been previously reported [101]. This is shorter than any value observed in this study; however, without a knowledge of how the samples were prepared for the NMR experiments in the previous study, a meaningful comparison can not be made.

Selenols

Spin Rotation accounts for the relaxation in the alkane selenols (Table III and Figure 9). The T_1's are small relative to the dialkyl selenides and are largely independent of the length of the alkyl chain, suggesting that in the long chain compounds there is enough segmental motion at the end of the chain to provide an efficient SR relaxation in spite of the molecules' long overall correlation times. The absence of a measureable NOE from the directly bound hydrogen in these compounds in in sharp contrast with what is commonly experienced in ^{13}C nmr, where the ^1H-^{13}C DD relaxation is a most important mechanism[134]. This situation reflects not only the much greater efficiency of SR relaxation for ^{77}Se as compared with ^{13}C, but also the inefficiency of ^1H-^{77}Se DD relaxation. If, under conditions of extreme narrowing, the ^{77}Se was relaxed exclusively by the DD process the maximum NOE enhancement of 2.61 (total intensity 3.61) would be observed [135]. The ^1H-^{77}Se DD relaxation is diminished primarily because of the long Se-H bond distances (1.44 A in ethanselenol[136] compared to 1.09A for alkyl C-H bonds) and the inverse sixth power dependence of the DD process on this distance (Eqn.[3])[140].

$$T_1^{-1}(DD) \propto \frac{\gamma_{Se}^2 \gamma_H^2}{r_{SeH}^6} \qquad [3]$$

The lower gyromagnetic ratio for ^{77}Se is also a factor and one may readily calculate from Eqn. [3] that, for a single bound hydrogen, the ratio of T_1 (DD) for ^{77}Se to T_1 (DD) for ^{13}C will be 9.4. Low molecular weight solutes have reorientational correlation times typically in the range of 10^{-11} to 10^{-13} sec/radian[132] and for these conditions a single hydrogen 1.44A away

will give rise to a ^{77}Se T_1 (DD) between 325 and 4270 sec. Thus, because the T_1(DD) in these compounds is on the order of hundreds of seconds it does not compete favorably with the SR mechanism. The correlation times for proteins are much longer[137] (ca. 10^{-8} to 10^{-7} sec/radian) in which case the ^{77}Se T_1(DD) will lie in the range of 0.3 to 2.0 sec. Under these conditions the T_1(DD) should have a greater influence on the T_1(OBS).

The use of $CDCl_3$ as solvent in these studies reduced the tendency of the Se-H protons to undergo intermolecular exchange. Evidence in support of this comes from the highly shielded chemical shift of the selenol protons (δ = 0.6 ppm in $CDCl_3$ relative to TMS) and the sharpness of the lines as well as the retention of the spin-coupling in both the ^{77}Se spectrum and the ^1H spectrum. Ionization of this sort may be expected to take place in aqueous solution, however, and considering that water is the most common biological environment it was deemed of interest to examine some selenols in aqueous solution to observe the effect on T_1.

The simple alkane selenols are insoluble in water but dissolve in basic solution. The T_1 for sodium methylselenolate (1.0 M in D_2O, pD$\sim$10) was found to be 16.3 sec at 43°. The resonance is shifted considerably to higher shielding compared to methaneselenol (-330 ppm relative to dimethyl selenide) and is split into a well resolved quartet due to coupling with the methyl hydrogens (J_{SeH}=6.6 Hz). The compound is apparently completely ionized at pD = 10 with very little chemical exchange, as evidenced by the sharpness of the lines and the shielded chemical shift.

A slightly more complicated situation was encountered with the amino acid selenocysteine, $HSeCH_2CH(NH_2)COOH$, which was prepared from the reduction of selenocystine. A 0.5 M solution of this compound (pH$\sim$5, 50% H_2O/D_2O) exhibited a broad resonance ($\nu_{1/2}$ = 150 Hz) centered at -141 ppm relative to dimethylselenide. Proton-decoupling had no effect on the linewidth which appears to be governed entirely by exchange effects. Unfortunately, the low signal-to-noise ratio and sample limitations prevented an examination of this compound in greater detail.

Instead, we investigated an analogous water soluble selenol, selenocysteamine, $HSeCH_2CH_2NH_2$. The resonance for this compound is very pH dependent. Its pK_a has been determined to be 5.01[128] and the graph of chemical shift versus pH has the form of a typical weak acid titration plot (Fig.10). At low pH the compound exists in the ammonium form 1 while at high pH it is predominantly

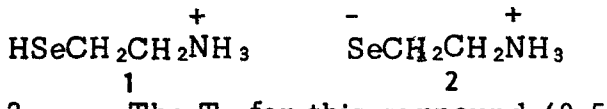

1 2

the Zwitterionic form 2 . The T_1 for this compound (0.5 M in either H_2O or D_2O) was determined to be 7.0 sec at pH 1.4 and 7.1 sec at pH 8.3 which would indicate that the T_1's are the same for both forms 1 and 2. The presence of chemical exchange is again evidenced by the breadth of the lines ($\nu_{1/2}$ = 13 Hz). From the graph it is apparent that the resonance for the RSeH species lies approximately 150 ppm to lower shielding of the RSe^- form and dynamic exchange between these sites could account for the observed decrease T_2, which

broadens the lines to the extent that any ^{1}H-^{77}Se spin coupling is obscured. The ionization process could also lead to an effect on T_2 through scalar coupling relaxation but this mechanism is unlikely to affect T_1 since it may be easily shown that, for the anticipated ^{1}H-^{77}Se one-bond coupling of 40-60 Hz, $T_1(SC)$ will be negligible at the Larmor frequencies of the experiment. Furthermore, the same T_1's in both H_2O and D_2O solutions serve to eliminate the possibility that modulation of the scalar coupling ineraction affects T_1. Finally, it may be noted that the T_1 for this compound demonstrated a marked sensitivity to dissolved oxygen. Prolonged exposure of an aqueous solution to the solution to the atmosphere converts the compound to the diselenide, selenocystamine, although the reaction requires several hours to reach completion [128]. It was found, however, that for solutions in the pH range 4-8, by simply opening the NMR tube to the atmosphere for 2 or 3 minutes, the small amount of oxygen so introduced resulted in a change of T_1 from 7 sec. to 0.1-0.3 sec.

In conjunction with this study we also prepared and investigated aqueous solutions of hydrogen and ammonium selenide. The ammonium selenide solutions were prepared on a vacuum line by co-dissolving hydrogen selenide and a 300% molar excess of anhydrous ammonia in D_2O. The resonance for this sample, at both 0.3 and 1.0 M, occurs at -511 ppm and is the most shielded selenium resonance yet reported. The linewidth is broad ($\nu_{1/2}$ = 37 Hz) no doubt due to an exchange between the species HSe^- and Se^{2-}, although as the shift would imply the predominant form is probably solvated Se^{2-}. Once again the breadth of the resonance led to such low signal-to-noise that an accurate T_1 could not be determined. A crude inversion recovery experiment indicated that the T_1 is relatively long and certainly greater than 5 sec. Attempts to observe a resonance for sodium selenide were fraught with difficulties as this compound is almost totally insoluble in water.

Hydrogen selenide in water primarily H_2Se and small amounts of HSe^-. The sample exhibits a resonance at -288 ppm which may be compared with that reported for neat H_2Se, -226 ppm[97,98]. The T_1's for this sample were found to be 0.9 and 0.7 sec at 10° and 34°, respectively. These values are similar to those for the alkaneselenols and we tentatively attribute the slight decrease in T_1 with an increase in temperature to a SR mechanism, although the temperature dependence is not large and SR and CSA may well both be contributing mechanisms.

Selenonium Compounds

Biologically important, naturally occurring forms of selenium in aqueous solution are selenonium ions, R_3Se^+. Trimethylselenonium ion, for example, is the normal excretory product arising from the ingestion and metabolism of many forms of selenium: it constitutes about 20-50% of the selenium excreted in the urine of rats fed a selenium diet [138]. The resonance for a 1.0 M solution of trimethylselenonium iodide at 32° appears at 258 ppm and the T_1 was found to be 13.7 sec. The material is insoluble in non-aqueous solvents and so to aid the interpretation of the T_1 mechanisms, a more detailed analysis of the selentine, $(CH_3)_2Se(Br)CH_2CO_2C_2H_5$ was undertaken. The T_1's for a 0.5 M solution of this compound in $CDCl_3$ are given in Table III. The values of T_1 are relatively small and increase only slightly over the sixty degree temperature range of the experiment. This behavior, along with the absence of a measureable NOE, can be taken to indicate that CSA is an important me-

chanism, although the temperature invariance suggests that CSA and SR may both be contributing mechanisms for spin-lattice relaxation. The magnitudes of the T_1's in aqueous solution are much greater than in the organic solvent and the increase in T_1 up to 35° followed by a decrease suggests again that both CSA and SR mechanisms are operative here. The greater rate of relaxation in $CDCl_3$ could reflect a lesser degree of mobility in the aqueous solution. However, the resonance position shifts from 140 ppm in $CDCl_3$ to 298 ppm in D_2O which indicates very different environments for the selenium in these two solvents. The selenonium compounds are believed to be completely ionized in aqueous solution[140] but some ion-pairing or even coordination of the bromide is likely to occur in the organic solvent. In the latter case it is, therefore, quite possible that the selenium is relaxing via a SC interaction with the bromine nucleus. There are two magnetic nuclei of bromine, ^{79}Br (I = 3/2, 50.5% nat. abundance) and ^{81}Br(i= 3/2, 49.4% nat. abundance) and at the magnetic field strength of these experiments, their Larmor frequencies are 24.89 and 26.83 MHz, respectively. Both of these nuclei have large electric quadrupole moments and in an asymmetrical environment such as in the selentine, their relaxation times, which are dominated by quadrupolar relaxation, will be on the order of microseconds or less. For a selenium-bromine SC interaction, the ^{77}Se T_1 is given by the expression [105a]

$$\frac{1}{T_1(SC)} = \frac{8\pi^2 J^2}{3} \quad S(S+1) \quad \frac{T_2}{1 + (\Delta\omega)^2 T_2^2} \qquad [4]$$

where J is the selenium-bromine scalar spin coupling constant, S is the bromine nuclear magnetic quantum number, T_2 is the spin-spin relaxation time of the bromine nucleus, and $\Delta\omega$ is the difference in Larmor frequencies for selenium and bromine. Since the value of $(\Delta\omega\ T_2)^2$ may conceivably approach unity in the case of the selentine one can see that for reasonable estimates of J the ^{77}Se T_1(SC) will be a few seconds or less. By analogy with the coupling of ^{77}Se to nuclei such as ^{19}F, ^{31}P and ^{195}Pt, wherein spin-spin coupling constants between 500 and 1600 Hz have been observed,[97,140] one can anticipate a large scalar coupling to ^{79}Br and ^{81}Br. In fact, by the judicious choice of J and T_2 one can reproduce on the basis of a SC relaxation alone the observed ^{77}Se T_1 and T_2 of the selentine in $CDCl_3$. Further experimentation is required to substantiate this argument but at this stage it should be pointed out that SC relaxation is the most plausible explanation for the T_1's of the dialkylselenides.

Oxyacids

Inorganic salts of the oxyacids H_2SeO_3 and H_2SeO_4 are common mineral forms of this element. They are readily absorbed and metabolized by a number of organisms, particularly the selenium accumulator plants, and likely to be present in natural biological extracts [141]. In addition, selenite ion is the most prevalent means by which selenium is administered in animal tests. Thus, an examination of some ^{77}Se T_1's for this class of compounds seemed

warranted.

It is apparent at the outset, given the polyprotic nature of these compounds, that their solutions are unlikely to consist of only one discrete species. Differing degrees of ionization are inevitable and for a given compound the composition of the solution will depend on pH, concentration and temperature. Indeed, a recent study[103] of the pH dependence of the chemical shift of ^{77}Se in aqueous H_2SeO_3 demonstrated the selenium resonance was sensitive to various equilibria and stepwise protonation or deprotonation. In our study, when selenous acid was examined as a function of pH, concentration and temperature, the T_1 was observed to vary sixfold over the range of conditions employed (Table III). The data thus serve to indicate that the T_1 sensitive to the changes in the average environment of the selenous ion, a behavior that parallels that of ^{31}P in phosphate ion [142]. The complexity of the system renders an exact interpretation of the data to be important relaxation mechanisms for the selenite ion. The possibility of a SC mechanism from rapid exchange of the acidic protons is unlikely for reasons presented earlier; it was also verified that the T_1's are virtually the same in both H_2O and D_2O solutions. The temperature dependence of the T_1 value for selenate ion (Table III) resembles that for selenite ion but must be regarded with the same discretion.

A very recent report by Koch, et al.[102] has appeared concerning ^{77}Se FT NMR studies of H_2SeO_3, Na_2SeO_3 and $NaHSeO_3$ and Na_2SeO_4 in H_2O. Their NOE determinations are in complete agreement with this study in that, for H_2SeO_3 and Na_2SeO_4, no NOE was observed. It is interesting to note, however, that for a 4.0 molal solution of Na_2SeO_3, an enhancement of 0.4 was observed. The T_1 measurements reported by Koch, et al.[102] were not obtained under comparable conditions and a direct comparison of the values is not possible. For Na_2SeO_4 (0.5 m, pH = 1-4) a T_1 = 1-.2 sec. was obtained at ambient temperature compared to our values of 6.5 sec (61°C) and 16.8 sec (15°C) using 0.5 M Na_2SeO_4 in D_2O at pH = 6.6 For H_2SeO_3 (4.0 m, pH = 1-4) Koch, et al. report[102] a T_1 value of 1.1 sec (H_2O) and 1.4 sec (D_2O) at ambient temperature. The concentration of H_2SeO_3 in our study was held at either 1.0 M or 0.5 M and for a 1.0 M H_2SeO_3 solution (pH = 1.5 in D_2O) we obtained T_1 values of 2.8 sec (63°C) and 8.5 sec (10°C). Our T_1 values are substantially longer in all H_2SeO_3 samples studied. It is possible that the samples of Koch, et al.[102] contained dissolved oxygen which would shorten the T_1 values and it is also known that at concentrations of ~4M or greater, pyroselenate ions, $Se_2O_5^{-2}$, are formed. Thus, further studies of relaxation times of seleno oxyacids are clearly needed.

The relaxation times of dimethylselenoxide and N,N-dimethylselenourea are included in Table III as further examples of multiply-bonded selenium. It appears that SR is the dominant relaxation mechanism for ^{77}Se in these cases. The generality of this result awaits further experimentation, however, not only because they are both low molecular weight examples of this class but also hydrogen bonding, hydration and enolization are characteristic properties of these functionalities and must be taken into consideration.

Summary and Conclusions

For the molecules studied in this work the spin-rotation and chemical shift anisotropy mechanisms were found to be the most important means of spin-lattice relaxation for the selenium-77 nucleus. The spin-rotation mechanism is very effective in reducing the T_1's of the small molecules but this

mechanism requires very rapid molecular rotation and freedom of movement and quickly becomes attenuated when the selenium atom is part of a large molecule. Solvation and/or aggregation also tends to reduce the efficiency of SR and this accounts for much of the difference in T_1 between organic and aqueous solutions of these selenium compounds. With the exception of perhaps the selenols, this mechanism will likely be unavailable for selenium-containing biopolymers. It was, however, illustrated that in these systems the CSA mechanism, which was evidenced in some of the larger molecules studied herein, will play an important role in determining the T_1.

The dipole-dipole mechanism, which is so beneficial to ^{13}C NMR studies, was found to be totally absent in the compounds studied. Thus, in spite of a potentially large NOE, no enhancement was observed upon proton decoupling. This is a consequence of not only the dominance of the more efficient SR and CSA mechanisms but also the marked inefficiency of the $^{1}H-^{77}Se$ DD mechanism. The long Se-H internuclear distances, even for directly bound protons, account for much of this ineffectiveness. This DD process has a strong dependence on the molecular correlation time, however, and it was shown that in biological macromolecules T_1 (DD) can be on the order of tenths of a second. These considerations indicate that the study of such large molecules by ^{77}Se FT NMR will not be encumbered by exceptionally long recycle times. It may be noted that under the conditions where DD relaxation becomes most effective (i.e., long correlation times) the maximum observable NOE is reduced to 1.1.

Prototropic ionization is a characteristic of several selenium compounds of potential biological interest. It was illustrated that this property has a definite effect on the observed T_1, although secondary in the sense that it does not contribute directly through a scalar coupling mechanism but controls the nature of the species under investigation. It was beyond the scope of the present study to provide a thorough interpretation of the data in terms of all the relevant physicochemical aspects but the data serve adequately to demonstrate the difficulties that may be encountered in analysing the ^{77}Se T_1's of ionizable compounds in aqueous solution. In a more optimistic vein, this type of data could lead to an understanding of the pKa of the ionizable group and information on the pH effects at a catalytic enzyme site containing selenium.[143]

V. Recent Advances in Multinuclear NMR Techniques.

In the course of the research performed under the auspices of this grant over the past two years, we have developed several innovative methods for improving our instrumental capability to do multinuclear nmr experiments. One facet of this research was the development of a multinuclear 18 mm nmr probe. This account has been published (R.A. Byrd and P.D. Ellis, J. Magn. Resonance, 26, 169 (1977), and is briefly summarized below. Two other aspects of our instrumental development research which are as yet unpublished deal with the efficiency of heteronuclear decoupling and the development of a synthesizer based modification of our XL-100 nmr spectrometer. The former has tremendous significance in high field application of multinuclear nmr studies and is described in detail following the 18 mm probe summary. The synthesizer based XL-100 facilitates the multinuclear magnetic resonance studies on any system, and it will be briefly summarized here.

The synthesizer mode of operation was designed to minimize our dependence upon Varian's rf observe related transmitters, local oscillators, and frequency controllers. The age of our spectrometer (8 years) and the intensive use made of it has resulted in an increasing amount of down time associated with these components. Furthermore, the maze of back-plane wiring, the interconnecting of these components, and their associated connections to the receiver and the nuclei-select module is a continuing source of problems. This modification removes our dependence upon these components.

Briefly, this project entailed the use of a General Radio synthesizer (GR-1061) as the observe frequency source for the spectrometer. Of course one must phase-lock the frequency synthesizer to the spectrometer. This was accomplished by building a 15.4/15.3 MHz high spectral purity frequency synthesizer that is phase-locked to the GR-1061. Thus, the output of this minisynthesizer becomes the ^{2}H-master clock for the spectrometer. The local oscillator function is provided by a Hewlett-Packard 230B tuned rf amplifier. A portion of the observe rf is mixed with the 10.7 MHz if available within the spectrometer and the desired mixing product, usually the first upper side band, is selected by the tuned rf amplifier. The low level observe frequency is routed through a network of rf switches, used for gating and phase alteration and then to a broad-band power amplifier, the ENI-3100L. Hence, with this relatively "simple" modification we have removed our dependency on over twenty rf modules and several hundred feet of trouble prone cable. This modification should prove to be very useful for any aging nmr spectrometer. A publication describing the implementation of this approach will be submitted to the Journal of Magnetic Resonance.

A. Development of a Multinuclear 18 mm Probe.

We would like to report the recent development of a probe for 18 mm spinning sample tubes which is capable of operating over the frequency range of 10-100 MHz on a standard Varian XL-100-15 NMR spectrometer. The improvement in signal-to-noise ratio achieved with this probe averages a factor of 3.4 over the standard 12 mm tube throughout the operable frequency range. This

corresponds to a reduction of approximately twelve in the time required for a given experiment. Allerhand and co-workers[144] have previously reported a probe for ^{13}C FT nmr which utilized 20 mm sample tubes. Large sample tube probes are now commercially available for the Bruker WH-180 and the Varian XL-100 (using the new 4418 probe for ^{13}C). In order to facilitate the investigation of various metal nuclides[96] and the more common nmr nuclides, e.g. ^{2}H, ^{13}C, ^{31}P, and ^{19}F, in biological systems, we have developed a single probe aimed at optimizing sensitivity subject to the constraint of minimizing the amount of sample required. This probe requires no additional preamps and is capable of performing any experiment already functional on a standard XL-100 spectrometer, including heteronuclear decoupling of nuclei other than protons, T_1 and T_2 experiments, ^{2}H, ^{1}H, and ^{19}F lock for field stabilization. The sensitivity improvements are measured relative to the identical experiment performed in a 12 mm tube on our modified XL-100, which includes the improvement attained through use of a crystal filter in a manner similar to that reported by Allerhand, et al.[144] . A brief description of the major design features of this probe as well as some examples of its performance are presented here.

The 18 mm probe was constructed using the body of a Varian 4415 probe and was incorporated into our XL-100-15 spectrometer. The probe design uses the cross-coil configuration and interchangeable plug-in inserts for the receiver coil. This feature provides tunability over the frequency range of 10-100 MHz in a manner analogous to the standard Varian XL-100 probes. The standard transmitter matching networks are easily modified such that they tune both our 4412 probe and the 18 mm probe for low power pulses, e.g. 100 W pulses. The standard decoupler matching networks tune both probes without modification. Due to the larger sample tube and the cross-coil configuration, a source of rf pulse power on the order of 1-2 kW is desirable for optimal 90° pulse widths, e.g. 20-30 μsec. We use an ENI Model 3100L side band amplifier, as a replacement for the tuned 100 W amplifier boards in the XL-100, to drive a Heathkit Model SB-220 amplifier. This combination produces approximately 1.6 kW of rf pulse power which is continuously tunable over the range of 7-32 MHz. Also, the Heathkit amplifier is easily modified to deliver 1 kW of rf power up to 40.5 MHz for observation of ^{31}P. We have constructed our own high power matching networks and attain representative 90° pulse widths of 54 μsec for ^{15}N (10.6 G), 22 μsec for ^{13}C (10.6 G), and 30 μsec for ^{31}P (4.8 G), all of which prove to be quite adequate for observation of the respective nuclides at 23.5 kG. In addition, we have constructed the necessary components for a Varian V4420 kilowatt amplifier, in order that we may obtain approximately 900 W of rf pulse power at 94 MHz. The proton rf field strength for decoupling is approximately 2.2 kHz (0.52 G) when the rf power is 9 W. For studies of large biomolecules, 4-6 W is generally sufficient[144] . The probe does not contain an upper dewar assembly for wide range variable temperature control; however, the lower dewar assembly and temperature controller of the standard 4415 probe are still part of our 18 mm probe and allow us to operate over a range of 5-75°C. Thermal stability of ±1°C is routinely achieved.

The spinner used on this probe was constructed in our machines shop and is capable of spinning rates up to 40 Hz with no difficulties. We use precision, thin walled 18 mm o.d. sample tubes supplied by Wilmad Glass Co., Inc., Buene, New Jersey. Teflon vortex-preventing plugs are supplied by the same manufacturer. Sample volume varies from 4-5 ml depending upon the insert and observe frequency employed.

We have encountered no problems with magnetic field inhomogeneity for resonance frequencies of 40 MHz and below. Half-height linewidths equal to those attainable on our 12 mm 4412 probe are routinely achieved with the 18 mm probe. However, for higher frequencies, e.g. ^{19}F at 94 MHz, we have observed approximately 0.5 Hz inhomogeneity broadening.

In Fig. 11 we show the natural-abundance ^{13}C nmr spectrum of 10 mM aqueous sucrose obtained on our 18 mm probe. This spectrum represents about 1 hr of signal accumulation and has a rms S/N ratio of 13:1. We feel it is significant that this spectrum using only 5 ml of sample represents slightly greater S/N than that reported by Allerhand et al.[144] using 12 ml of sample. Consequently, the sensitivity per unit volume, which is a very important criteria when considering nmr investigations of large biomolecules, is considerably higher in our probe.

Figures 12-14 demonstrate the sensitivity improvements attained for ^{19}F, ^{31}P and ^{113}Cd with the 18 mm probe. The ability to observe metal nuclide resonances, e.g. ^{113}Cd, at low concentrations is important if one wishes to use nmr to directly probe the metal binding sites of metalloproteins [82]. The two spectra in Fig. 16 are of 32 mM aqueous $CdCl_2$; however, the lower spectrum was obtained in 1 hr using an 18 mm sample tube whereas the upper spectrum was obtained using identical acquisition parameters, after 12 hrs of accumulation in a 12 mm sample tube. These spectra indicate that detection of ^{113}Cd resonances at concentrations as low as 4 mM in isotopically enriched ^{113}Cd (this equivalent to 32 mM in natural abundance) bound to a protein is quite practical using this probe.

B. Utilization of Chirp Frequency Modulation with 180°-Phase Modulation for Heteronuclear Spin Decoupling.

Modulation of the decoupling rf with psuedo random noise as described by Ernst [145] is now routinely used as a method for broadband heteronuclear spin decoupling. However, there are some drawbacks to this technique. The main problem arises because of the relatively high rf power levels that are necessary to decouple all protons within a sample at 100 MHz, i.e. approximately 10 watts of power. This situation can become critical when superconducting magnets are employed, especially when high salt concentrations are employed with biological samples. For such samples the dielectric heating due to the intense and continuous rf decoupling fields is more efficient at the higher frequencies.

In an attempt to alleviate this experimental problem, Grutzner and Santini[146] have introduced a 180°-phase modulation scheme for heteronuclear spin decoupling. They have shown that under the most common experimental situations that this method is more efficient than noise decoupling. That is, with 10 watts of power a reasonably uniform decoupling can be obtained over a bandwidth of approximately 1.3 kHz. By bandwidth we mean the range of decoupling frequencies that will maintain the signal-to-noise ratio of a given nucleus, e.g. ^{13}C, at a value of at least 1/2 that of the on resonance coherent decoupling signal-to-noise. Although their method does provide more uniform decoupling than noise decoupling, it is clear that the achieved bandwidth is less than ideal for superconducting magnets. Further, the required power levels still do not avoid the rf heating problems.

Clearly what is needed is a decoupling method that has a bandwidth in excess of 2KHz with lower power levels. Further, to have the most efficient utilization of the available power the power spectrum should be uniform throughout the decoupling bandwidth. A modulation scheme that meets this latter requirement is a linear frequency modulation method, i.e. a Chirp[147]. Originally developed for radar applications, Chirp modulation has been shown to produce an rf power distribution which is almost constant as a function of frequency within the bandwidth of the Chirp, followed by a sharp drop off at frequencies outside of the bandwidth [147]. Furthermore, a Chirp pulse has been demonstrated to be useful as a low rf power substitute for the usual high power short pulse excitation of the nuclei in a Fourier transform (FT) nmr experiment [148]. It will be shown here, that Chirp frequency modulation in combination with a 180°-phase modulation scheme is more efficient than phase modulation alone, and further, that one can obtain decoupling bandwidths in excess of 2KHz with significantly lower levels.

The coupled IS two-spin system has been analyzed by Anderson and Freeman [149] for the case when two rf fields are being applied. One of these is the decoupling rf field with its frequency near the Larmor frequency of the S nuclei, and the other, the observing rf field, with its frequency near the Larmor frequency of the I nuclei. In modern FT nmr experiments, the decoupling rf field is generally strong and the observing rf pulse field averaged over its duty cycle is generally weak. The Hamiltonian for this system can, therefore, be separated into two parts **H** and **H'** where the latter, the contribution from the observing rf pulse field, can be treated as a small perturbation. The Hamiltonian is given by the following expressions;

$$\mathbf{H} = -[\omega_I I_z + \omega_S S_z - 2\pi J \underset{\sim}{I} \cdot \underset{\sim}{S} + \gamma_I H_2 (I_X \cos\omega_2 t - I_y \sin\omega_2 t)$$

$$+ \gamma_S H_2 (S_X \cos\omega_2 t - S_y \sin\omega_2 t)] \qquad [5]$$

and

$$\mathbf{H'} = -[\gamma_I H_1 (I_x \cos\omega_1 t - I_y \sin\omega_1 t) + \gamma_S H_1 (S_x \cos\omega_1 t - S_y \sin\omega_1 t)] \qquad [6]$$

where I is the spin of the I nuclei whose Larmor frequency is ω_I; S is the spin of the S nuclei whose Larmor frequency is ω_S; J is the value of the spin-spin coupling in Hz; γ_I and γ_S are the gyromagnetic ratios of the nuclei with spin I and S respectively; $2H_2$ is the magnitude of the decoupling rf field of angular frequency ω_2; $2H_1$ is the magnitude of the observing rf pulse field of angular frequency ω_1.

In order to analyze the effect of amplitude and frequency modulation of the decoupling rf field, we must assume that both H_2 and ω_2 are time dependent. Let us now transform the Hamiltonian to a rotating coordinate system defined by the following transformation:

$$R = \exp[-i\,\omega_2(t)\,(S_z + I_z)t] \qquad [7]$$

The transformed Hamiltonian is given by:

$$\mathbf{H}_R = R\mathbf{H}R^{-1} - i\,R\,\dot{R}^{-1}$$

$$= -(\omega_I - \omega_2(t) - t\dot{\omega}_2(t))I_z - (\omega_S - \omega_2(t) - t\,\dot{\omega}_2(t))S_z$$

$$-2\pi J \underset{\sim}{I} \cdot \underset{\sim}{S} - \gamma_I H_2(t) I_x - \gamma_S H_2(t) S_x \qquad [8]$$

and

$$\mathbf{H'}_R = R\mathbf{H'}R^{-1} = -\{\gamma_I H_1 [I_x \cos(\omega_1 - \omega_2(t))t - I_y \sin(\omega_1 - \omega_2(t))t] +$$

$$+ \gamma_S H_1 [S_x \cos(\omega_1 - \omega_2(t))t - S_y \sin(\omega_1 - \omega_2(t))t]\} \qquad [9]$$

Since we are interested in heteronuclear decoupling, the weak coupling approximation, $|\omega_I - \omega_S| >> 2\pi|J|$, is strictly valid. For such a case, only the diagonal matrix elements of $J\,\underset{\sim}{I} \cdot \underset{\sim}{S}$ are kept in the Hamiltonian [149]. Furthermore, since $\omega_2(t)$ is near ω_S, and assuming that $|t\omega_2(t)| << |\omega_2(t)|$, then $|\omega_I - \omega_2(t) - t\dot{\omega}_2(t)| >> \gamma_I H_2$, so that the term $\gamma_I H_2 I_x$ can be neglected in eq.[8] . Similarly, the terms involving $\gamma_S H_1$ can be neglected in eq. [9]. Equations [8] and[9] can now be rewritten in the following form:

$$\mathbf{H}_R = -\Omega_I(t) I_z - (\Omega_S(t) - 2\pi J I_z) S_z - \gamma_S H_2(t) S_x \qquad [10]$$

and

$$\mathbf{H}_{R'} = -\gamma_I H_1 [I_x \cos(\omega_1 - \omega_2(t))t - I_y \sin(\omega_1 - \omega_2(t))t] \qquad [11]$$

where

$$\Omega_I(t) = \omega_I - \omega_2(t) - t\dot{\omega}_2(t) \qquad [12]$$

and

$$\Omega_S(t) = \omega_S - \omega_2(t) - t\dot{\omega}_2(t) \qquad [13]$$

At this point we no longer need to condider H'_R, since it only involves the sampling of the I magnitization. Hence, we will focus our attention of H_R. In order to bring the Hamiltonian in eq [10] to diagonal form, let us carry out the transformation defined by:

$$V = \exp[i\,\theta(m)\,S_y] \qquad [14]$$

where

$$\theta(m) = \tan^{-1}[\gamma_S H_2(t)/(\Omega_S(t) - 2\pi Jm)] \qquad [15]$$

where m represents the eigenvalue of the operator S_z. Then the transformed Hamiltonian has the following form:

$$\begin{aligned} H_V = &-[(\Omega_S(t) - 2\pi Jm)^2 + (\gamma_S H_2)^2]^{\frac{1}{2}} S_z - \Omega_I(t) I_z \\ &-S_y\{[\gamma_S \dot{H}_2(t)/(\Omega_S(t) - 2\pi Jm)] + [\gamma_S H_2(t)\dot{\Omega}_S(t)/(\Omega_S(t) - 2\pi Jm)^2]\} \\ &[1 + (\gamma_2 H_2/(\Omega_S(t) - 2\pi Jm))^2]^{-1} \end{aligned} \qquad [16]$$

In order to make eq. [16] useful we must now consider explicit forms for $\Omega(t)$.

Chirp decoupling

Chirp modulation corresponds to a frequency modulation using a periodic linear ramp. Thus, for one cycle of the Chirp, the frequency of the decoupling rf field is given by:

$$\omega_2(t) = \omega_o + 2\pi rt \qquad \text{for } -\frac{t_c}{2} \leq t < \frac{t_c}{2} \qquad [17]$$

where $2\pi r$ is the rate of change of the angular frequency, given in rad/sec^2, and t_c is the length of one cycle of the Chirp in seconds. Using eq.[17] and eq.[13], we get the following expression for $\dot{\Omega}_S(t)$:

$$\dot{\Omega}_S(t) = -2\dot{\omega}_2(t) - t\ddot{\omega}_2(t) = -4\pi r \qquad [18]$$

Substituting eq.[18] in eq. [16], and making $H_2(t)$ independent of time, the Hamiltonian with Chirp modulation is the following:

$$H_V = -\Omega_I(t)I_z - [(\Omega_s(t) - 2\pi Jm)^2 + (\gamma_s H_2)^2]^{\frac{1}{2}} S_z$$
$$-S_y\, 4\pi r\gamma_s H_2/[(\Omega_s(t) - 2\pi Jm)^2 + (\gamma_s H_2)^2] \qquad [19]$$

If the coefficient of the S_y term in eq.[19] is small enough, it can be neglected and the diagonalized Hamiltonian would have the form:

$$H_V = -\Omega_I(t)I_z - [(\Omega_s(t) - 2\pi Jm)^2 + (\gamma_s H_2)^2]^{\frac{1}{2}} S_z \qquad [20]$$

In order to find the conditions under which the coefficient of the S_y term in eq.[19] can be neglected, we must carry out another diagonalizing transformation defined by:

$$V_1 = \exp[i\,\theta_1(m)\, S_x] \qquad [21]$$

where

$$\theta_1(m) = \tan^{-1}\{4\pi r\gamma_s H_2/[(\Omega_s(t) - 2\pi Jm)^2 + (\gamma_s H_2)^2]^{3/2}\} \qquad [22]$$

Then, the z component of the transformed Hamiltonian will be:

$$(H_{V_1})_z = -\Omega_I(t)I_z - \{(\Omega_s(t) - 2\pi Jm)^2 + (\gamma_s H_2)^2$$
$$+[(4\pi r/\gamma_s H_2)/(1 + (\Omega_s(t) - 2\pi Jm)^2/(\gamma_s H_2)^2)]^2\}^{\frac{1}{2}} S_z \qquad [23]$$

The eq. [20] will be valid under the following condition:

$$(\gamma_s H_2)^2 >> \{(4\pi r/\gamma_s H_2)/[1 + (\Omega_s(t) - 2\pi Jm)^2/(\gamma_s H_2)^2]\}^2 \qquad [24]$$

however,

$$(4\pi r/\gamma_s H_2)/[1 + (\Omega_s(t) - 2\pi Jm)^2/(\gamma_s H_2)^2] \leq 4\pi r/\gamma_s H_2 \qquad [25]$$

since the minimum value for the expression in brackets in inequality [25] is 1.0. Then inequality [24] will be satisfied if the following inequality is satisfied:

$$(\gamma_s H_2)^2 >> (4\pi r/\gamma_s H_2)^2 \qquad [26]$$

which reduces to:

$$(\gamma_s H_2)^2 >> 4\pi r \qquad [27]$$

The Hamiltonian of eq[19] cannot be completely diagonalized. However, it can be shown that if inequality[27] is valid, then all further transformations will lead to a further reduction in the value of coefficient of the Sy in eq. [19]. Then, under the condition of inequality[27], eq[20] will be valid.

Substituting eq.[16] in eq.[13] and eq.[12] , and the result in eq.[20] , the following expression for the diagonalized Hamiltonian is obtained:

$$H_V = -(\omega_I - \omega_o - 4\pi rt)I_z - A(m)S_z \qquad [28]$$

where

$$A(m) = [(\omega_s - \omega_o - 4\pi rt - 2\pi Jm)^2 + (\gamma_s H_2)^2]^{\frac{1}{2}} \qquad [29]$$

This Hamiltonian has the same form as that for the case when no modulation if applied to the decoupling rf field, as discussed by Anderson and Freeman[149]. The Hamiltonian of eq.[28] then differs from that discussed by Anderson and Freeman by replacement of $\omega_o + 4\pi rt$ for ω_2. The frequencies and intensities of the allowed transitions are identical to those presented in Table I of the Anderson and Freeman paper with $\omega_2 = \omega_o + 4\pi rt$. For $\gamma_s H_2 >> 2\pi J$, with $I = \frac{1}{2}$ and $S = \frac{1}{2}$, there are only two allowed transitions of frequencies:

$$\omega_A = \omega_I + \tfrac{1}{2}[A(\tfrac{1}{2}) - A(-\tfrac{1}{2})] \qquad [30]$$

and

$$\omega_B = \omega_I - [A(\tfrac{1}{2}) - A(-\tfrac{1}{2})] \qquad [31]$$

Then, the residual coupling J_R is given by:

$$J_R = \frac{1}{2\pi}(\omega_A - \omega_B) = \frac{1}{2\pi}[A(\tfrac{1}{2}) - A(-\tfrac{1}{2})] \qquad [32]$$

Replacing the values of $A(\frac{1}{2})$ and $A(=\frac{1}{2})$ from eq.[29] in eq.[32], the residual coupling is given by:

$$J_R = \frac{1}{2\pi}\{[(\omega_s - \omega_o - 4\pi rt - \pi J)^2 + (\gamma_s H_2)^2]^{\frac{1}{2}}$$

$$-[(\omega_s - \omega_o - 4\pi rt + \pi J)^2 + (\gamma_s H_2)^2]^{\frac{1}{2}}\} \qquad [33]$$

The effect of Chirp modulation is similar to chemical exchange. That is, the Chirp leads to a time dependent chemical shift term with eq.[25]. For large enough Chirp frequencies, sharp resonances should be observed. Under such conditions of large Chirp modulation frequencies, the observed residual coupling will be given by the average of the residual coupling over one Chirp cycle. This average coupling will be given by:

$$(J_R)_{av} = \frac{1}{t_c}\int_{-\frac{t_c}{2}}^{\frac{t_c}{2}} J_R(t)\, dt$$

$$= \frac{1}{2\pi t_c}\int_{-\frac{t_c}{2}}^{\frac{t_c}{2}} \{[(\omega_s - \omega_o - 4\pi rt - \pi J)^2 + (\gamma_s H_2)^2]^{\frac{1}{2}} - [(\omega_s - \omega_o - 4\pi rt + \pi J)^2 + (\gamma_s H_2)^2]^{\frac{1}{2}}\}dt \quad [34]$$

Evaluating the integral within eq. [34], the following expression is obtained:

$$(J_R)_{av} = -\frac{1}{16\pi^2 rt_c}\{A\sqrt{A^2 + (\gamma_s H_2)^2} - B\sqrt{B^2 + (\gamma_s H_2)^2} - C\sqrt{C^2 + (\gamma_s H_2)^2} + D\sqrt{D^2 + (\gamma_s H_2)^2} + (\gamma_s H_2)^2 \ln\left[-\frac{(A + \sqrt{A^2 + (\gamma_s H_2)^2})(D + \sqrt{D^2 + (\gamma_s H_2)^2})}{(B + \sqrt{B^2 + (\gamma_s H_2)^2})(C + \sqrt{C^2 + (\gamma_s H_2)^2})}\right]\} \quad [35]$$

where A, B, C and D are given by the following expressions:

$$A = \omega_s - \omega_o - 2\pi rt_c - \pi J$$

$$B = \omega_s - \omega_o + 2\pi rt_c - \pi J$$

$$C = \omega_s - \omega_o - 2\pi rt_c + \pi J$$

$$D = \omega_s - \omega_o + 2\pi rt_c + \pi J$$

Equation [35] will give the residual coupling provided that the Chirp modulation frequency is high enough to give sharp lines and that inequality [27] is satisfied.

Square wave modulated decoupling

This type of modulation consists of a periodic phase reversal, that is, the rf field is being phase modulated by a square wave so the rf decoupling

field is described by:

$$H_2(t) = -H_2 \qquad -t_{c/2} \leq t < O \qquad [36]$$

and

$$H_2(t) = H_2 \qquad O \leq t < t_{c/2} \qquad [37]$$

where t_c is the cycle time in seconds, and H_2 is the magnitude of the rf field. In eq. [16], $\Omega s(t)$ would be independent of time. However, $H_2(t)$ as defined by eqs. [36] and [37] has a discontinuity for t = O, making $H_2(O) = \infty$. Thus, the analysis of Chirp decoupling cannot be used.

The method of analysis of Anderson and Freeman[150], based on a Fourier series expansion of the modulating waveform requires low rf decoupling power and a small modulation index. The function described by eqs. [36] and [37] is certainly not one of small modulation index. Furthermore, we are presently interested in high power rf decoupling fields. Therefore, the analysis provided by Anderson and Freeman[150] cannot be used for analysis of square wave modulated decoupling. Hence, the theoretical conclusions reached by Grutzner and Santini[149] should be considered as only zero-order approximations.

All spectra were obtained on a Varian XL-100-15 NMR spectrometer operating at 25.2 MHz, in the FT mode. The decoupling frequency was generated using a General Radio 1061 frequency synthesizer. The output frequency of the synthesizer was partially controlled by an analog sawtooth function, in order to create the Chirp. The average frequency was measured using a Hewlett Packard 5328A universal counter, and the bandwidth of the modulation set using an oscilloscope to match the extremes of the sawtooth modulating signal to values predetermined using a DC voltage at the modulation port and measuring the output frequency. Phase modulation was accomplished using a double balanced mixer with a square wave at the modulation port. The DC offset of the square wave was adjusted so that the absolute value of the first half of the cycle was equal to that of the second half of the cycle, in order to keep the rf amplitude constant throughout the cycle.

The decoupling coil matching network was tuned to less than 1% reflected power as measured with a Bird Electronic Corp. model 4370 R.F. wattmeter. The effective decoupling rf field was determined from residual splittings in single frequency off resonance experiments, using the following equation:

$$\gamma_s H_2/2\pi = (\Delta\nu^2 - J_R^2/4)^{\frac{1}{2}}(J^2 - J^2_R)^{\frac{1}{2}}/J_R \qquad [38]$$

where $\Delta\nu$ is the difference between the proton resonance frequency and the decoupling frequency in Hz. Equation [38] can be obtained by reformulating the equation obtained for the residual coupling J_R in the AX case from the results given by Anderson and Freeman[149]. For a decoupling power of 10 watts the value of the term $\gamma_S H_2/2\pi$ was determined to be 3300 Hz ± 100 Hz, for a decoupling power of 4 watts it was 2300 Hz ± 100 Hz and for a decoupling power of 2 watts it was 1640 Hz ± 50 Hz.

The sample used contained methyl formate and ~20% of deuterochloroform for locking purposes. The frequency of the center of the formyl proton doublet

was determined to ±1 Hz using single frequency decoupling with 0.5 W of rf power, by changing the decoupling frequency until best decoupling was observed.

Chirp Decoupling

The residual coupling constant for the formyl carbon resonance of methyl formate was measured for various Chirp rates and bandwidths. The results are given in Table IV , along with the results predicted from eq.[35] .

Inequality [27], describes the conditions under which eq.[35] is valid. It can be rewritten in the following form:

$$(\gamma_s H_2/2\pi)^2 >> r/m \qquad [39]$$

All experimental results of Table IV show good agreement with the results of eq.[35] except for the case when the Chirp repetition frequency is 2.0 kHz and the bandwidth is of 10.0 kHz. For this case $r/\pi \cong 6.4 \times 10^6$ sec^{-2} and $(\gamma_s H_2/2\pi)^2 \cong 1.0 \times 10^7$ sec^{-2}, and inequality[39]in not obeyed.

At Chirp repetition frequencies of 1.0 kHz or higher, the observed spectra consisted of sharp lines, that is, the linewidth of the individual lines of the observed doublet were the same as that for on resonance decoupling. At lower Chirp rates, the resonances showed increased broadening especially when the average decoupling frequency was very far from the center of the proton doublet. At very low Chirp frequencies (less than 100 Hz), the ^{13}C spectrum disappeared completely!

None of these results can be considered as giving good decoupling. However, these results are instructive in the understanding of the experiment using Chirp and square wave modulation simultaneously, which will be discussed subsequently. The best Chirp decoupling is observed when using the maximum bandwidth allowed by inequality [39].

Chirp and Square Wave Modulation

It will be shown here that a combination of Chirp and square wave modulation, applied simultaneously to the decoupling rf, decouples over a wider range than with either type of modulation alone. As exploratory experiments, using various ratios of Chirp to square wave frequencies, were carried out it became quickly evident that the ratio of Chirp to square wave frequencies must be four-to-one in order to obtain good decoupling. This can be understood if we look at the Fourier series components of the modulated rf. A spectrum analyzer was used to look at the frequency components of the resultant rf. With Chirp modulation alone, the spectrum consisted of sidebands of equal intensity going out from the center frequency $\nu_o \pm \frac{rt_c}{2}$, where rt_c is the bandwidth of the Chirp. These sidebands were equally separated, the separation being equal to the modulating sawtooth frequency f_c. Outside the range $\nu_o \pm \frac{rt_c}{2}$, the sidebands decreased in intensity very quickly.

With square wave modulation alone, the spectrum consisted of sidebands with frequencies, $\nu_o \pm (2n + 1)f_s$, where f_s is the frequency of the square wave,

and n is a positive integer. Since the Chirp is a frequency modulation, while square wave phase modulation is equivalent to an amplitude modulation, square wave modulation of the Chirp can be analyzed as a modulation of each of the sidebands of the Chirp. Therefore, sidebands will be created at the following frequencies:

$$\nu_o \pm (nf_c \pm (2n' + 1)f_s)$$

where n and n' are positive integers. Unless the ratio of frequencies is an integer, a large number of unequal intensity sidebands will be generated within the bandwidth of the Chirp.

At integral ratios, with $f_s > f_c$, the sideband separation will be that of the Chirp alone. The same will be true if $f_c/f_s = 2$ or $f_c/f_s = 1$. However, with $fc/f_s = 4$, the number of sidebands will be doubled, their intensities being equal to each other within the bandwidth of the Chirp since each line is the sum of the first square wave modulation sideband of one Chirp sideband with the second of another, the third of another and so on. With $f_c/f_s = 3$, the number of sidebands will be 1.5 times the number of sidebands of the Chirp alone for a fixed bandwidth. Careful examination will show that there will be two different intensities of sidebands. One of these corresponds to the sum of the odd square wave modulation sidebands of alternating Chirp sidebands, and the other to the sum of the second sideband of one Chirp sideband with the second of another and all higher even order sidebands of alternating Chirp sidebands.

Any higher ratios of f_c/f_s will create a larger number of sidebands. However, their intensities are not all equal since the first sideband of one Chirp cannot coincide with the second of the next, therefore creating at least two different intensities of sidebands. Analysis of the resulting rf modulated with both Chirp and square wave, using a spectrum analyzer, showed that in fact only with a ratio $f_c/f_s = 4$, the sidebands within the bandwidth of the Chirp were all of the same intensity.

In order to measure the effectiveness of the decoupling methods, the formyl carbon resonance of methyl formate was used. This carbon should represent a worse case due to its large value of J_{CH}, i.e. 226 Hz. The decoupling frequency was changed until the observed carbon linewidth doubled. This would lead to reduction in the signal-to-noise ratio of a factor of two. Hence, the resulting decoupling bandwidth will correspond to the effective 3db points of the power distribution. The linewidth with proton decoupling frequency exactly at the center of the proton doublet was kept at 2.0 Hz. This means that the additional broadening or residual coupling was of 2.0 Hz at the 3db point. The effective decoupling bandwidth for the Chirp/square wave modulation scheme under a variety of Chirp bandwidths and Chirp repetition frequencies are summarized within Tables V (with 10 watts of power) and VI (with 4 watts and 2 watts of power). Further, Figure 15 depicts the results of a Chirp/square wave decoupling experiment when the decoupling power is 10 watts. Figure 16 summarizes the same experiment with only 2 watts of power. Table VII summarizes the effective decoupler bandwidth for decoupling experiments with square wave alone for 10 and 4 watts of decoupling power. Figure 17 graphically demonstrates the decoupling efficiency of the square wave method with 4 watts of decoupling and a square wave rate of 100 Hz.

Table IV
Residual Coupling Constants for Chirp Decoupling

$\Delta\nu$[(a)] (Hz)	Case I		Cases II&III	Case II	Case III	J_R(S.F.)[(c)]
	J_R(calc.)[(b)]	J_R(obs)	J_R(calc.)[(b)]	J_R(obs.)	J_R(obs.)	
100	5.9	5.5	2.2	4.0	2.6	6.7
200	11.8	12.0	4.3	9.0	5.5	12.5
300	17.7	17.3	6.4	12.5	7.5	19.5
500	29.4	31.0	10.8	20.0	11.8	33.3
1000	57.7	60.0	21.5	29.5	20.8	65.3

Case I: Chirp repetition frequency 1000 Hz, Chirp bandwidth 2.0 kHz.
Case II: Chirp repetition frequency 2000 Hz, Chirp bandwidth 10.0 kHz.
Case III: Chirp repetition frequency 1000 Hz, Chirp bandwidth 10.0 kHz.
(a) $\Delta\nu$ = difference between the average decoupling frequency and the center of the proton doublet.
(b) calculated using equation [35]
(c) results for single frequency decoupling
(d) the decoupling power for all these experiments was of 10 watts ($\gamma_s H_2/2\pi$ = 3300 Hz).

Table V
Decoupling Range with Chirp and Square Wave Modulation at 10 W of Decoupling Power

Chirp Freq. (Hz)	Bandwidth (kHz)	Decoupling range[(a)] (Hz)
790	2.0	1600
400	2.5	1700
400	5.0	2100
1600	10.0	poor decoupling
800	10.0	2000
400	10.0	2200

(a) proton frequency range within which the residual coupling or broadening of the observed carbon resonance is less than 2.0 Hz.

Table VI

Decoupling Range with Chirp and Square Wave Modulation

at 4W[(a)] and 2W[(b)] of Decoupling Power.

Chirp (Hz) freq.	(kHz) Bandwidth	(Hz) Decoupling range
400[a]	5.0	1800
400[a]	6.4	2000
400[a]	10.0	2200
800[a]	5.0	poor decoupling
348[b]	8.0	2200
404[b]	8.0	2100
500[b]	8.0	1100

(a) $\gamma_S H_2/2\pi = 3200$ Hz

(b) $\gamma_S H_2/2\pi = 1640$ Hz

Table VII

Decoupling Range with Square Wave Modulation

Square wave rate (Hz)	Decoupling power (watts)	Decoupling range (Hz)
100	10	1400
202	10	1900
100	4	1300
200	4	600
40	2	500
50	2	700
60	2	600

Examination of Tables V and VI shows that best decoupling was obtained when the Chirp bandwidths was of 5.0 kHz or more, and when the Chirp repetition frequency was of about 400 Hz. The reason for good decoupling with large Chirp bandwidths can be understood from the theory and experiments for Chirp modulation alone. Only at large bandwidths was the residual coupling considerably reduced from that expected for single frequency decoupling. Furthermore, if the condition of the inequality depicted by eq [35]is violated, the spectra obtained showed very poor decoupling when both Chirp and square wave modulation was used.

From Table VII the largest decoupling range at 10 W decoupling power was of 1900 Hz for the square wave decoupling. From Table V , the largest decoupling range at 10 W decoupling power for modulation with both Chirp and square wave, is of 2.2 kHz, which is roughly a factor of 1.2 larger than the best decoupler with square wave modulation alone.

From a comparison of Tables V and VII for Chirp rates of 400 Hz, the results for 4 W of power are almost the same as the results at a decoupling power of 10 W. However, with a Chirp bandwidth of 5.0 kHz, 4 W of decoupling power and a Chirp repetition frequency of 800 Hz, conditions which do not violate inequality [39], very poor decoupling was observed. At this Chirp repetition frequency, the square wave rate, which is fixed by the four-to-one ratio, is of 200 Hz. When square wave modulation alone was used, at a decoupling power of 4W and rate of 200 Hz, the effective decoupling bandwidth was only 600 Hz. This poor decoupling with square wave modulation alone may be the reason for the poor decoupling observed when both Chirp and square wave modulation is used.

At 4 W of decoupling power, the largest decoupling range for modulation with both Chirp and square wave is of 2200 Hz. The largest decoupling range with square wave modulation alone, at this power level, was of 1300 Hz. Thus, at 4 W of decoupling power, the decoupling range has been nearly doubled when both Chirp and square wave modulation is used. Furthermore, at 2 W of decoupling power, the largest decoupling range with Chirp and Square wave was of 2000 Hz while the largest range with square wave alone was of only 700 Hz. At this power level the decoupling range with Chirp and square wave modulation is a factor of three larger than with square wave modulation alone. From these results, it would be anticipated that the same decoupling bandwidth could be achieved on systems not employing a Faraday shield with only 1 to 2 watts of decoupling power.

Modification of commercial nmr spectrometers for decoupling with Chirp and 180°-phase modulation.

Generation of this decoupling scheme was done using a swept frequency synthesizer as described in the experimental section. It would be more useful, however, to use a simpler, less expensive method of generating the Chirp. This can be done using a voltage controlled oscillator (VCO) with a phase lock loop circuit which is locked to the 1.0 MHz reference used as a frequency standard in many nmr spectrometers. With a low pass filter in the control loop the modulation can be introduced as an additional voltage to the frequency control input of the VCO. The loop circuit maintains the average frequency at a fixed value.

Such a circuit was developed here, as shown in Fig. 18 using SN 74324 for the VCO. The average frequency in this case is 5.0 MHz. For phase detection this frequency is divided by a factor of 100, while the 1.0 MHz reference is divided by a factor of 20. The 50 kHz signals go to the phase detector (MC 4044). The output of the phase detector goes through an integrator and a filter to generate the control voltage for the VCO. A sawtooth wave is introduced at this point through a summing network. Fig. 19 shows the circuit used to generate the sawtooth wave and square wave, at exactly 1/4 of the frequency of the sawtooth wave, to be used for the 180°-phase modulation.

While a frequency of 500 kHz could have been used for the phase detection, it was found experimentally that 50 kHz provides a more stable output frequency. Care must also be taken to isolate the VCO from the control circuits.

The 5.0 MHz output of this oscillator is mixed with a fixed frequency from the original decoupler. The output is then 180°-phase modulated and filtered to remove the component at a frequency 10.0 MHz from the desired decoupling frequency. The output is then amplified in the normal way. Additional amplification may be needed at this stage.

The output of the 5.0 MHz oscillator was analyzed through a spectrum analyzer. The error in the frequency of the modulated oscillator was of about ±50 Hz. This uncertainty represents a reduction of about 100 Hz in the decoupling range, which is a small reduction for a decoupling range of 2.0 - 2.2 kHz. This system operated satisfactorily and is now routinely used in our laboratory.

A Non-trivial Application of the Modification

As an illustration of the utility of this method, the ^{19}F decoupled ^{13}C spectrum of $(CH_3)_2BC_2F_3$ was obtained and is shown in Fig. 22 . The fluorine spectrum of this compound consists of one multiplet at δ-79.6 ppm (relative to $CFCl_3$) another at δ -94.6 ppm and a third one at δ-184.5 ppm [151] . At 94.1 MHz, the ^{19}F spectrum is spread over a range of nearly 10.0 kHz. However, the two multiplets to higher shielding are separated by 1.4 kHz, which is certainly within the decoupling range of 2.2 kHz when Chirp and 180° phase alternation are used at 4 watts of decoupling power under optimum Chirp rate and bandwidth (2 watts would also be sufficient). In order to also decouple the deshielded resonance, a final 100% amplitude modulation with a sine wave of 4.58 kHz was used. In this example 8 watts of rf power were used so that there were 4 watts of decoupling power for each band (a reduction of the power by a factor of 2 would have been sufficient to decouple all fluorines. The Chirp rate used was 500 Hz and the Chirp bandwidth was 8 kHz.

As Fig. 20 illustrates, there are two broad resonances at 6.8 ppm and 136.4 ppm, and one sharp resonance at 162.6 ppm relative to TMS. The resonance at 136.4 ppm can be assigned to the perfluorovinyl carbon bonded to boron. It is directly bonded to boron, and is broadened by interaction with the nuclear quadrupole of the boron nucleus. The resonance at 6.8 ppm can be assigned to the methyl carbons. It is broad due to boron coupling, quadrupolar broadening and coupling to the protons of the methyl group.

Perfluoromethylcyclohexane has a similar spread of ^{19}F resonances [152] . There are three groups of resonances. Two separated from each other by 1.4 kHz and the third 4.9 kHz away from the average of the first two as observed at 84.64 MHz. Complete decoupling of all fluorine resonances was accomplished by Ovenall and Chang [152] using noise modulation with a 100% amplitude modulation

using a sine wave, in addition to the noise modulated output of a second synthesizer. The total power used in these experiments as they have been reported was of 30 watts! Block-Siegert shifts were also observed in those experiments and were of the order of 4 kHz. Our present experiments for $(CH_3)_2B\text{-}C_2F_3$, using only 8 watts of decoupling power, is estimated to have Block-Siegert shifts of <1 kHz.

VI. Summary

During the course of this research project we have investigated, in detail, the ^{113}Cd nmr of three metalloproteins; con-A, carboxypeptidase-A, and bovine superoxide dismutase. Although we were not the first research group to publish on the importance of this particular approach, it is evident from the progress report that our studies are not merely reporting chemical shifts of new species. But rather, our work on all three systems is providing new and significant information to the biochemist with respect to the fundamental mode of action of these proteins and the interelationship between the function of the proteins and the metal associated with it.

Furthermore, we have been involved in an intensive effort to find other nmr active spin 1/2 nuclei that could be exploited in biological applications. Such a nucleus is ^{77}Se. Although extensive chemical shift information is available for ^{77}Se, little, if any, relaxation time information was available before our efforts in this area of research. The spin lattice relaxation time is a parameter of paramount importance in determining the overall utility of a given nucleus in a biological application, that is, it is intimately related to the signal-to-noise per unit time. To this end, we have carried out an extensive study on the nature of the specific mechanism(s) of spin lattice relaxation and the corresponding values of T_1 . The systems that we have investigated to date are; organoselenium compounds, RSeR', selenols RSeH, diselenides, RSeSeR', selenates, SeO_4^{-2} , and selenocysteamine. As a result of this research it is clear that ^{77}Se nmr may be very useful to studying active site sulfhydryls in sulfhydryl proteins.

In order to pursue these research topics in the most efficient fashion, it was necessary for us to develop some novel modifications of our nmr instrumentation. One of these is a unique nmr probe, capable of spinning 18 mm nmr tubes, decoupling at any frequency, and observing any nmr active nucleus. Further, the most important design parameter was signal-to-noise on a 5 ml coil volume. The net result is that the probe leads to a timesaving of approximately a factor of twelve over conventional 12 mm nmr systems.

Finally, we have solved a rather severe experimental problem in nmr spectroscopy. That is, the required power levels for efficient broad band hetero-nuclear spin decoupling. This problem reaches critical proportions when examining biological systems, e.g. proteins in high salt concentrations, on nmr spectrometers employing superconducting magnets. The basic approach employs a linear frequency modulation scheme, i.e. a "Chirp" followed by a 180° -phase modulation of the "Chirp". The relative rates of "Chirp" to 180° -phase modulation must be kept in a 4 to 1 ratio for the method to succeed. The net results is that uniform decoupling can be achieved over a range in excess of 2kHz with only 2 watts of power. For those systems not employing a Faraday shield, efficient decoupling can be affected with power levels between 1 and 2 watts.

VII. References

1. B. Bergersson, R.E. Carter, and T. Drakenberg, J. Magn. Resonance, 28, 299 (1977).

2. I.M. Armitage, R.T. Pajer, A.J.M.S. Miterkamp, J.F. Chleborski, and J.E. Coleman, J. Amer. Chem. Soc., 98, 5710 (1976).

3. J.L. Sudmeir and S.J. Bell , ibid, 99, 4499 (1977).

4. J.F. Chlebowski, I.M. Armitage and J.E. Coleman, J. Biol. Chem. 252, 7053 (1977).

5. D.B. Bailey, A.D. Cardin, P.D. Ellis, W.D. Behnke, J. Amer. Chem. Soc., 100, 5263 (1978).

6. A.R. Palmer, P.D. Ellis, W.D. Behnke, D.B. Bailey, A.D. Cardin, submitted to J. Amer. Chem. Soc.

7. A.R. Palmer, D.B. Bailey, P.D. Ellis, W.D. Behnke, and A.D. Cardin, submitted to Proc. Nat. Acad. Sci.

8. G.L. Nicholson, Int. Rev. Cytol., 39, 90 (1974).

9. T.K. Choudhary, and S.K. Weiss, (eds), Adv. Exp. Med. Biol., 55 (1974).

10. Concanavalin A as a Tool, ed. H. Bittiger, (John Wiley and Sons, New York, New York (1977).

11. M. Inbar, and Z. Sachs, Proc. Nat. Acad. Sci., U.S.A., 67, 1418(1969).

12. S.D. Douglas, R.M. Kamin, and H.H. Fridenberg, J. Immunol., 103, 1185-1195 (1969).

13. L. Stavy, A.J. Treves, and M. Feldman, Nature, 232, 56 (1971).

14. M.A. Leon, and H.J. Schwartz, Proc. Exp. Biol. Med., 131, 735 (1969).

15. I.J. Goldstein, C.E. Hollerman, and E.E. Smith, Biochemistry, 4, 876 (1965).

16. G.M. Edelman, B.A. Cunningham, G.N. Reeke Jr., J.W. Becker, M.J. Waxdal, and J.S. Wang, Proc. Nat. Acad. Sci. U.S.A., 69, 2580 (1972).

17. K.D. Hardman, and C.L.F. Ainsworth,Biochemistry, 11, 4910-19 (1972).

18. J.W. Becker, G.N. Reeke Jr., J.L. Wang, B.A. Cunningham, and G.M. Edleman, J. Biol. Chem., 250, 1513 (1975).

19. G.N. Reeke, Jr., J.W. Becker, and G.M. Edelman, J. Biol. Chem., 1525 (1975).

20. K. D. Hardman Adv. Exp. Med. Biol., 40, 103 (1973).

21. J.W. Becker, G.N. Reeke, Jr., B.Z. Cunningham, and G.M. Edelman, Nature, 259, 406 (1976).

22. C. Nicolav, A.J. Kalb and J. Yariv, Biochem. Biophys. Acta, 194,71 (1969).

23. G.M. Alter, E.R. Pandolfino, D.J. Christie, and J.A. Magnuson, Biochemistry, 16, 4034 (1977).

24. J.J. Grimaldi and B.D. Sykes, J. Biol. Chem., 250, 1618 (1975).

25. C.F. Brewer, H. Sternlicht, D.M. Marcus, and A.P. Grollman, Proc. Nat. Acad. Sci., U.S.A., 70, 1007 (1973).

26. C.F. Brewer, H. Sternlicht, D.M. Marcus and A.P. Grollman, Biochemistry, 12 4448 (1973).

27. J.J. Villafranca and R.E. Viola, Arch. Biochem. Biophys., 160, 465 (1974).

28. G.M. Alter and J.A. Magnuson, Biochemistry, 13, 4038 (1974).

29. B.H. Barber and J.P. Carver, J. Biol. Chem., 248, 3353 (1973).

30. J.J.Grimaldi and B.D. Sykes, J.Biol. Chem., 250, 1618 (1975).

31. E. Meirovitch and A.J. Kalb, Biochem. Biophys. Acta, 303, 258 (1972).

32. A.D. Sherry and G.L. Cottam, Arch. Biochem. Biophys., 156, 665 (1973).

33. B.H. Barber and J.P. Carver, Can. J. Biochem., 53,371 (1974).

34. R.D. Brown, III, C.F. Brewer and S.H. Koenig,Biochem. Biophys. Res. Commun., 43, 660 (1977).

35. W.D. McCubbin, K. Oikawa and C.M. Kay, Biochem. Biophys. Res. Commun., 43, 660 (1971).

36. A.J. Kalb and A. Lustig, Biochem. Biophys. Acta, 168, 366 (1968).

37. W.D. McCubbin and C.M. Kay, Biochem. Biophys. Res. Commun., 44, 101 (1971).

38. A.J. Kalb and A. Levitzki, Biochem. J., 109, 669 (1968).

39. M. Shoham, A.J. Kalb and I. Pecht, Biochemistry, 12, 1914 (1973).

40. A.D. Sherry, A.D. Newman and C.G. Gutz, Biochemistry, 14, 2191 (1973).

41. C.S. Peters, R. Codrington, H.C. Walsh and P.D. Ellis, J. Mgn. Reson., 11, 431 (1973).

42. D.D. Traficante, J.A. Simms, and M. Mulcay, J. Magn. Reson., 15 484 (1974).

43. A.G. Marshall, L.D. Hall, M. Hatton and J. Gallos, J. Magn. Reson., 13, 392 (1974).

44. R.A. Byrd and P.D. Ellis, J. Magn. Reson., 26, 169 (1977).

45. R.A. Byrd, D. Sinclair, A.R. Garber and P.D. Ellis, manuscript in preparation.

46. R.J. Kostelnik, and A.A. Bothner-By, J. Magn. Resonance, 14, 141 (1974).

47. G.E. Maciel and M. Borzo, J. Chem. Soc. Chem. Commun., 394 (1973).

48. A.D. Cardin, P.D. Ellis, J.D. Odom, and J.W. Howard, J. Am. Chem. Soc., 97, 1672 (1975).

49. R.A. Haberkon, L. Quz, W.O. Gillum, R.H. Holm, C.S. Zin and R.L. Lord, Inorg. Chem., 15, 240 (1976).

50. B. Birgersson, R.F. Carter and T. Drakenberg, J. Magn. Reson. 28, 299 (1977).

51. B.B.L. Agrawal and I.J. Goldstein, Biochem. Biophys. Acta, 147, 262 (1967).

52. J. Yariz, A.J. Kalb and A. Levitzke, Biochem. Biophys. Acta, 165, 303 (1968).

53. J.L. Wang, B.A. Cunningham and G.M. Edelman, Proc. Nat. Acad. Sci., U.S.A. 70, 1625 (1971).

54. International Union of Pure and Applied Chemistry, Pure Appl. Chem., 45, 219 (1976).

55. R.D. Brown, personal communication.

56. C.E. Richardson and W.D. Behnke, J. Mol. Biol., 102, 441 (1976).

57. D.B. Bailey, P.D. Ellis, and J.A. Fee, submitted to Proc. Nat. Acad. Sci. (U.S.A.).

58. A.M.Michelson, J.M.McCord, and I. Fridovich (Eds.) "Superoxide and Superoxide Dismutases" Academic Press, London, (1977).

59. J.A. Fee, A.M. Michelson, J.M. McCord, and I. Fridovich (Eds.) "Superoxide and Superoxide Dismutases" Academic Press, London, 173 (1977).

60. J.S.Richardson, K.A. Thomas, Bitt. Rubin, and D.C. Richardson, Proc. Nat. Acad. Sci., 72, 1349 (1975).

61. J.S. Richardosn, K.A. Thomas, and D.C. Richardson, Biochem, Biophys. Res. Commun, 63, 986 (1975).

62 B.P. Gaber, R.D. Brown, S.H. Koenig, and J.A. Fee Biochim. Biophys. Acta, 271, 1 (1972).

63. D. Klug-Roth, I. Fridovich, and J. Rubin, J. Am. Chem. Soc., 95, 2786 (1973).

64. E.M. Fielder, P.B. Roberts, R.D. Bray, D.J. Lowe, G.N.Mautner, G. Rotrlio, and L. Calabrese, Biochem. J. 139, 49 (1974).

65. J.A. Fee, and P.D. DiCorleto, Biochemisty, 12, 4893 (1973).

66. T.H. Moss and J.A. Fee ,Biochem. Biophys. Res. Commun. 66, 799 (1975).

67. M.E. McAdam, E.M.Fielder, F. Lavelle, L. Calabrese, D. Cocco, and G. Rotrilio, Biochem. J. 167, 271 (1977).

68. W.E. Blumberg, J. Peisach, P. Eisenberger, and J.A. Fee, Biochemistry, 17, 1842 (1978).

69. J.M.McCord and I. Fridovich, J.Biol. Chem. 244, 6049 (1969).

70. J.A. Fee, J. Biol. Chem., 248, 4229 (1973).

71. K.M. Beem, W.E. Rich, and K.V. Rajagopalan, J. Biol. Chem. 249, 7298 (1974).

72. O.H. Lowry, N.J. Rosebrough, A.L. Farr, and R.J. Randcoll, J. Biol. Chem., 193, 265 (1951).

73. A.R. Garber, and P.D. Ellis, manuscript in preparation.

74. R.A. Byrd and P.D. Ellis, J. Magn. Reson., 26, 169 (1977).

75. R. Freeman and H.E.W. Hill, J. Chem. Phys., 54, 3367 (1971).

76. T.C. Farrar and E.D. Becker "Pulse and Fourier Transform NMR" Acadmice Press, New York (1971).

77. "Interatomic Distances Supplement", Special Publication No. 18, Chemical Society, London (1965).

78. Reference 19 p 55.

79. a. D.B. Bailey, P.D. Ellis, A.D. Cardin, and W.D. Behnke, J. Amer. Chem. Soc., 100, 5263;bA.R. Palmer, P.D. Ellis, W.D. Behnke, D.B. Bailey, and A.D. Cardin, submitted to J. Amer. Chem. Soc.

80. G.M. Edelman, B.A. Cunningham, G.M. Reeke, Jr., J.W. Becker, M.J. Waxdal, and J.L. Wang,Proc. Nat. Acad. Sci., 69, 2580 (1972).

81. G.N. Reeke, J.A. Hartsuck, M.L. Ludwig, F.A. Quiocho, R.A. Steitz, and W.N. Kipscomb, Proc. Nat. Acad. Sci. (U.S.A.), 58, 2220 (1967).

82. J.L. Sudmeier and S.J. Bell, J. Am. Chem. Soc., 99, 4499(1977).

83. I.M. Armitage, A.J. M.Schoot-Uiterhamp, J.F. Chlebowski, and J.E. Coleman, J. Magn. Res. 29, 375 (1978).

84. I.M. Armitage, R.T. Pajer, A.J.M.Schoot Uiterkamp, J.F. Chlebowski, and J.E. Coleman, J. Am. Chem. Soc., 98, 5710 (1976).

85. J.L. Sudmeier, personal communication.

86. K.K.Kannan B. Nostrano, K. Fridborh, S. Lougren, A. Ohilss and M. Petef, Proc. Nat. Acad. U.S.A. 72, 51 (1975).

87. J.A. Fee and R.G. Briggs, Biochim. Biophys. Acta 400, 439 (1975).

88. J.A. Fee and R.L. Ward, Biochem. Biophys. Res. Commun. 71, 427 (1976).

89. E.K. Hodgson and I. Fridovich, Biochemistry, 14, 5294 (1975).

90. J. Rabani, D. Klug-Roth, and J. Lilie, J. Phys. Chem., 77, 1169 (1973).

91. An excellent review of carboxyepetidase-A and its physical and chemical properties has been published by M.L. Ludwig and W.N. Lipscomb, in Inorganic Biochemistry, edited by G.I. Eichhorn, Elsevier, Chapter 15, (1973).

92. B.L. Vallee and H. Neurath, J. Biol. Chem., 217, 253 (1955).

93. G.N. Reeke, J.A. Hartsuck, M.L. Ludwig, F.A. Quiocho, T.A. Stietz and W.N. Lipscomb, Proc. Nat. Acad. Sci. U.S.A., 58, 2220,(1967);W.N. Lipscomb J.A. Hartsuck, G.N.Reeke, F.A. Quiocho, Brokhaven Symp. Biol., 21, 24 (1968); W.N. Lipscomb, G.N. Reeke, J.A. Hartsuck, F.A. Quiocho, and P.H. Bethge, Phil Trans Royal Soc., B257, 177 (1970).

94. R. Breslow and D.L. Wernick, Proc. Natl. Acad. Sci. U.S.A., 74, 1303 (1977).

95. L.D. Byers and R. Wolfenden, Biochemistry, 12, 2070 (1973).

96.(a)D.L. Klayman and W.H.H. Gunther, Ed., "Organic Selenium Compounds, Their Chemistry and Biology", Wiley-Interscience, New York, 1973.

(b)R.A. Zingaro and W.C. Cooper, Ed., "Selenium", Van Nostrand-Reinhold, New York, 1974.

97.(a)A.D. Cardin, P.D. Ellis, J.D. Odom and J.W. Howard, J. Am. Chem. Soc., 97, 1672 (1975).

(b)M.A. Sens, N.K. Wilson, P.D. Ellis and J.D. Odom, J. Magn. Resonance, 19, 323 (1975).

(c) W.H. Dawson and J.D. Odom, J. Am. Chem. Soc., 99, 8352 (1977).

(d) D.B. Bailey, P.D. Ellis, A.D. Cardin and W.D. Behnke, J. Am. Chem. Soc., 100, 5263 (1978).

98. T. Birchall, R.J. Gillespie and S.L. Vekris, Can. J. Chem., 43, 1672 (1965).

99. W.M. McFarlane and R.J. Wood, J. Chem. Soc., A, 1397 (1972).

100.(a)S. Gronowitz, I. Johnson and A.B. Hornfedlt, Chem. Scr., 3, 94 (1973).

(b)ibid., 8,8 (1975).

(c) A. Fredga, S. Gronowitz and A.B. Hornfeldt, ibid., 8, 15 (1975).

(d)S. Gronowitz, A. Konar and A.-B. Hornfeldt, Org. Magn. Resonance, 9, 213 (1977).

101. W-H. Pan and J.P. Fackler, J. Am. Chem. Soc., 100, 5783 (1978).

102. O.A. Gansow, W.D. Vernon and J.J.Dechter, J. Magn. Resonance, 32, 19 (1978).

103. W. Koch, O. Lutz and A. Noelle, Z. Naturforsch, 33a, 1025 (1978).

104. H. Kolshorn and H. Meier, J. Chem. Research (s), 338 (1977).

105.(a)J.R. Lyerla, Jr. and D.M. Grant in "International Review of Science. Phys. Chem. Series", C.A. McDowell, Ed., Medical and Technical Publishing Co., Bol. 4, Chap. 5 (1972).

(b)D. Shaw, "Fourier Transform NMR Spectroscopy", Elsevier, New York, (1976).

106.(a)A. Abragam, "Principles of Nuclear Magnetism", Oxford University Press, London, 1961.

(b) E. Oldfield and A. Allerhand, J. Biol. Chem., 250, 6403 (1975).

(c)E. Oldfield, R.S. Norton and A. Allerhand, ibid., 250,6468 (1975).

(d)W.E. Hull and B.D. Sykes, J. Mol. Biol., 98, 121 (1975).

107. Personal communication,Varian Associates Applications Laboratory.

108.(a)R.L. Vold, J.S.Waugh, M.P.Klein and D.E. Phelps,J. Chem. Phys., 48, 3831(1968).

(b)R. Freeman and H.D. W. Hill, ibid., 51, 3140 (1969).

109(a)J.L.Markley, W.J. Horsley and M.P.Klein, J. Chem. Phys., 55, 3604 (1971).

(b)G.C.McDonald and J.S. Leigh, J. Magn, Reson., 9, 358 (1973).

110. J.H. Noggle and R.E. Schirmer, "The Nuclear Overhauser Effect. Chemical Applications" ,Academic Press, New York, 1971.

111.(a)M. Sass and D. Ziessow, J. Magn. Reson.,25, 263(1977).

(b)D. Canet, ibid., 23, 361(1976).

112. The choice of dimethylselenide as the ^{77}Se chemical shift reference conforms with that of McFarlane and Wood.[99] The other common standard is selenophene[160]which is reported to be 617 ppm deshielded relative to demethylselenide. [101]

113. G. Ayrey, D. Barnard and D.T. Woodbridge, J. Chem. Soc., 2089 (1962).

114. M.L. Bird and F. Challenger, J. Chem. Soc., 570 (1942).

115. G. Cohen, C.M Murphy, J.G. O'Rear, H. Rauner and W.A. Zisman, ind. Eng. Chem., 45, 1766 (1953).

116. L. Brandsma and H.E. Wijers, Rec. Trav. Chim., 82,68 (1963).

117. G.E. Coates, J. Chem. Soc., 2839 (1953).

118. W.H.H. Gunther, J. Org. Chem., 31, 1202 (1966).

119. J. von Bruan, W. Teuffert and K. Weissbach, Liebigs Ann. Chem., 472, 121 (1929).

120. H.J. Backer and W. van Dam, Rec. Trav. Chim., 54, 531 (1935).

121. T. Zincke and K. Fries, Liebigs Ann. Chem., 334, 342 (1904).

122. D.L. Klayman and T.S. Griffin, J. Am. Chem. Soc., 95, 197 (1973).

123. P.G. Foster, Org. Syn., Coll. Vol. 3, 771 (1955).

124. E. Rebane, Arkiv. Kemi, 25, 363 (1966).

125. I.G.M. Campbell, R.C. Cookson and M.B. Hocking, J. Chem. Soc., 2184 (1965).

126. R. Paetzold and G. Bochmann, Z. Anorg. Allg. Chem., 360, 293 (1968).

127. D.L. Klayman, J. Org. Chem., 30, 2454 (1965).

128. H. Tanaka, H. Sakurai and A. Yokoyama, Chem. Pharm. Bull. (Tokyo) 18, 1015 (1970).

129. Reference 110 pages 34-37.

130.(a)C. Deverell, Mol. Phys., 18, 319 (1970).

(b)A.A. Maryott, T.C. Farrar and M.S. Molmberg, J. Chem. Phys., 54, 64 (1971).

131(a)S.O. Chan and L.W. Reeves, J. Am. Chem. Soc., 96, 404 (1974).

(b)M. Bacon and L.W. Reeves, ibid., 95, 272 (1973).

(c)J.F. Hinton and R.W. Briggs, J. MAgn. Reson., 25, 379 (1977).

132.(a)Y.K.Levine, N.J.M.Birdsall, A.G. Lee, J.C. Metcalfe, P. Parrington and G.C.K. Roberts, J. Chem. Phys., 60, 2890 (1974).

133.(a)A. Koma and S. Tanaka, Solid State Commun., 10, 823 (1972).

(b)A. Koma, Stat. Sol., 57b, 299 (1973).

(c)M. Mehring, "NMR Basic Principles and Progress:, R. Diehl, E.Fluck, and R. Kosfeld, eds., Springer Verlag, New York, 1976,Vol. 11, p. 191.

134. D. Doddrell, V. Glushko and A. Allerhand, J. Chem. Phys., 56, 3683 (1972).

135.(a)K.F. Kuhlmann and D.M. Grant, J. Am. Chem. Soc., 90, 7355 (1968).

(b)K.F. Kuhlmann, D.M. Grant and R.K. Harris, J. Chem. Phys., 52, 3439 (1970).

136. J.R. Durig and W.E. Bucy, J. Mol. Spectrosc., 64, 474 (1977).

137(a)B.D. Sykes, Biochem. Biophys. Research Commun., 39, 508 (1970).

(b)B.D. Sykes, P.G. Schmidt and G.R. Stork, J. Biol. Chem., 245, 1180 (1970).

138.(a)J.L. Byard, Arch. Biochem. Biophys., 130, 556 (1969).

(b) I.S. Palmer, D.D. Fisher, A.W. Halverson and O.E. Olson, Biochem. Biophys. Acta, 177, 336 (1969).

(c)I.S. Palmer, R.P. Bonsalus, A.W. Halverson and O.E. Olson, ibid, 208, 260 (1970).

139. Reference 1(a) pages 239-240.

140.(a)D.W. W. Anderson, E.A.V. Ebsworth, G.D. Meikle and D.W.H. Rankin, Mol. Phys., 25, 381 (1973).

(b)W.M. McFarlane, Chem. Commun., 755 (1968).

141. Reference 1(a) Chaps. XIII A-E.

142. T. Glonek, P.J. Wang and J.R. VanWazer, J. Am. Chem. Soc., 98, 7968 (1976).

143. Ref. 15, p. 58.

144. A. Allerhand, R.F. Childers, and E. Oldfield, J. Magn. Resonance, 11, 272 and references cited therein (1973).

145. R.R. Ernst, J. Chem. Phys., 45, 3845 (1966).

146. J.B. Grutzner and R.E. Santini, J. Magn. Res., 19, 173 (1975).

147. J.R. Kluander, A.C. Price, S. Darlington and W.J. Albersheim, Bell System Technical Journal, XXXIX (4), 746 (1960).

148. J. Delayre and J.J. Dunand, Abstracts 17th Experimental NMR Conference.

149. R. Freeman and W.A. Anderson, J. Chem. Phys., 37, 85 (1962).

150. R. Freeman and W.A. Anderson, J. Chem Phys., 42, 1199 (1965).

151. E.J. Stampf and J.D. Odom, Journal of Organometallic Chemistry, 108, 1 (1976).

152. D.W. Ovenall and J.J. Chang, J. Magn. Res., 25, 361 (1977).

VIII. Figures and Figure Captions

Figure Captions

Figure 1

(a) Cadmium-113 nmr spectrum of Concanavalin A to which 2.2 equivalents of $^{113}Cd\ Cl_2$ per monomer have been added to the previously metal-free protein. The sample is 2.3 mM in Con A protomer. The buffer used in these experiments was 0.2 M NaCl, 50 mM NaAc, pH = 5.2, with D_2O added to provide an internal lock. The experimental conditions used to obtain all spectra shown were: flip angle = 45°, recycle time = 0.4 sec, spectral window = 10,000 Hz, number of data points collected = 1024. These spectra required 70000 transients. A 5 kHz enlargement of the spectra is displayed with Hz of line broadening for sensitivity enhancement. Resonances occur at 68, 46 and -125 ppm.
(b) Cadmium-113 spectrum of Con A containing 2.2 equivalents of $^{113}Cd(II)$ and one equivalent of Mn(II). The resonances are at 68, 46, and -125 ppm.
(c) Cadmium-113 nmr spectrum of Con A containing 2.2 equivalents of $^{113}Cd(II)$ and one equivalent of Ca(II). The large resonances occur at 68 and 41 ppm. The small resonance is at 46 ppm.

Figure 2

(Δ) The chemical shift of the free $^{113}Cd(II)$ resonance in a Cd:Cd Con A sample vs chloride ion concentration. The sample contains 2.2 mM Con A protomer, 5.0 mM $Cd(NO_3)_2$, and .05 M sodium acetate buffer pH 5.2. Sodium Chloride was added to give the desired Cl^- concentration.
(o) The chemical shift of 4 mM $^{113}Cd(NO_3)_2$ in the absence of protein but in the same buffer as above.

Figure 3

(a) Cadmium-113 nmr spectrum of "unlocked" Con A containing two equivalents of $^{113}Cd(II)$. One resonance is observed at 68 ppm. The same experimental conditions are used in Fig. 1 with a protomer concentration of 1.1 mM.
(b) Cadmium-113 nmr spectrum of 3a after the addition of Zn(II). The resonance occurs at 72 ppm.
(c) Cadmium-113 nmr spectrum of unlocked 2 Cd(II)-Con A in nitrate containing buffer. The protomer concentration is 1.8 mM with the resonance occurring at -12 ppm.

Figure 4

(a) The cadmium-113 nmr spectrum of Con A containing 2 equivalents of $^{113}Cd(II)$ and an equivalent of methyl α-DOmanno-pyranoside. The sample is 1.6 mM in Con A protomer. The resonances occur at 43 and -131 ppm.
(b) Cadmium-113 nmr spectrum of 2 Cd(II)-Con A for reference. The resonances occur at 68, 43 and -125 ppm.

Figure 5

(a) The ^{113}Cd nmr spectrum on 2 Cd(II)-SOD. The spectrum was obtained on a 5000 Hz spectral window using a 45° flip angle with a 0.8 second delay between pulses. Five thousand transients were accumulated. The spectrum shown is a 2000 Hz expansion of the transformed spectrum. One resonance appears at 311 ppm.
(b) The ^{113}Cd spectrum of 2 Cd(II)-2 Cu(II)-SOD ran under the same conditions as (a).
(c) The ^{113}Cd spectrum of 2 Cd(II)-2 Cu(I)-SOD obtained using the same conditions as in (a). One resonance appears at 321 ppm.

Figure 6

The spectra obtained in a progressive saturation experiment on 2 Cu(II)-SOD. The sequence $(90°-\tau)_n$ was used where τ included the data acquisition interval. The spin lattice relaxation time was determined using a non-linear least squares program.

Figure 7

The spectra obtained in determining the NOE enhancement for 2 Cd(II)-SOD. The sequence $(90°-PD)_n$ was used where $PD \geq 7\ T_1$. Fig. 2 (a) is proton coupled spectrum and 2 (b) the proton decoupled spectrum.

Figure 8

Arrhenius plots of the temperature dependence of the observed relaxation rates ($R \equiv 1/T_1$) of dialkylselenides.

Figure 9

Arrhenius plots of the temperature dependence of the observed relaxation rates ($R \equiv 1/T_1$) of alkaneselenols.

Figure 10

pH profile of the chemical shift of a 0.5 M solution of selenocysteamine in D_2O. The experimentally determined pK_a is indicated on the graph.

Figures 11 - 14

See figures.

Figure 15

The ^{1}H decoupled ^{13}C spectrum of methyl formate (formyl carbon) using

Chirp and Square wave modulation at 10 watts of power (Chirp repetition rate was 400 Hz and Chirp bandwidth was 10 kHz). The left most signal corresponds to an on resonance condition for the ^{1}H decoupling. Each resulting signal corresponds to a 100 Hz offset of the decoupler to higher frequency.

Figure 16

The ^{1}H decoupled ^{13}C spectrum of methyl formate (formyl carbon) using Chirp and Square wave modulation with 2 watts of decoupling power (Chirp repetition frequency equal to 300 Hz and a Chirp bandwidth of 6.0 kHz). The format of this figure is the same as that employed in Figure 2.

Figure 17

The ^{1}H decoupled ^{13}C spectrum of methyl formate (formyl carbon) using square wave modulation at 4 watts os decoupling power. The optimum modulation rate of 100 Hz was employed. The format of this figure is the same as that employed in Figure 2.

Figure 18

Circuit diagram for a frequency modulated 5.0 MHz oscillator.

Figure 19

Circuit diagram for a sawtooth function generator and synchronous square wave at 1/4 of the sawtooth frequency.

Figure 20

The ^{19}F decoupled ^{13}C spectrum of perfluorovinyl dimethyl borane, $(CH_3)_2BC_2F_3$. See text for chemical shifts.

Figure 1

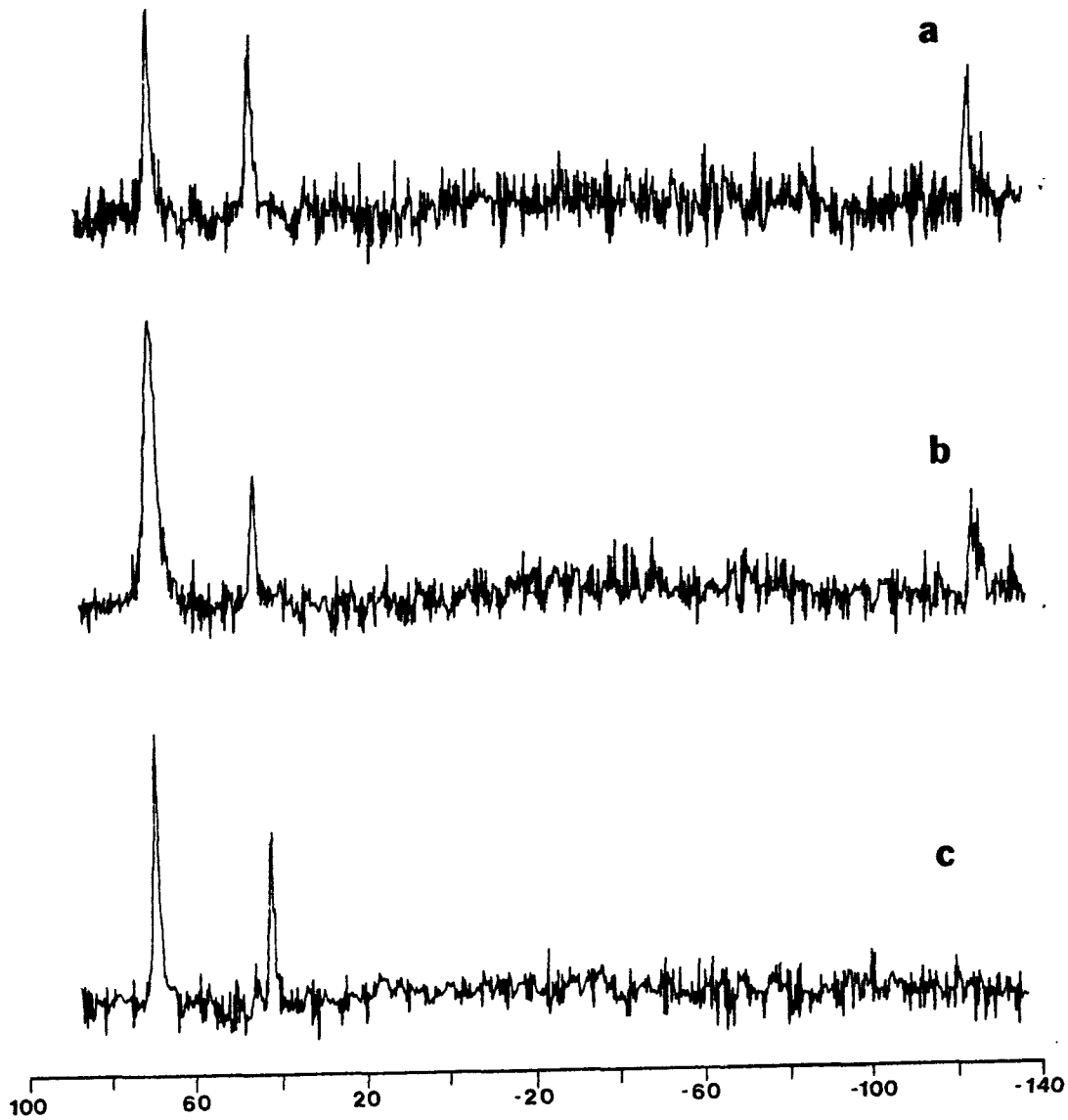

Figure 2

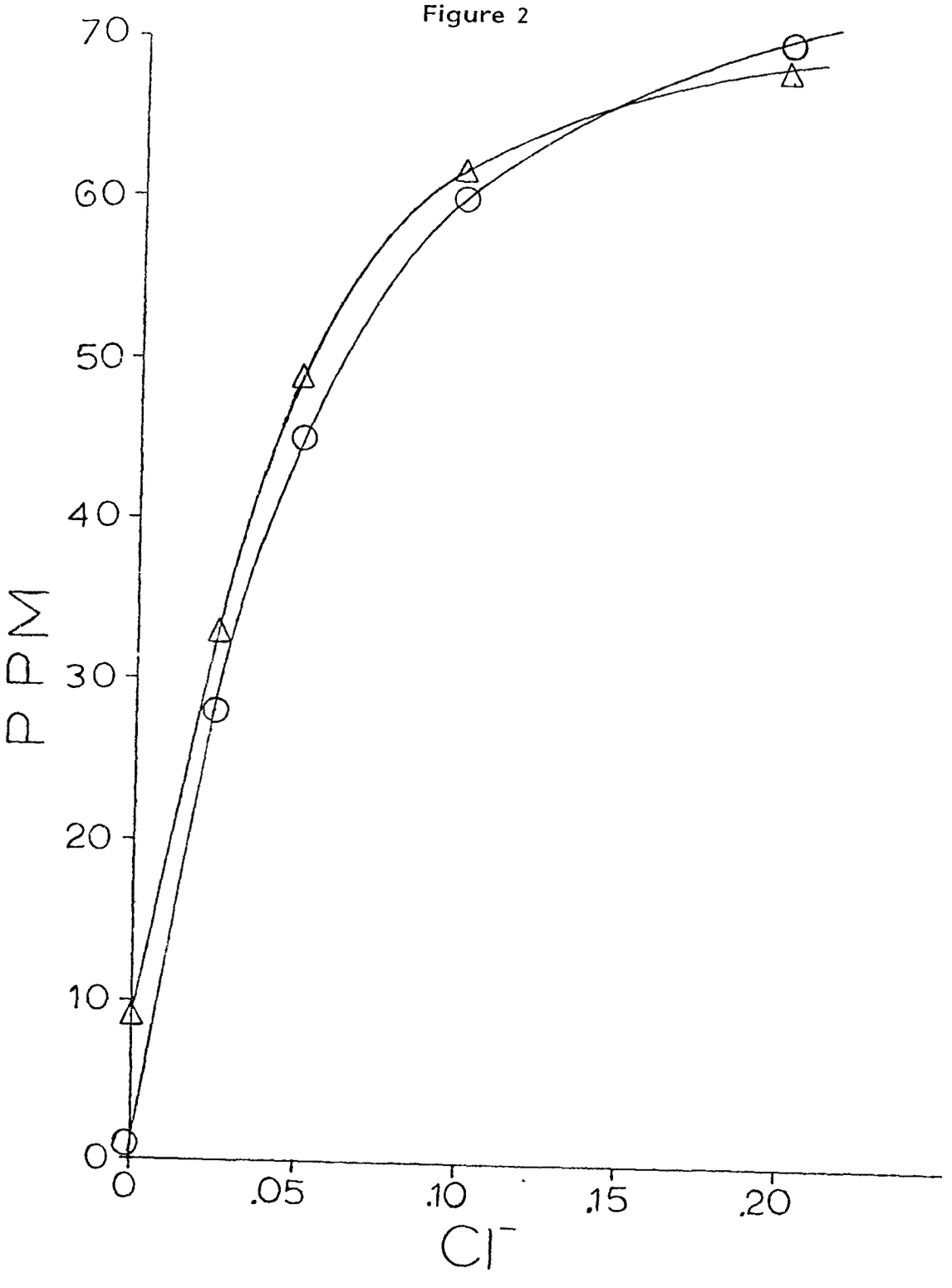

Figure 3

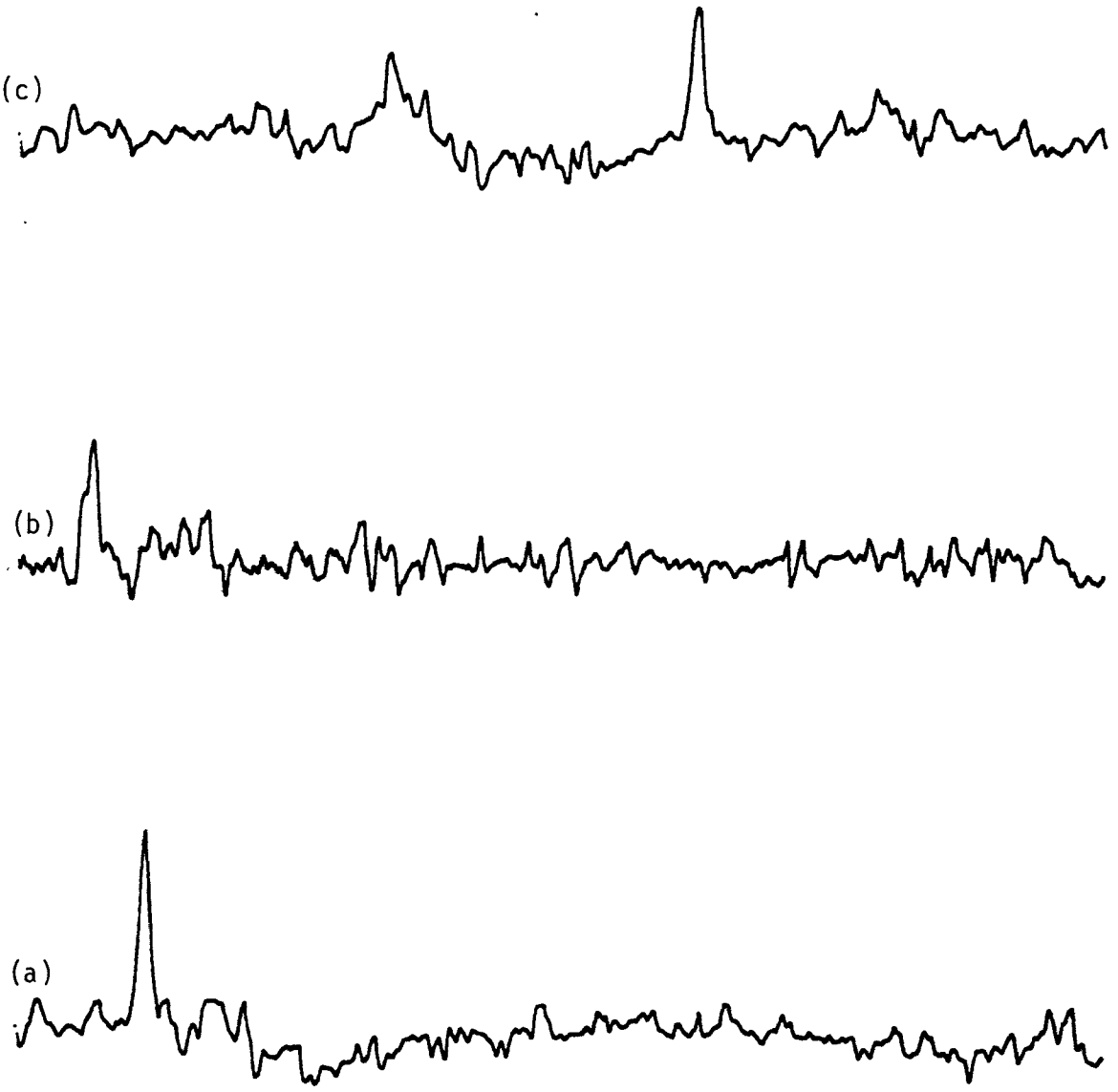

Figure 4

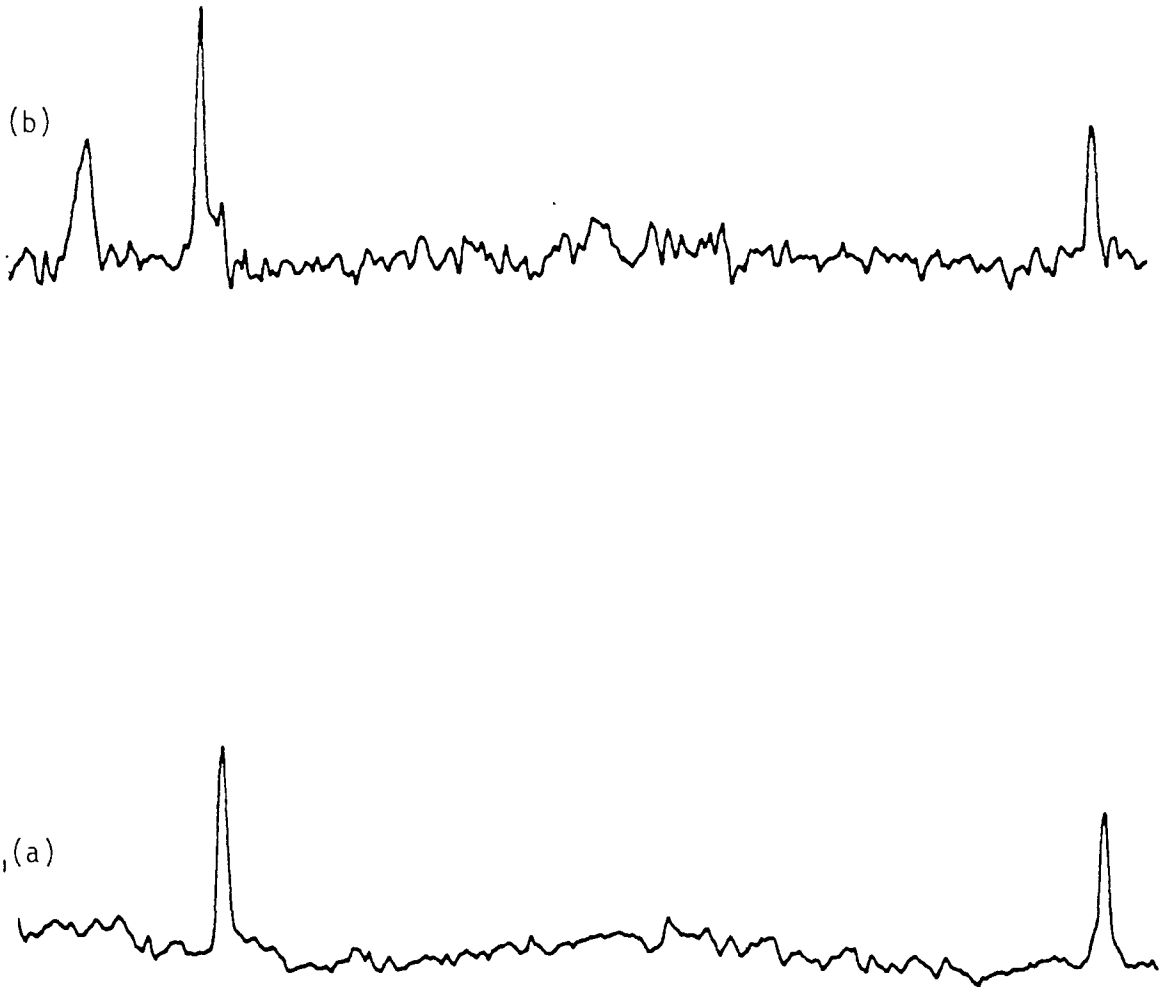

Figure 5

SUPEROXIDE DISMUTASE

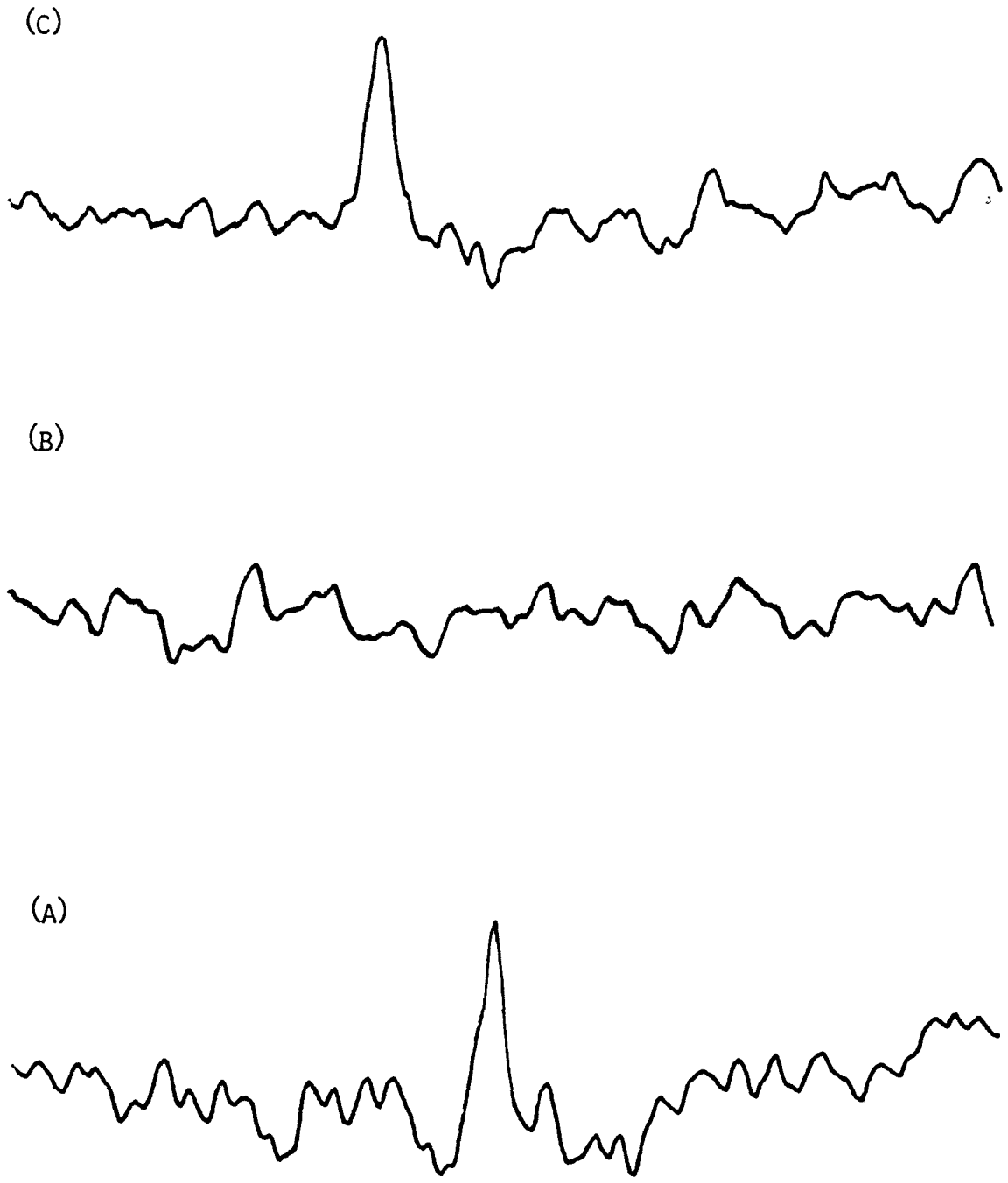

Figure 6

T_1 PLOT (PROGRESSIVE SATURATION) OF $2Cd^{2+}$ - SOD

T_1 = 1.2 sec

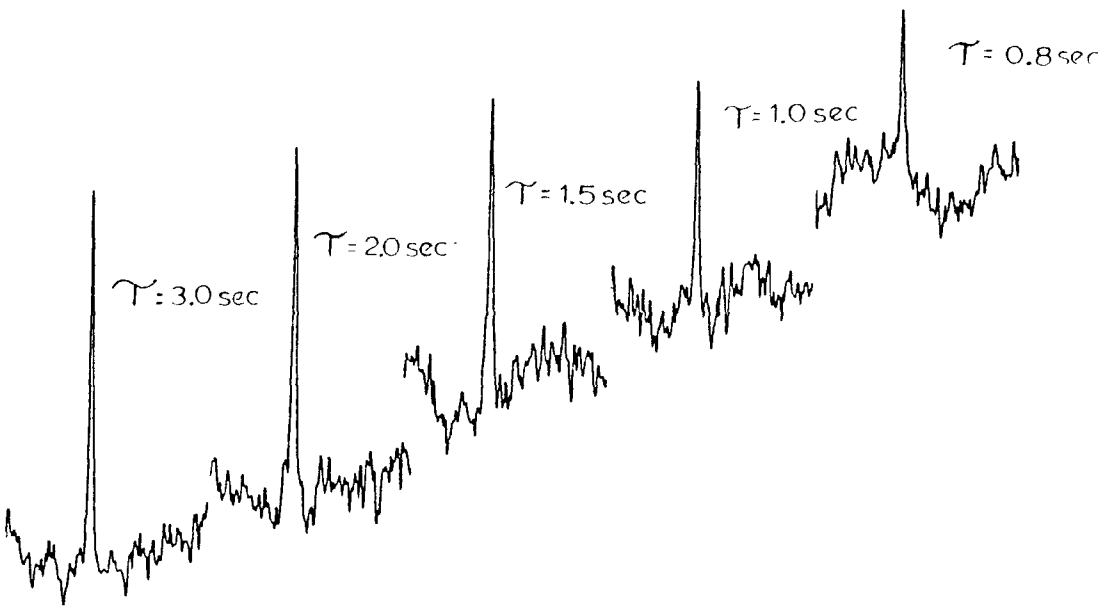

Figure 7

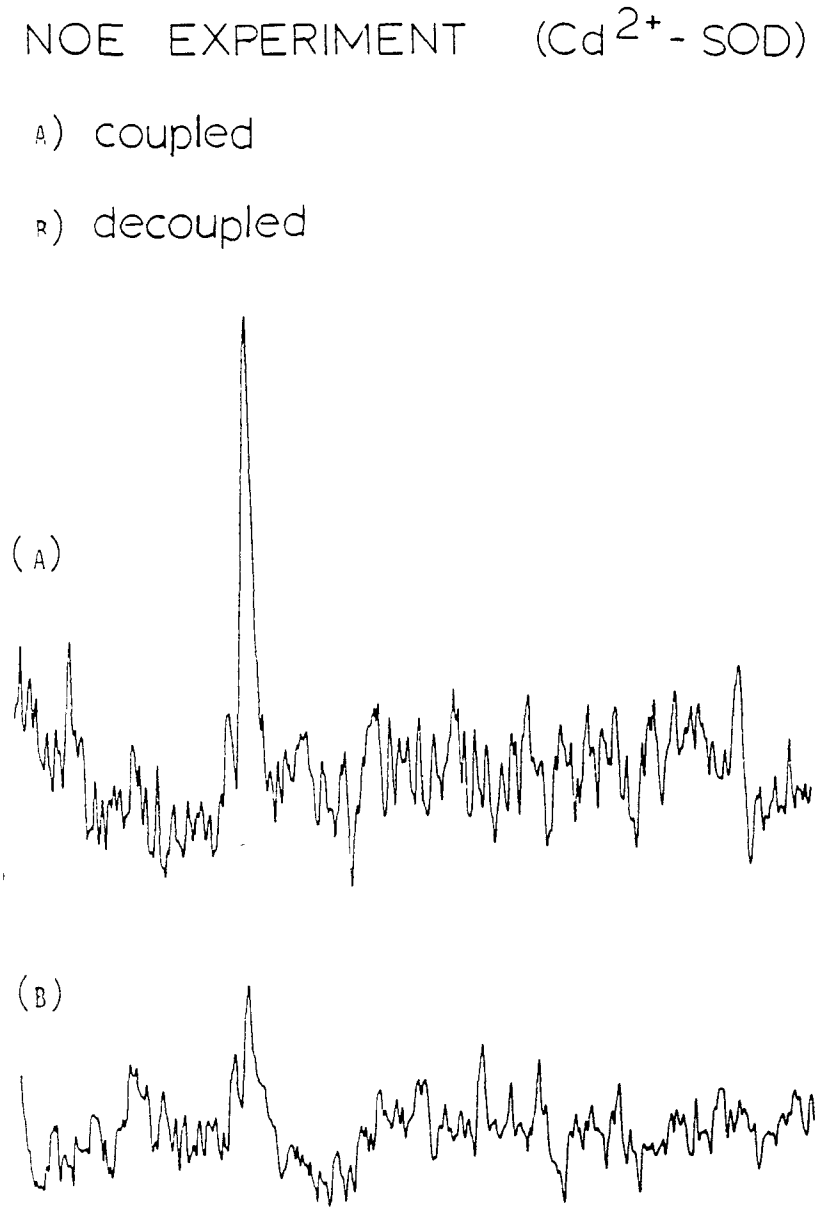

Figure 8

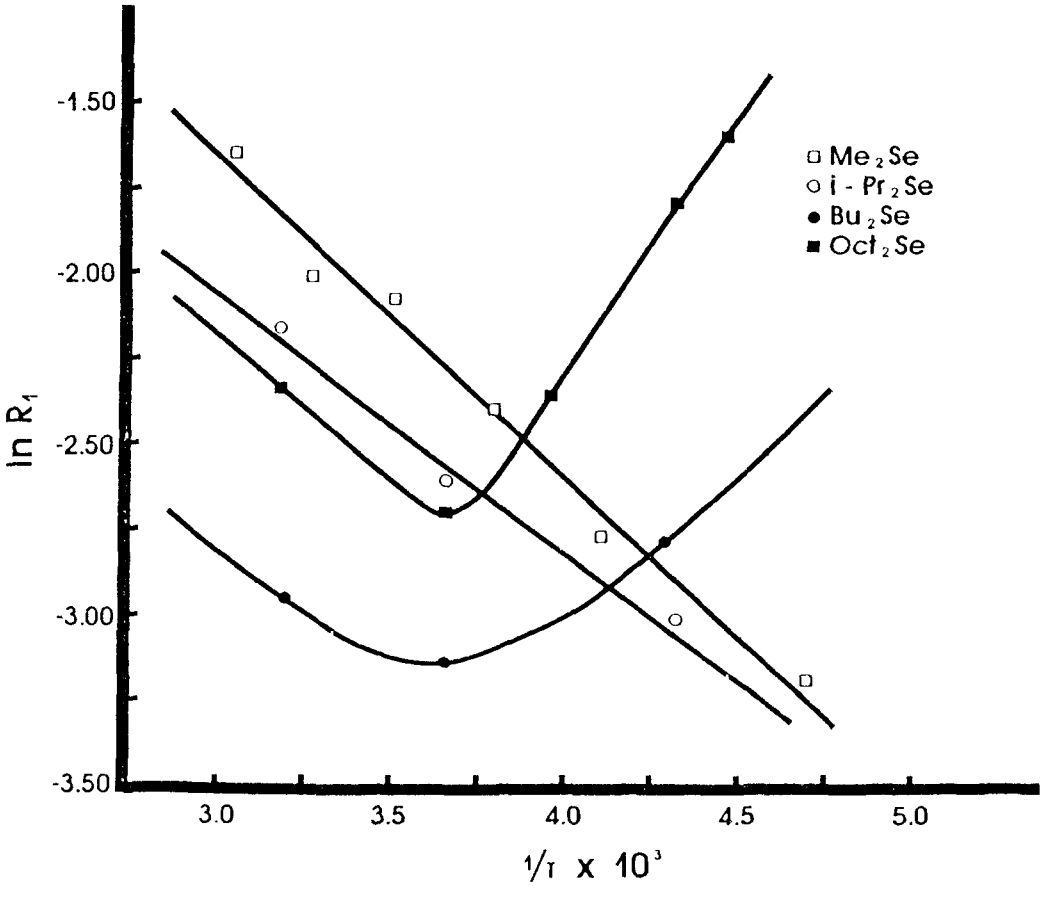
-1.50
-2.00
-2.50
-3.00
-3.50
ln R_1
3.0
3.5
4.0
4.5
5.0
1/T x 10^3
Me$_2$Se
i - Pr$_2$Se
Bu$_2$Se
Oct$_2$Se

Figure 9

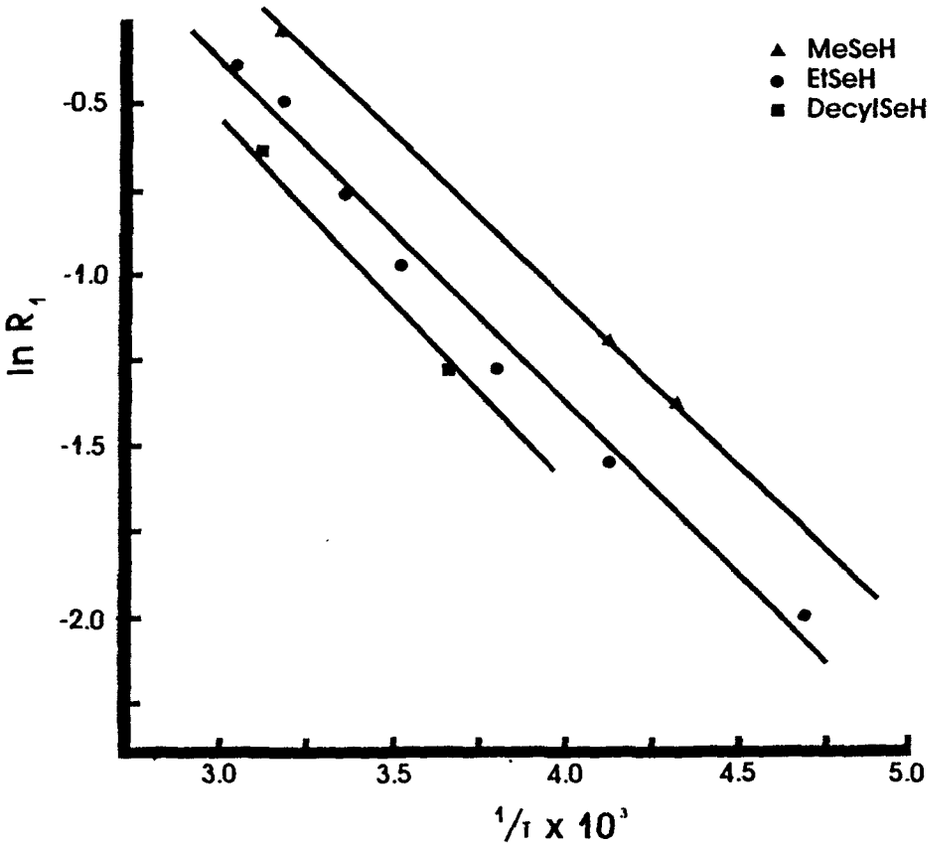

Figure 10

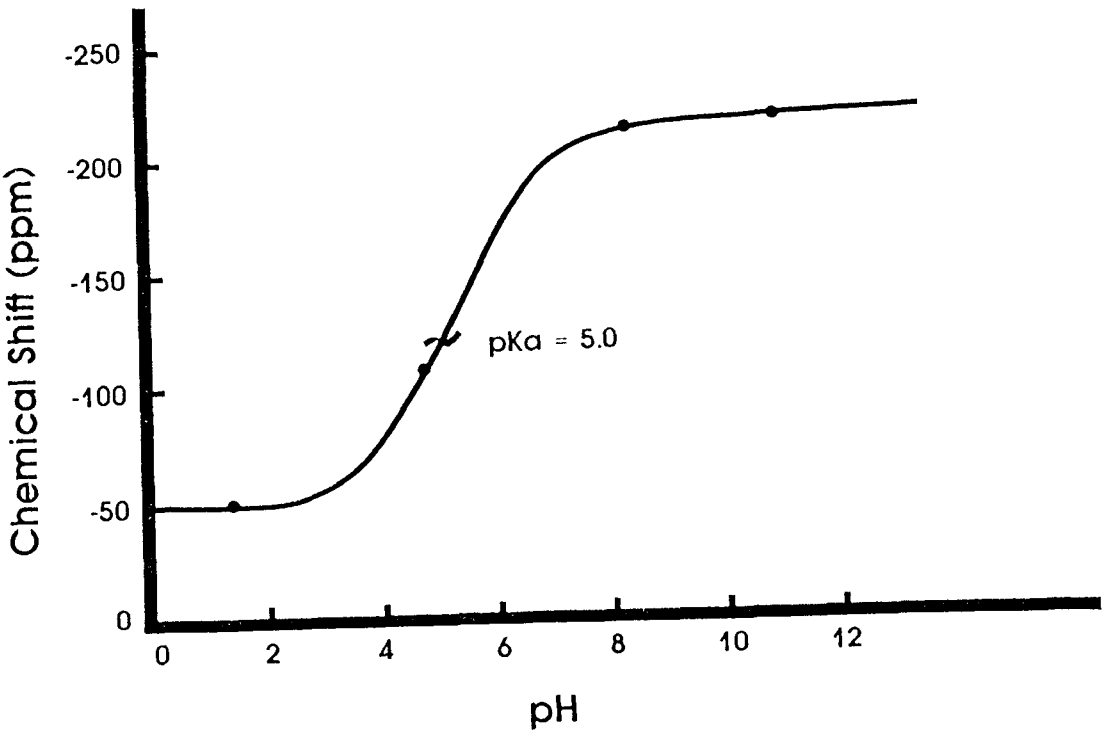

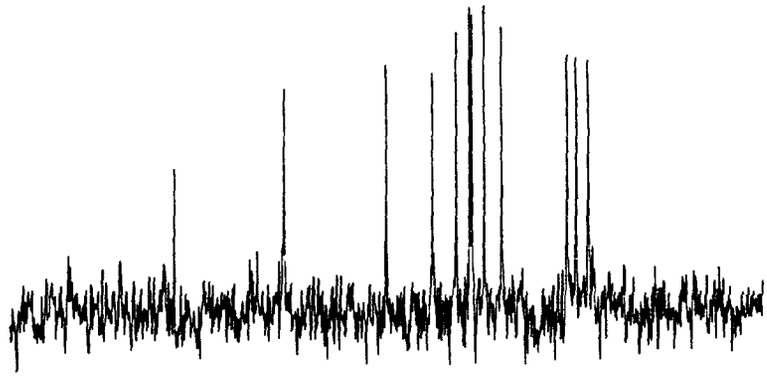

Fig. 11 Proton-decoupled natural-abundance ^{13}C spectrum of aqueous sucrose at 32°C. This spectrum represents 4096 accumulations using 90° rf pulses, 8192 points in the time domain, a spectral width of 4000 Hz, and a recycle time of 1.0 sec. Exponential multiplication equal to 1-Hz broadening was used for this plot which is a 2000-Hz portion of the entire frequency sepectrum.

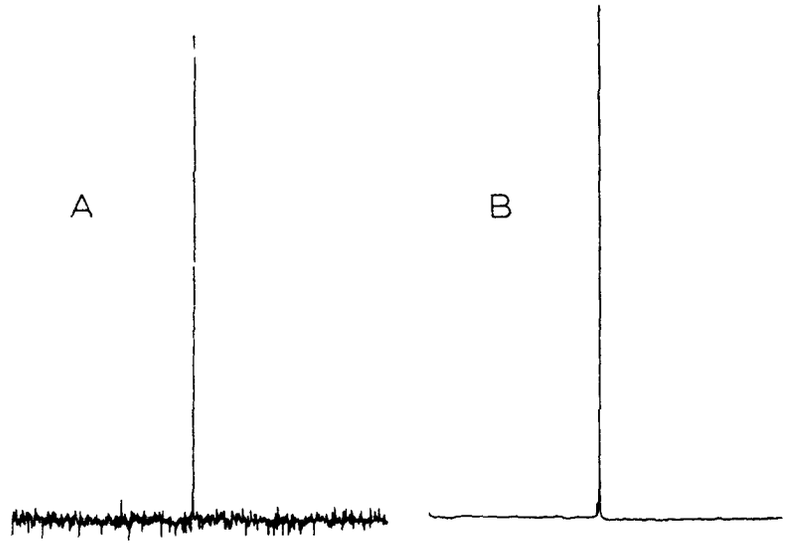

Fig. 12 ^{19}F spectra of trifluoroacetic acid (20 m*M* in ^{19}F) at 94.1 MHz. Both spectra were recorded using the same sample following a single 90 rf pulse, with a sweepwidth of 2000 Hz and 0.3-Hz broadening due to exponential multiplication. Spectrum (A) was recorded in a 12-mm tube and (B) was recorded in an 18-mm tube.

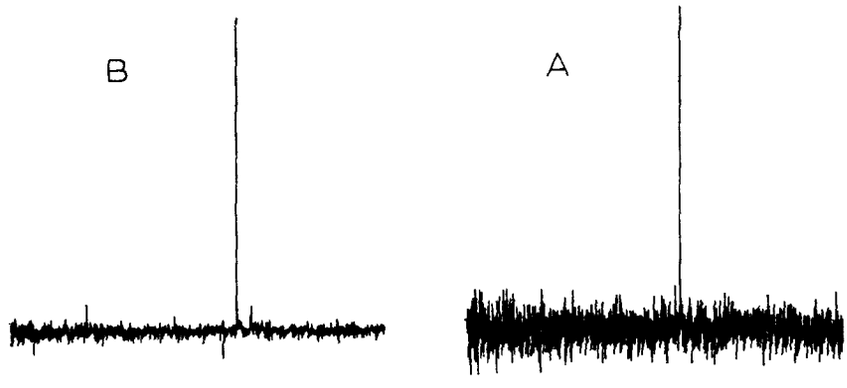

Fig. 13 ^{31}P spectra of 25-m*M* aqueous potassium phosphate at 40.5 MHz. Both spectra were recorded using the same sample following a single 90° rf pulse, with a sweepwidth of 2500 Hz, 8192 points in the time domain, and 0.4-Hz broadening due to exponential multiplication. Spectrum (A) was recorded in a 12-mm tube and (B) was recorded in an 18-mm tube.

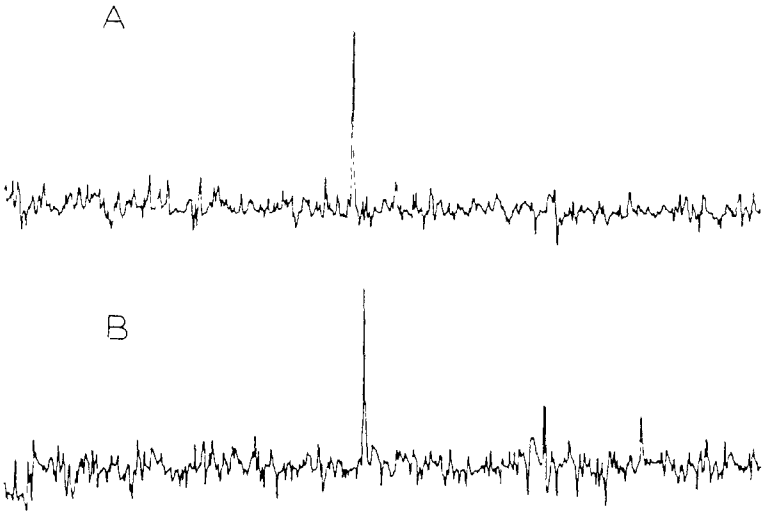

Fig. 14 Natural-abundance ^{113}Cd spectra of 32-m*M* $CdCl_2$ at 22.2 MHz. Both spectra were recorded using 30° rf pulses, a 5000-Hz sweepwidth, 8192 points in the time domain, and 0.8-Hz broadening due to exponential multiplication. (A) Fifty thousand accumulations in a 12-mm tube. (B) Four thousand accumulations in an 18-mm tube.

Figure 15

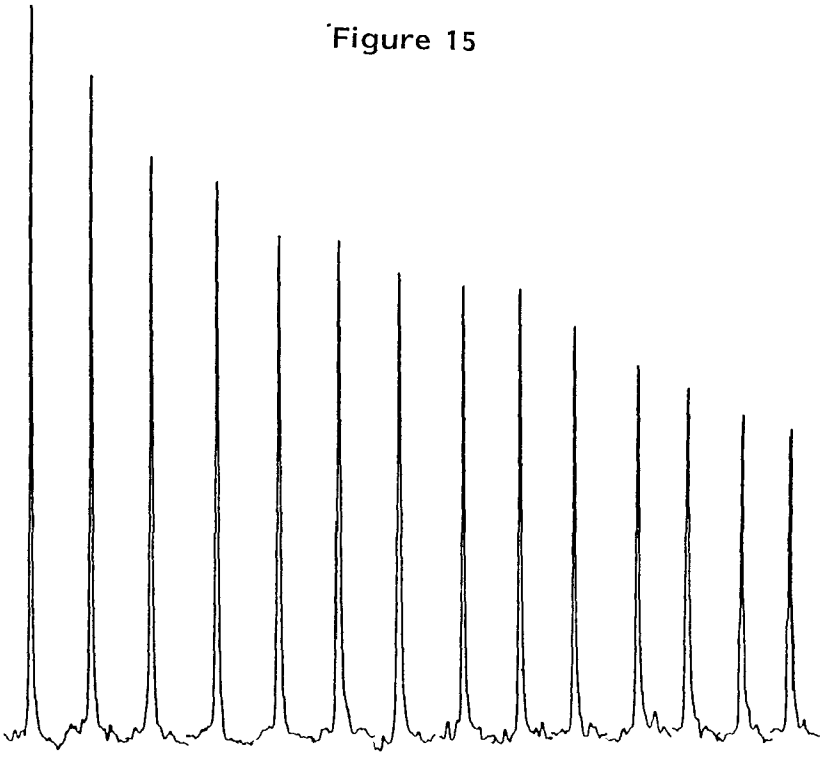

Figure 17

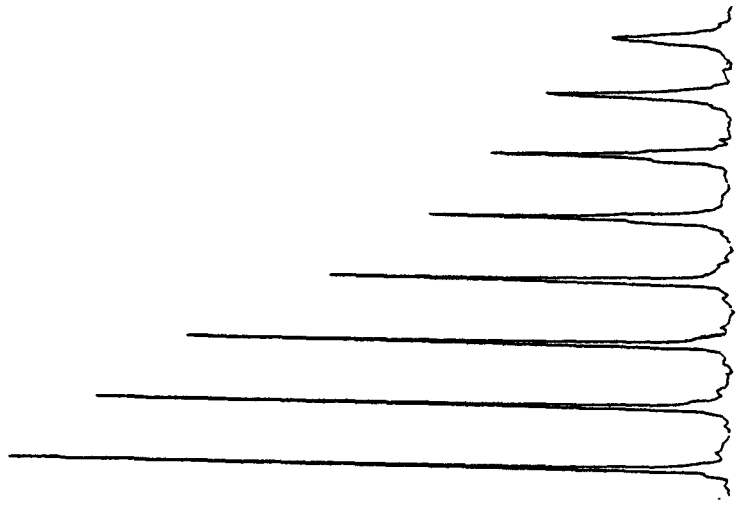

Figure 16

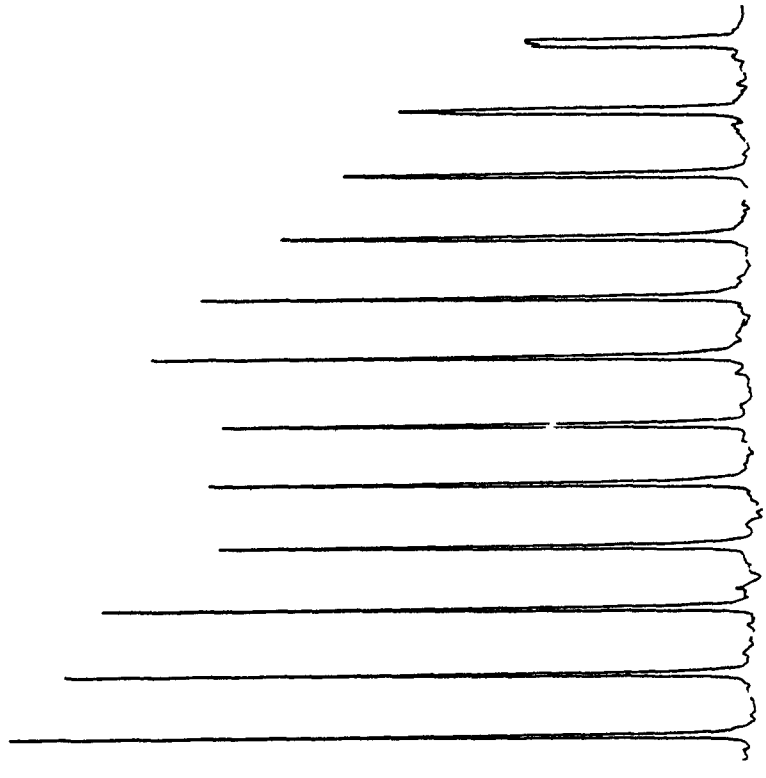

Figure 18

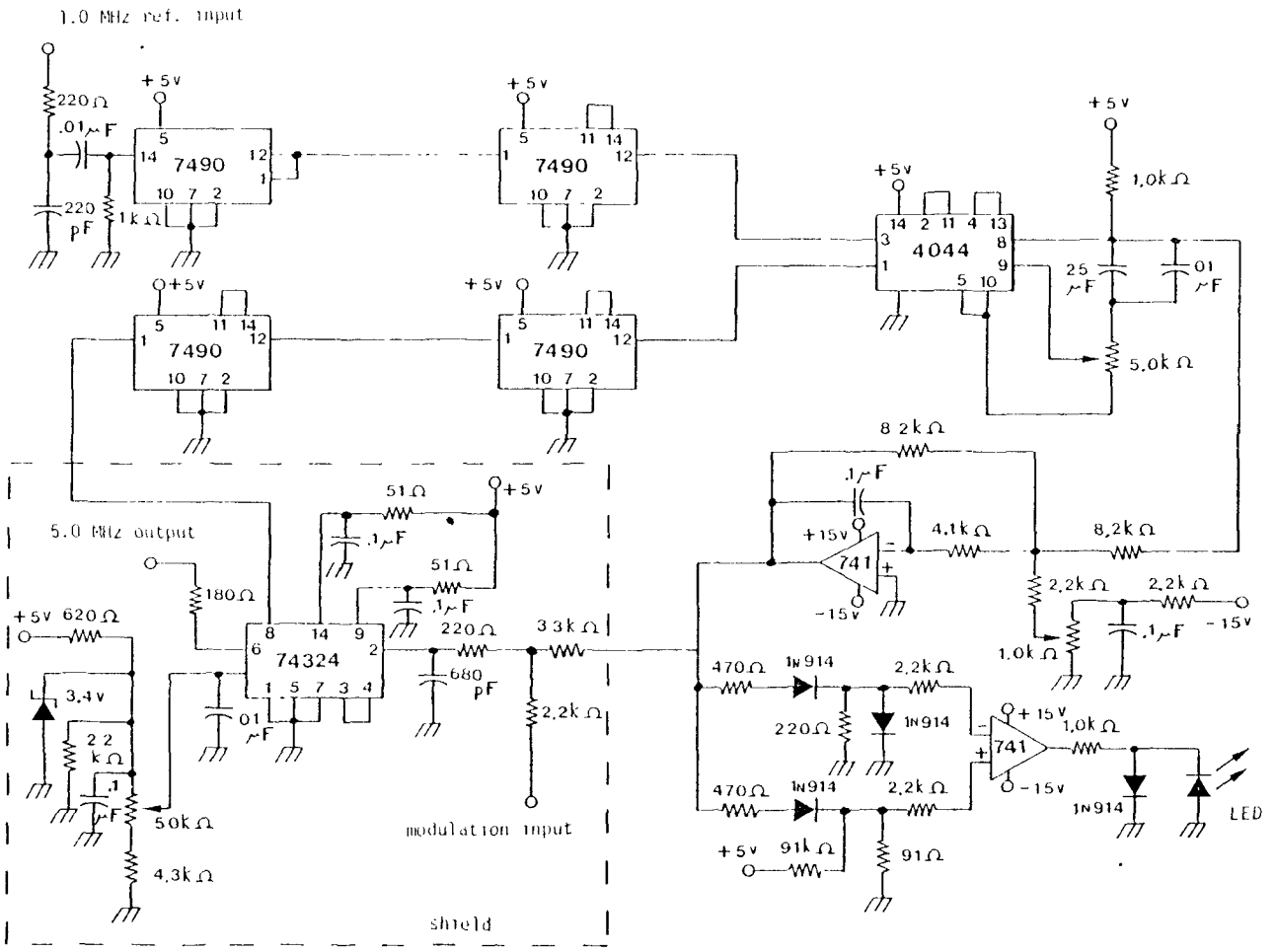
1.0 MHz ref. input
220Ω
.01μF
220 pF
1kΩ
+5v
7490
5.0 MHz output
180Ω
+5v 620Ω
3.4v
22 kΩ
.1μF
50kΩ
4.3kΩ
51Ω
74324
.01 μF
680 pF
220Ω
33kΩ
2.2kΩ
modulation input
shield
4044
25 μF
5.0kΩ
8.2kΩ
4.1kΩ
741
+15v
-15v
2.2kΩ
1.0kΩ
470Ω
1N914
220Ω
91kΩ
91Ω
LED

Figure 19

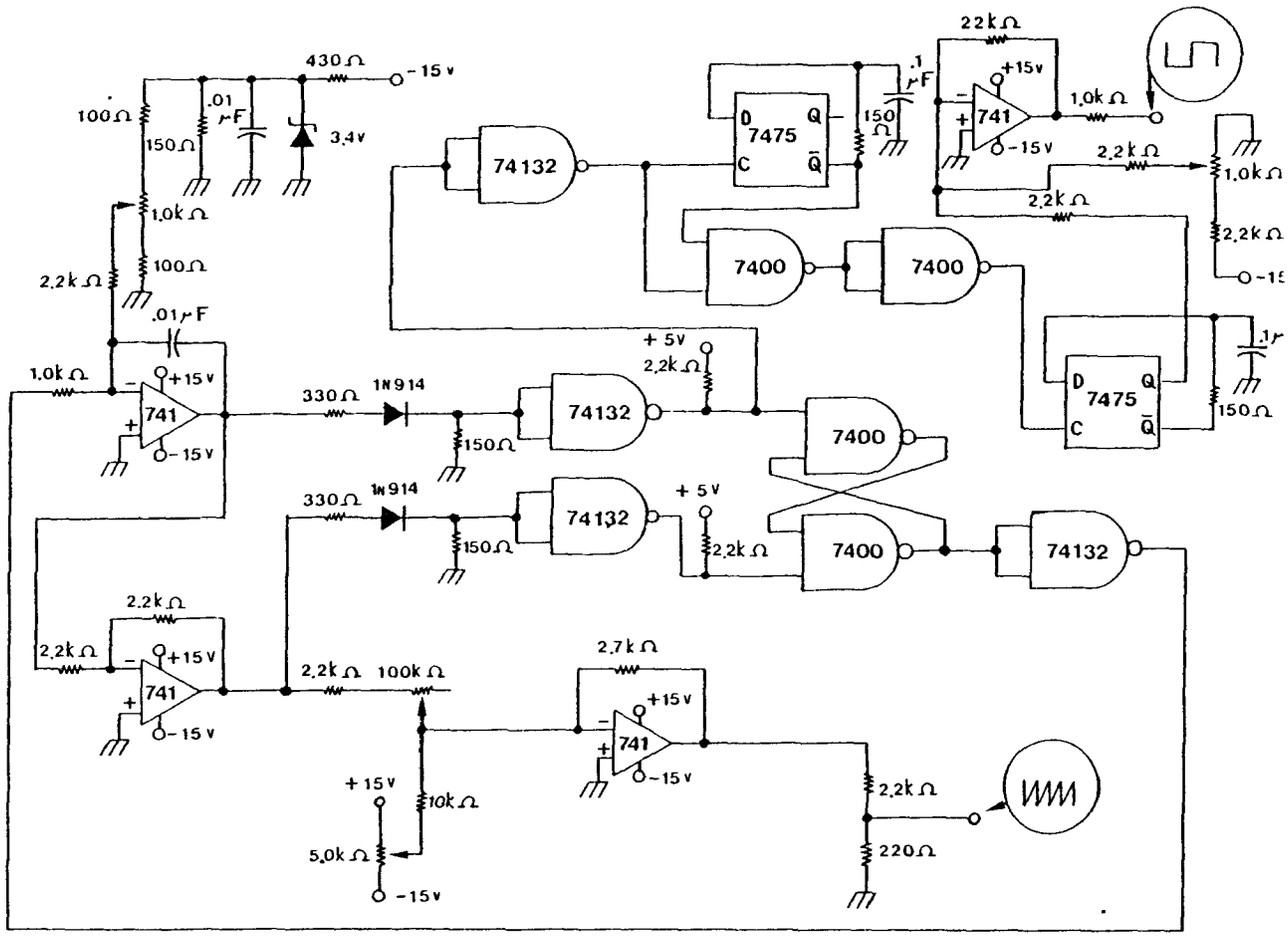
430Ω
-15v
100Ω
.01μF
150Ω
3.4v
1.0kΩ
100Ω
2.2kΩ
.01μF
1.0kΩ
+15v
741
-15v
330Ω
1N914
150Ω
74132
+5v
2.2kΩ
7400
D
7475
C
Q
Q̄
.1μF
150Ω
22kΩ
+15v
741
-15v
1.0kΩ
2.2kΩ
2.2kΩ
1.0kΩ
2.2kΩ
7400
7400
D
7475
C
Q
Q̄
.1μ
150Ω
330Ω
1N914
150Ω
74132
+5v
2.2kΩ
7400
74132
2.2kΩ
2.2kΩ
+15v
741
-15v
2.2kΩ
100kΩ
2.7kΩ
+15v
741
-15v
+15v
10kΩ
5.0kΩ
-15v
2.2kΩ
220Ω

Figure 20

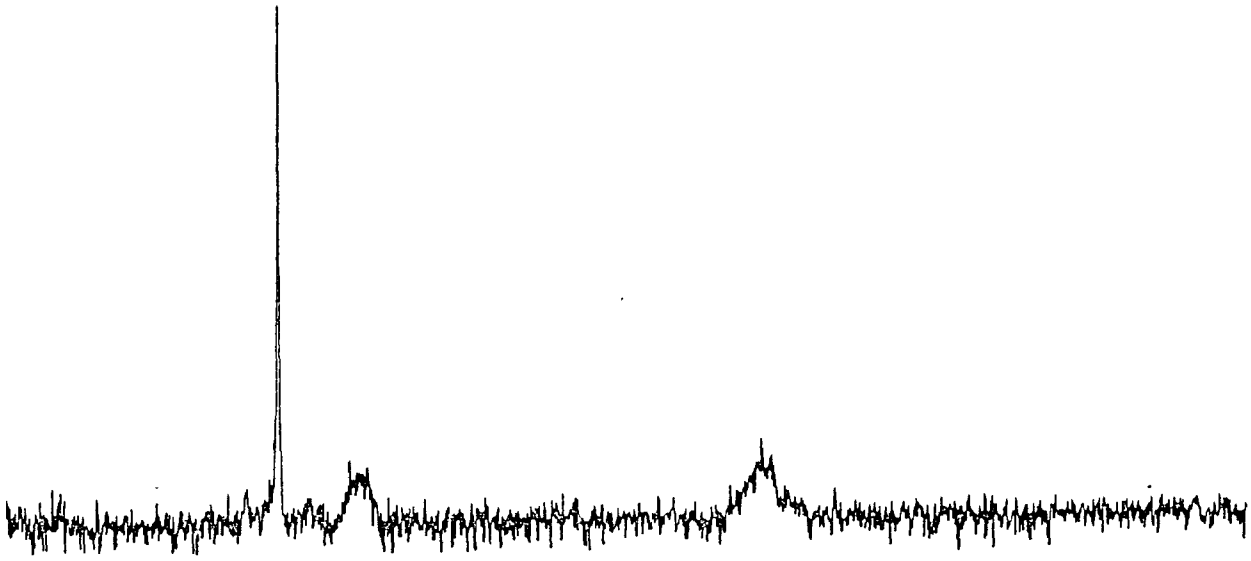

TECHNICAL REPORT DATA
(Please read Instructions on the reverse before completing)

REPORT NO.	2.	3. RECIPIENT'S ACCESSION NO.
EPA-600/1-79-035		

TITLE AND SUBTITLE	5. REPORT DATE
COMPREHENSIVE PROGRESS REPORT FOR FOURIER TRANSFORM NMR OF METALS OF ENVIRONMENTAL SIGNIFICANCE	September 1979
	6. PERFORMING ORGANIZATION CODE

AUTHOR(S)	8. PERFORMING ORGANIZATION REPORT NO.
Paul D. Ellis and Jerome D. Odom	

PERFORMING ORGANIZATION NAME AND ADDRESS	10. PROGRAM ELEMENT NO.
Department of Chemistry University of South Carolina Columbia, South Carolina 29208	1EA615
	11. CONTRACT/GRANT NO.
	Grant R804359

SPONSORING AGENCY NAME AND ADDRESS	13. TYPE OF REPORT AND PERIOD COVERED
Health Effects Research Laboratory RTP, NC Office of Research and Development U.S. Environmental Protection Agency Research Triangle Park, NC 27711	14. SPONSORING AGENCY CODE EPA 600/11

SUPPLEMENTARY NOTES

ABSTRACT

Interactions of the metals cadmium and selenium with various biologically important substrates were studied by nuclear magnetic resonance (NMR) spectroscopy. Cadmium-113 NMR was used for a critical examination of three metalloproteins: concanavalin A, bovine superoxide dismutase and carboxypeptidase A. The NMR parameters of selenium-77 were investigated, with a view to using this nucleus as a probe of active site sulfydryl groups in proteins.

Several advances in NMR instrumentation were developed to further the aims of this project. One is a unique NMR probe, capable of spinning large (18 mm) NMR tubes, decoupling at any frequency, and observing any NMR-active nuclei. A decoupler modification, "Chirp" decoupling, was developed. This modification allows good experimental results with approximately 1/10 the power required without modification.

KEY WORDS AND DOCUMENT ANALYSIS

DESCRIPTORS	b. IDENTIFIERS/OPEN ENDED TERMS	c. COSATI Field/Group
Fourier Analysis Fourier Transformation Nuclear Magnetic Resonance		06B,T

DISTRIBUTION STATEMENT	19. SECURITY CLASS *(This Report)*	21. NO. OF PAGES
RELEASE TO PUBLIC	UNCLASSIFIED	91
	20. SECURITY CLASS *(This page)*	22. PRICE
	UNCLASSIFIED	

EPA Form 2220-1 (Rev. 4-77) PREVIOUS EDITION IS OBSOLETE